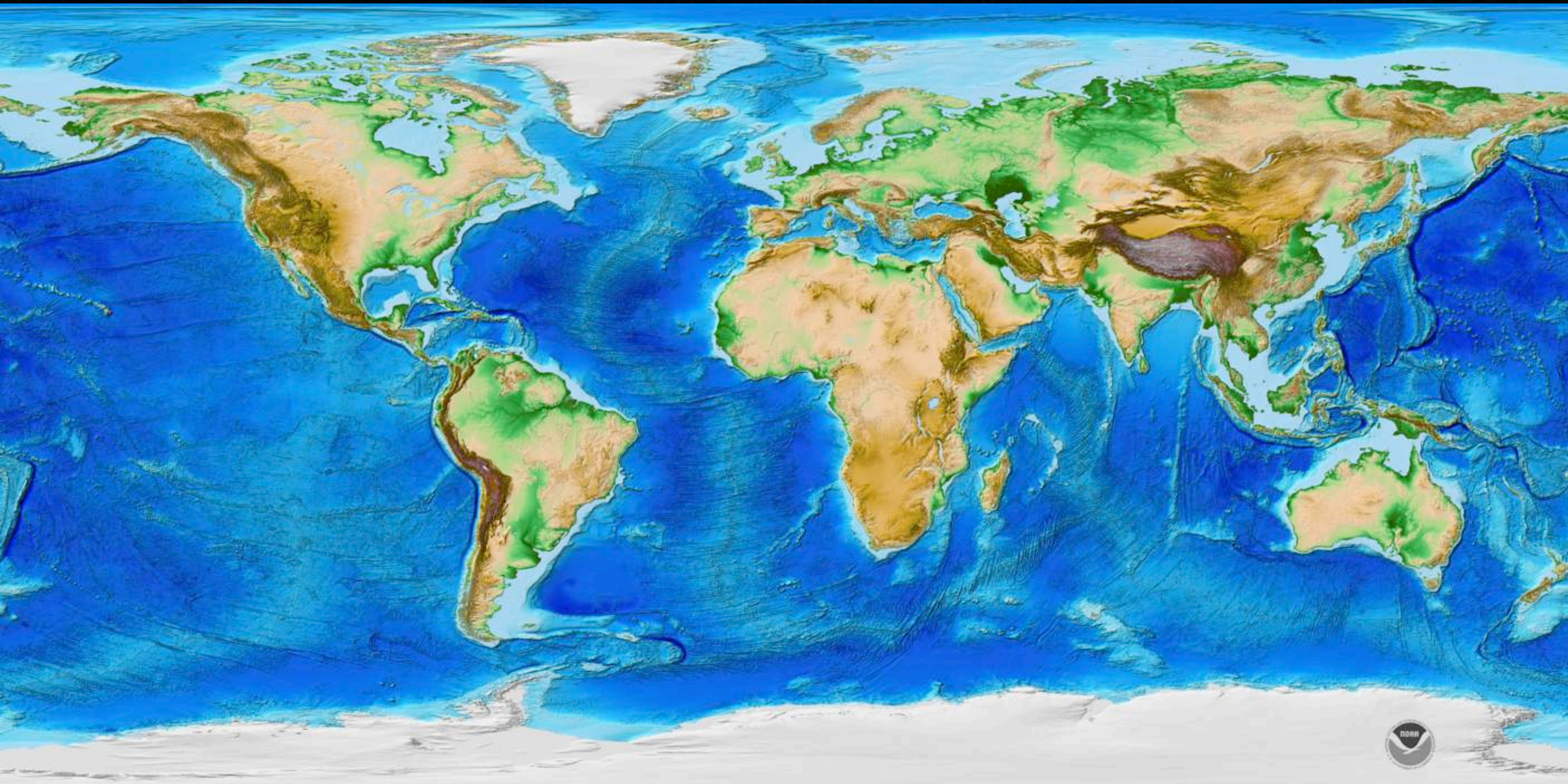

LabEx UnivEarthS Fall School
17-23 October 2015 – Santorini

Phase changes and eruptions in the Universe: VOLCANOLOGY

Edouard Kaminski

Institut de physique du globe de Paris
Université Paris Diderot
Sorbonne Paris Cité

Physical framework: Earth as a thermal system

Structure of the Earth according to Kircher (1665) with an ancient sun cooling down at its center that produces volcanoes.

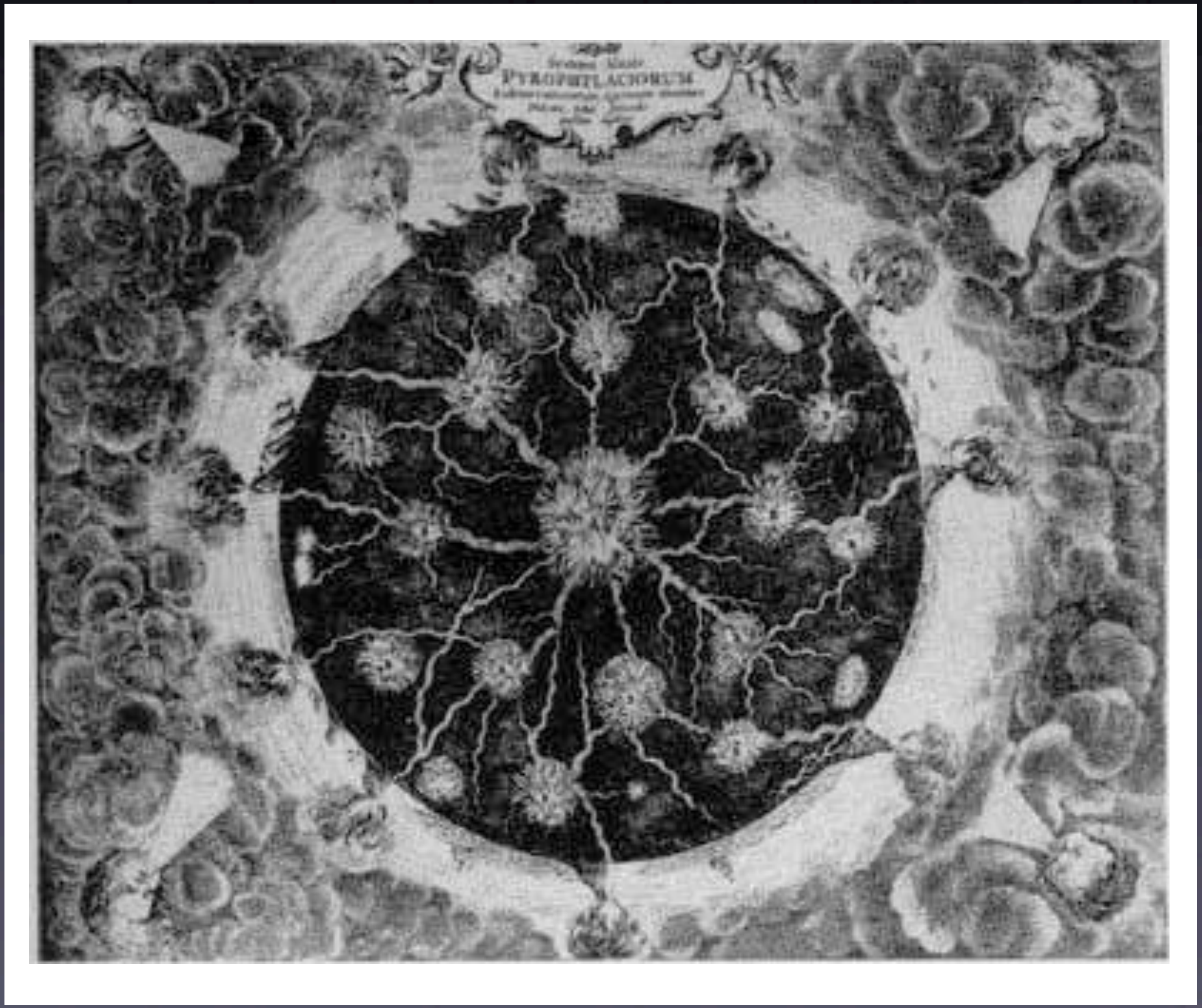

Modern view of the cooling of the Earth

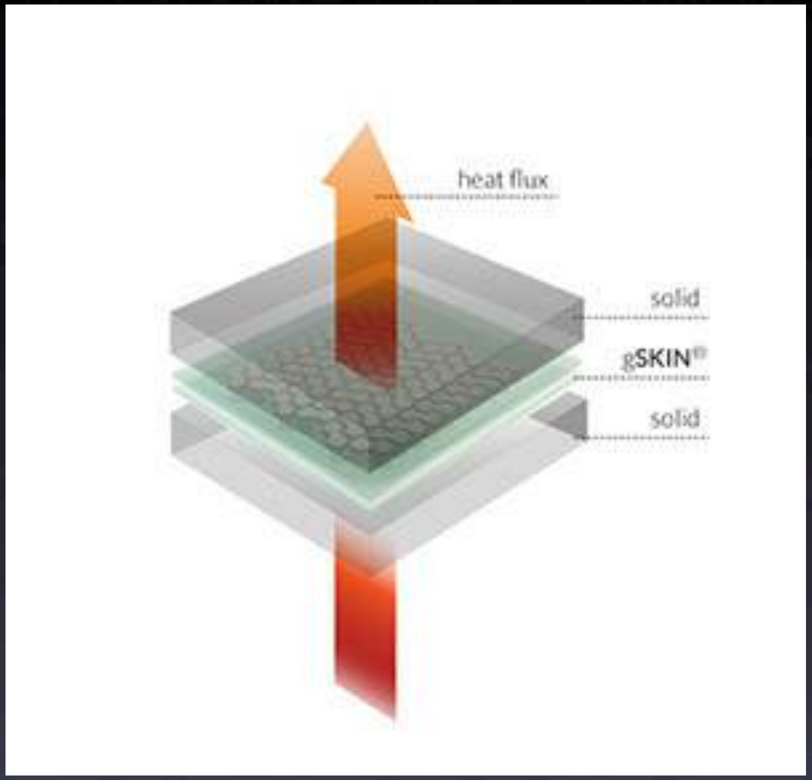

$q = -k\, dT/dz$ ($J/s/m^2 = W/m^2$)

k = thermal conductivity ~ 1 W/m/K

dT/dz = vertical temperature gradient = geotherm

Continental heat flux

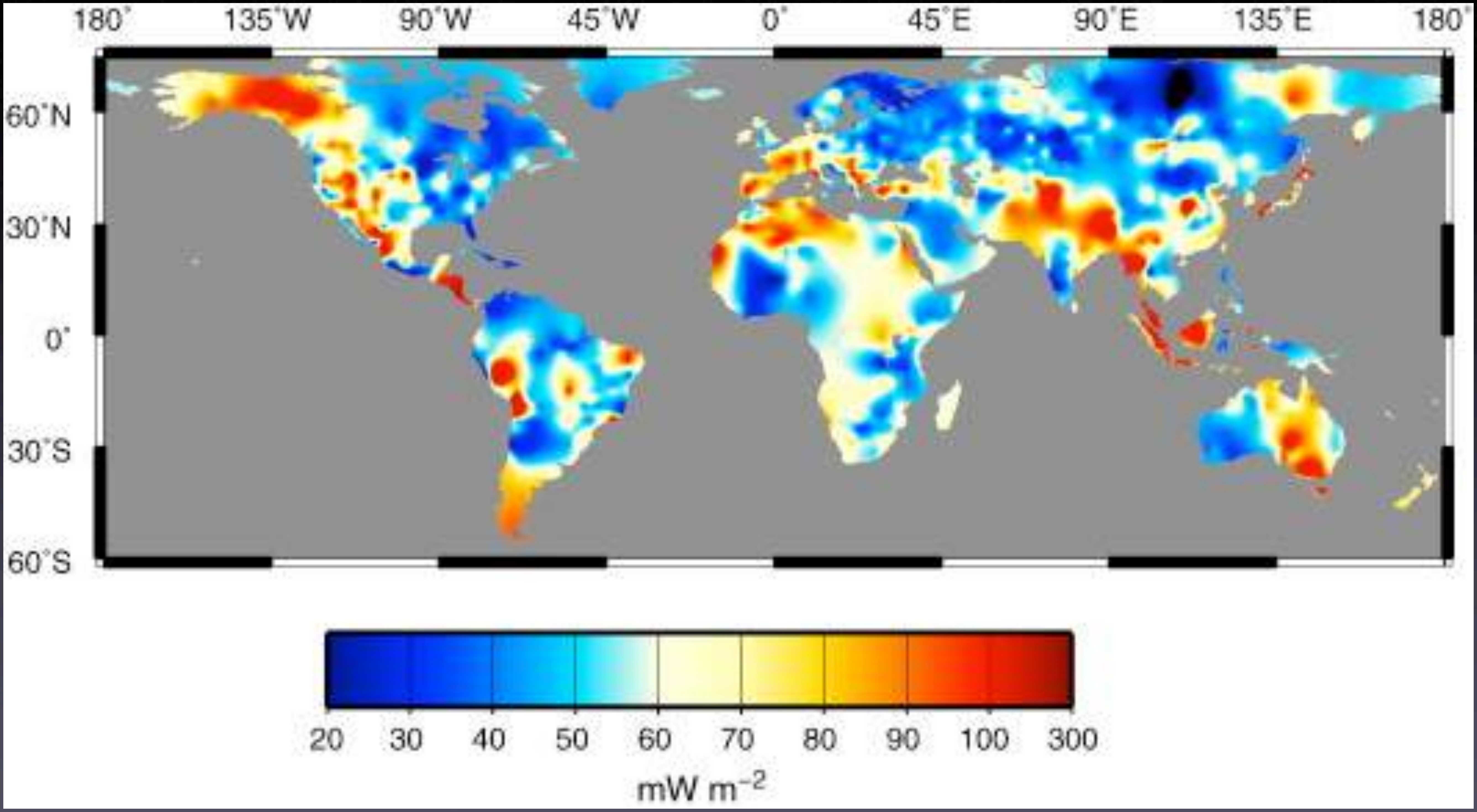

Jaupart & Mareschal

Oceanic heat flux

from 50 mW/m^2 (blue) to more than 500 mW/m^2 (red)

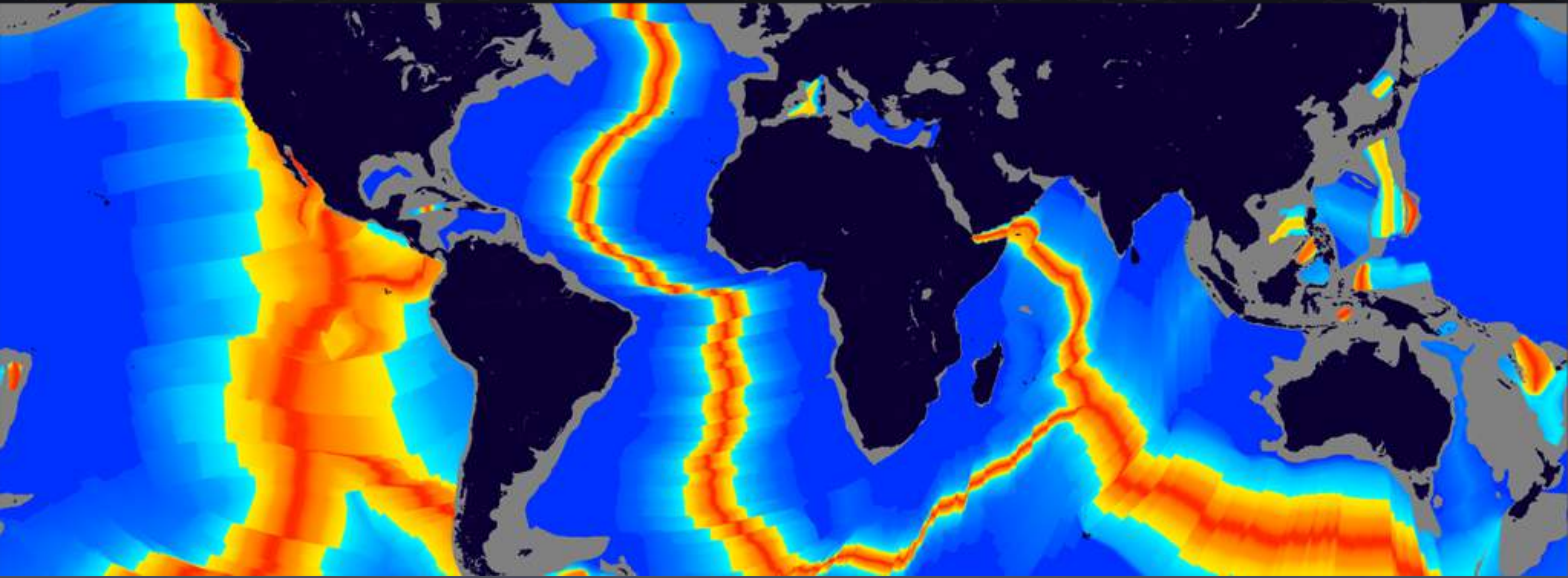

Labrosse

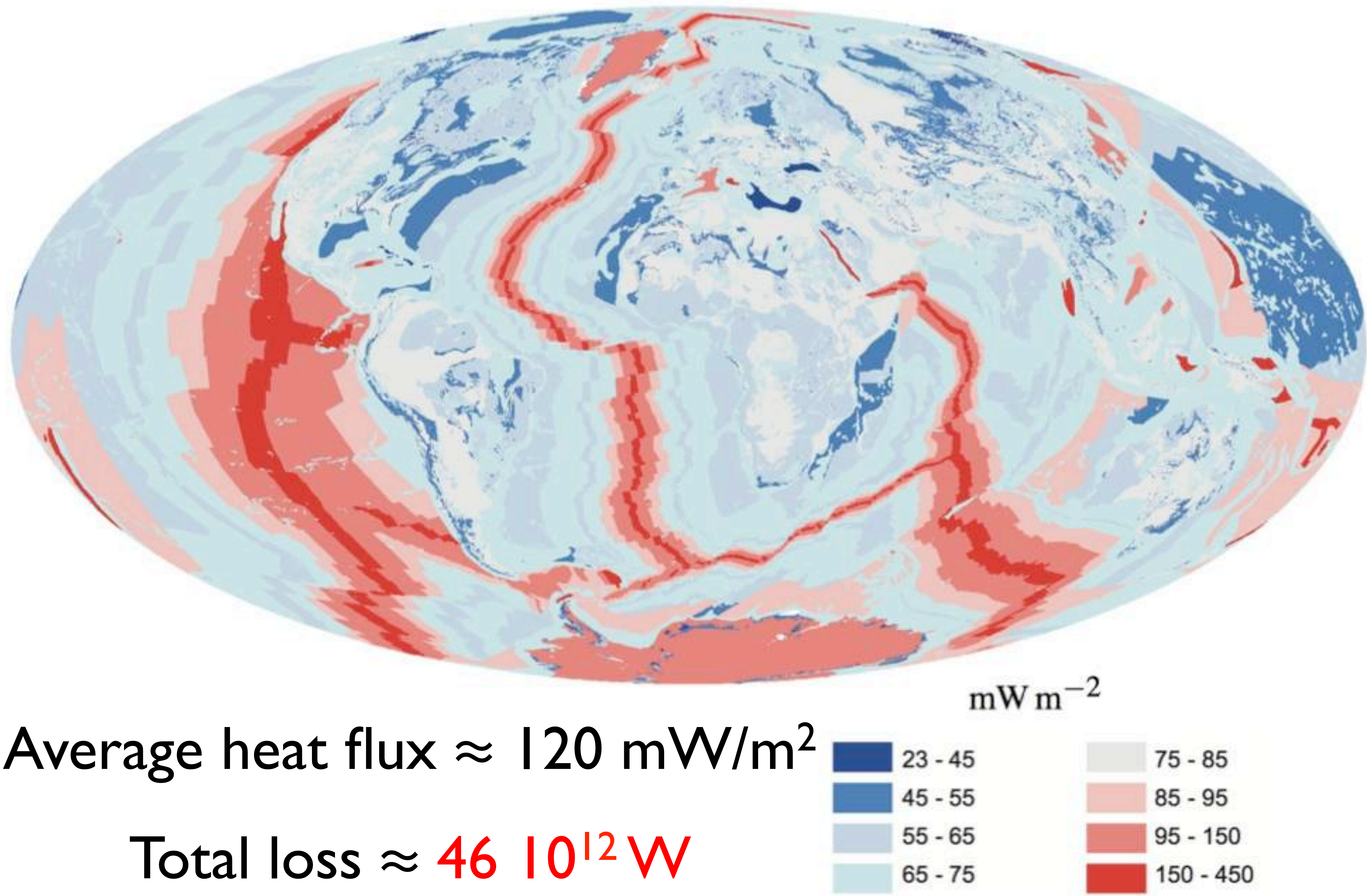

Average heat flux ≈ 120 mW/m^2

Total loss ≈ 46 10^{12} W

Quantitative estimate (present day)

Rate of variation of energy = production - loss

$$\color{red}{dE/\ dt} = M\ C_p\ dT/dt = \color{red}{S - P,}$$

$$dT/dt = (S - P)\ /\ M\ C_p$$

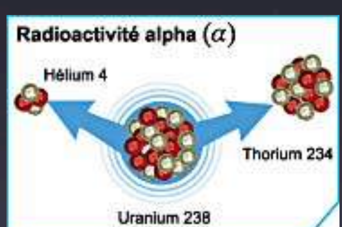

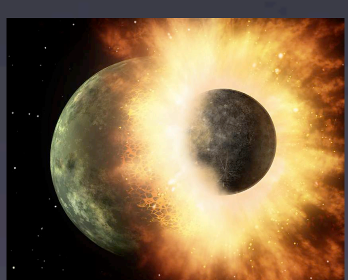

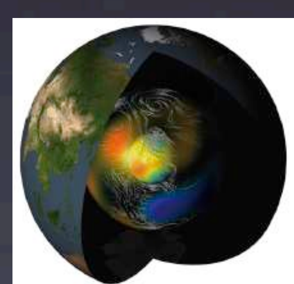

Heat production = 30 TW

Loss = 46 TW

Cp = 1200 J/s/K

$M = 6\ 10^{24}$ kg

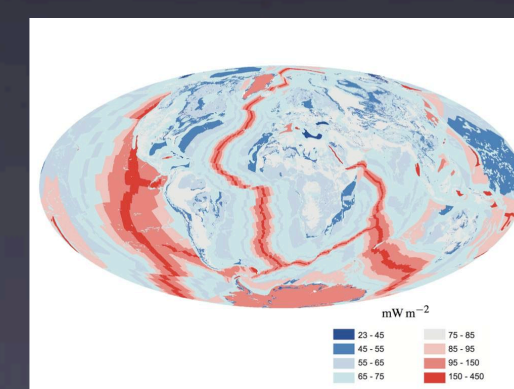

$$\color{red}{dT/dt \approx -70\ K/Ga}$$

Quantitative estimate (past)

based on the composition of lava

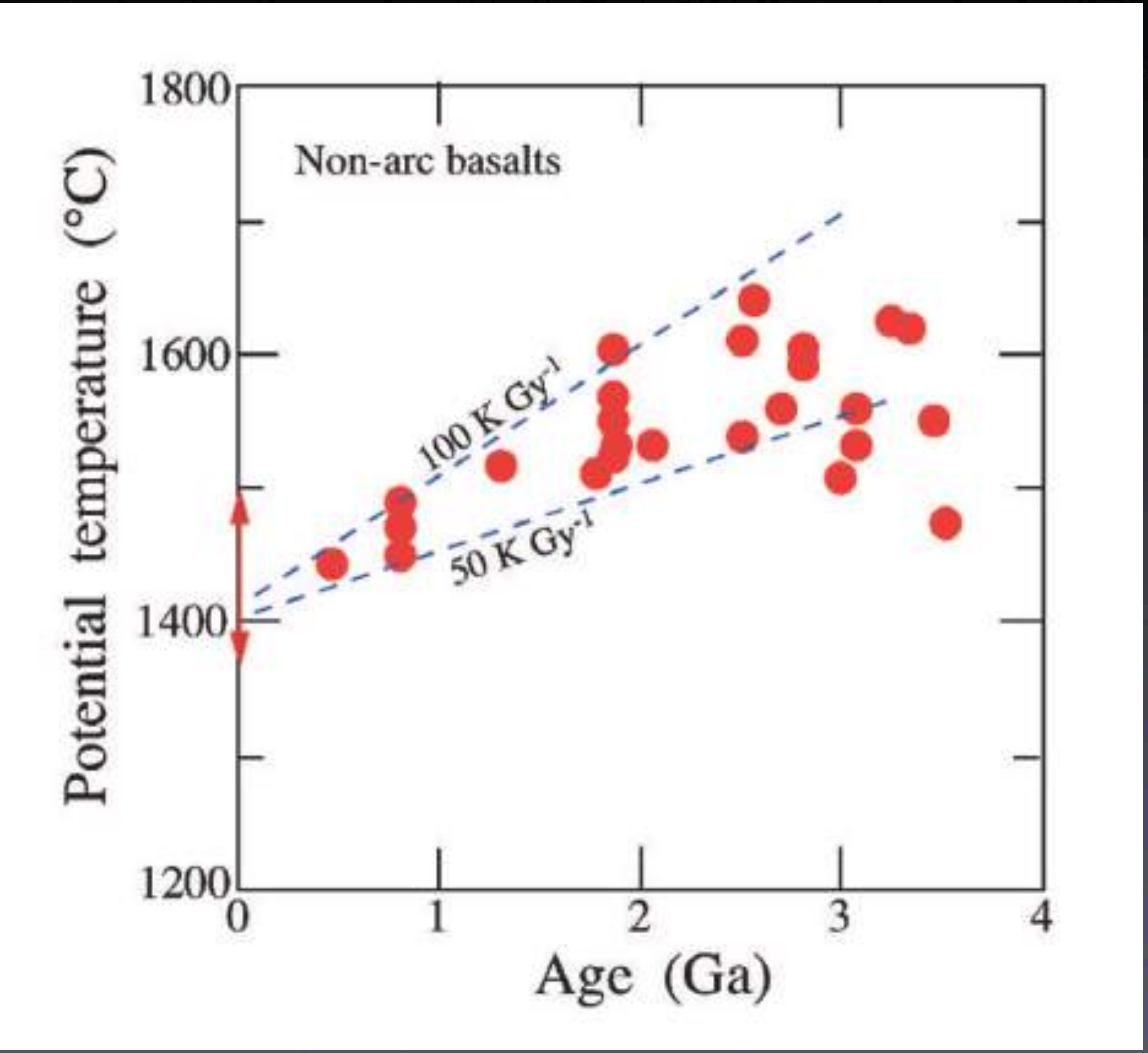

Implies a magmatic ocean at the surface of the early Earth following the giant impact

Structure of the present day Earth: a solid mantle

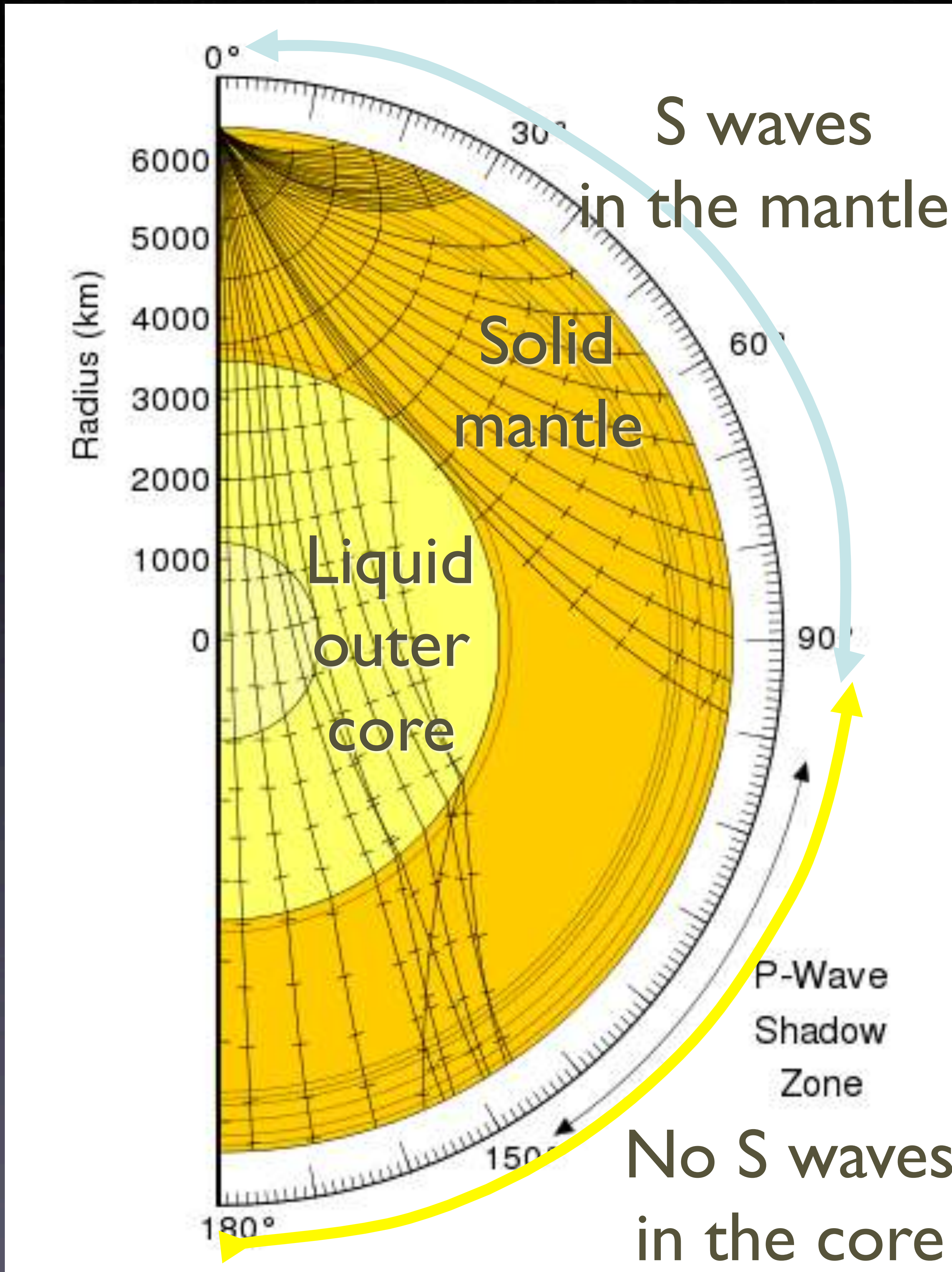

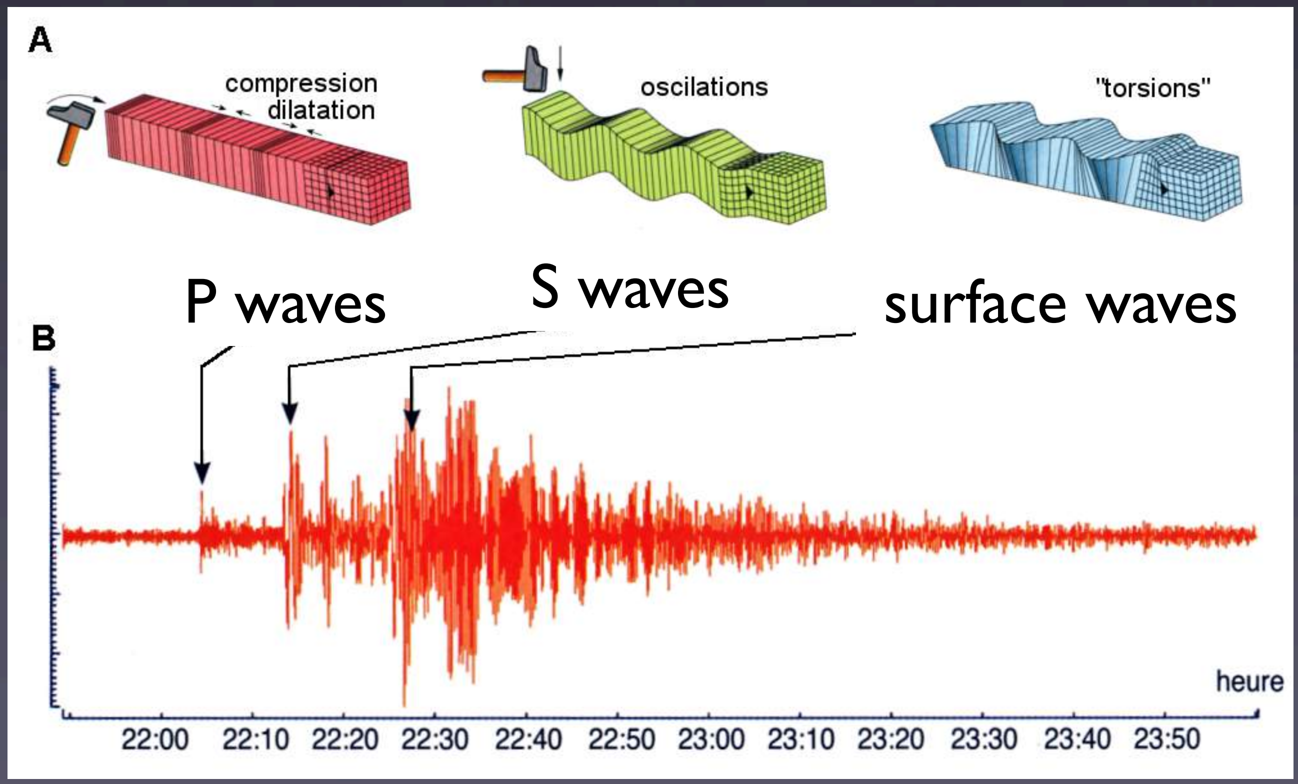

Heat transfer in the mantle: convection

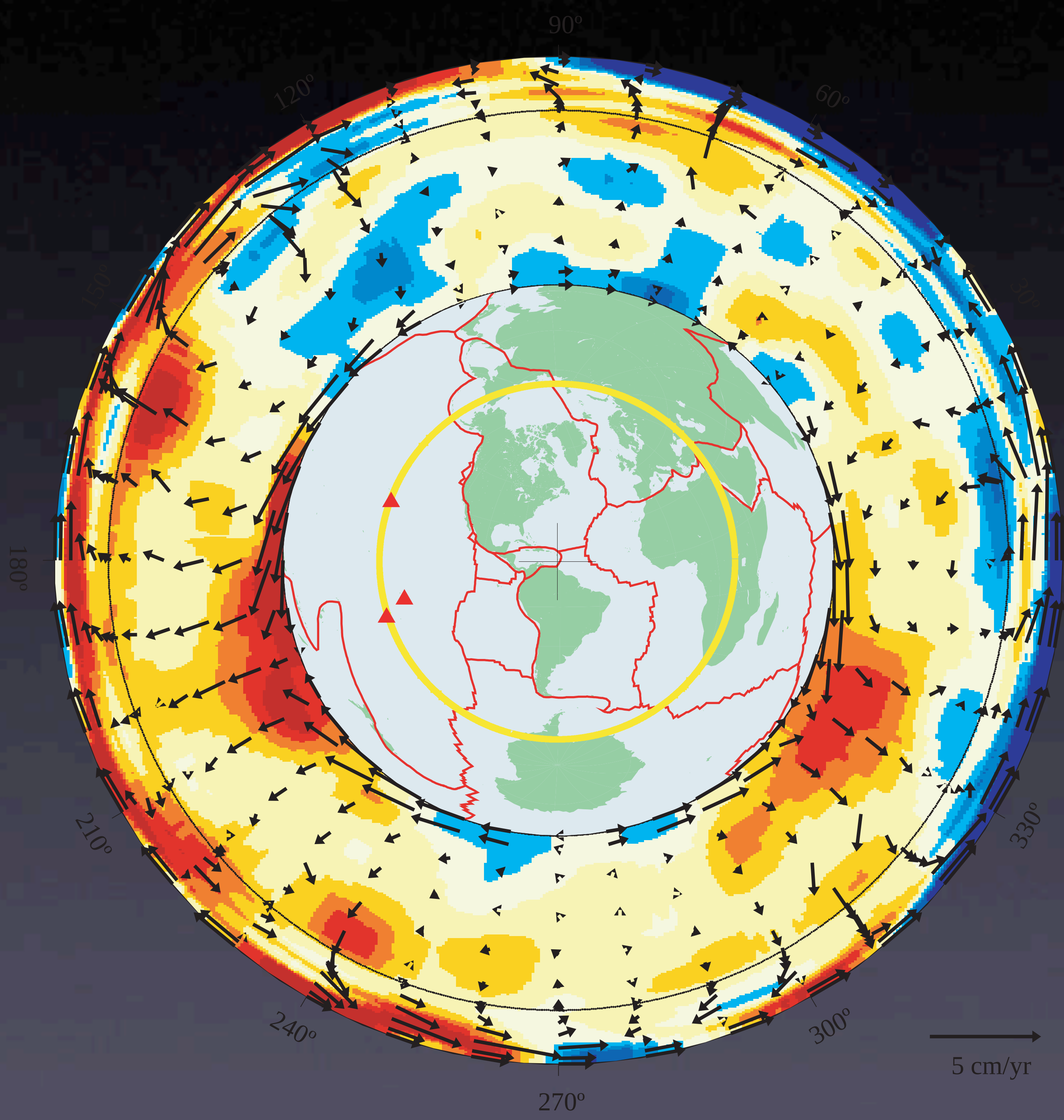

Forte

Rayleigh number = convection/diffusion =

$\rho\, g\, \alpha\, \Delta T\, h^3 / \kappa\, \mu$

>> 10^3 (Ra critique)

Surface expression of convection: plate tectonics

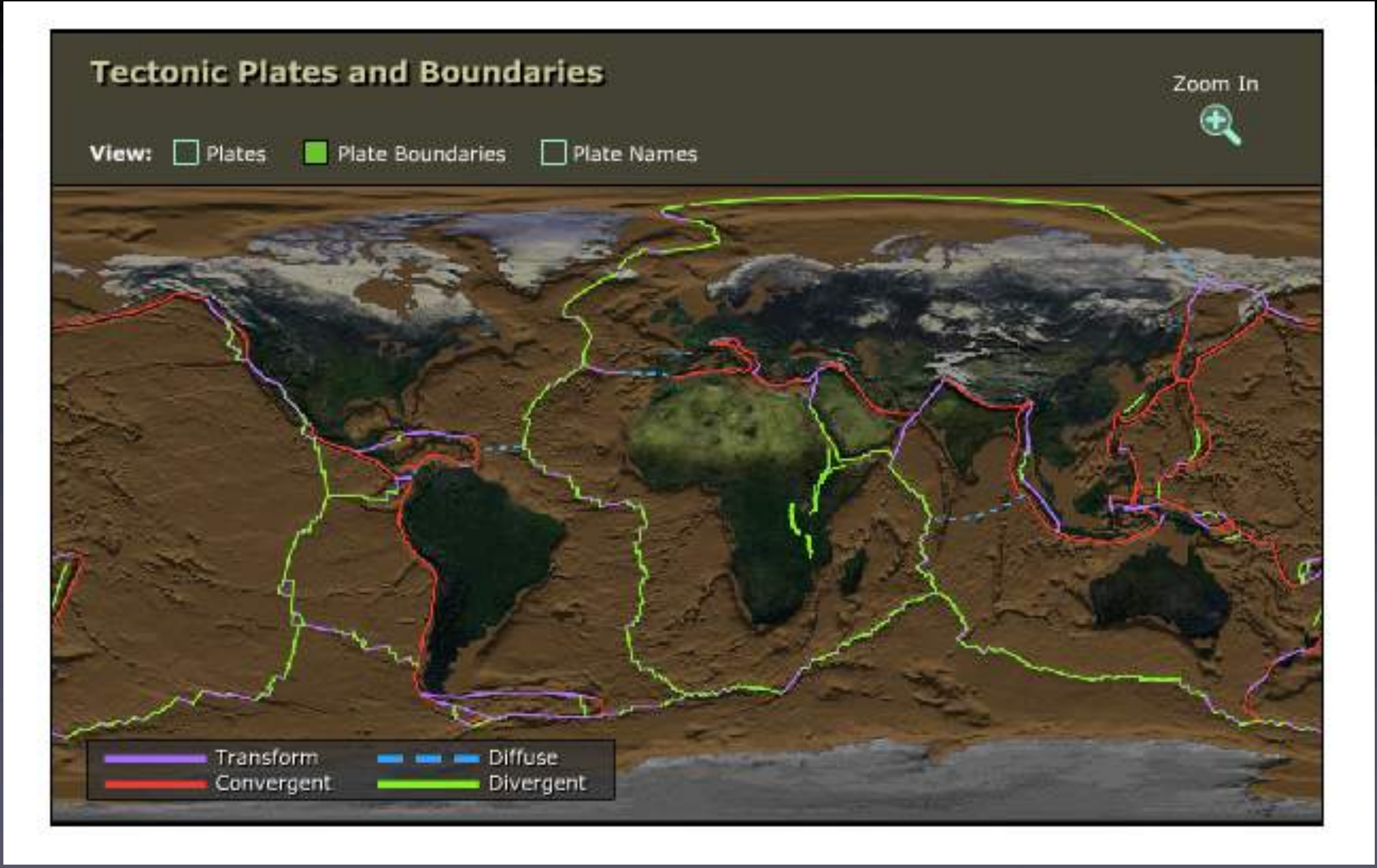

Plate tectonics in the last 260 Ma

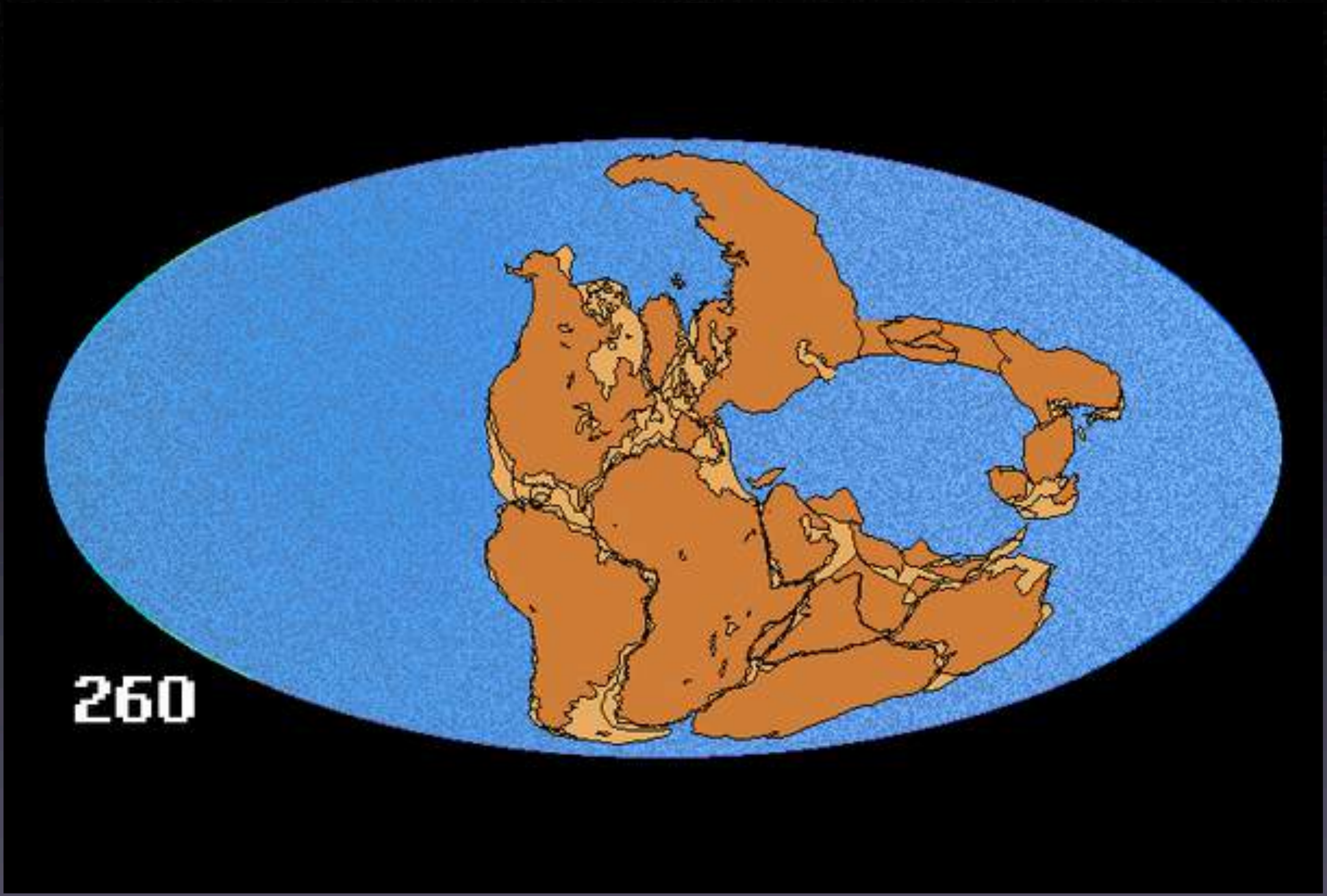

Besse

Magma are mainly produced at plate boundaries

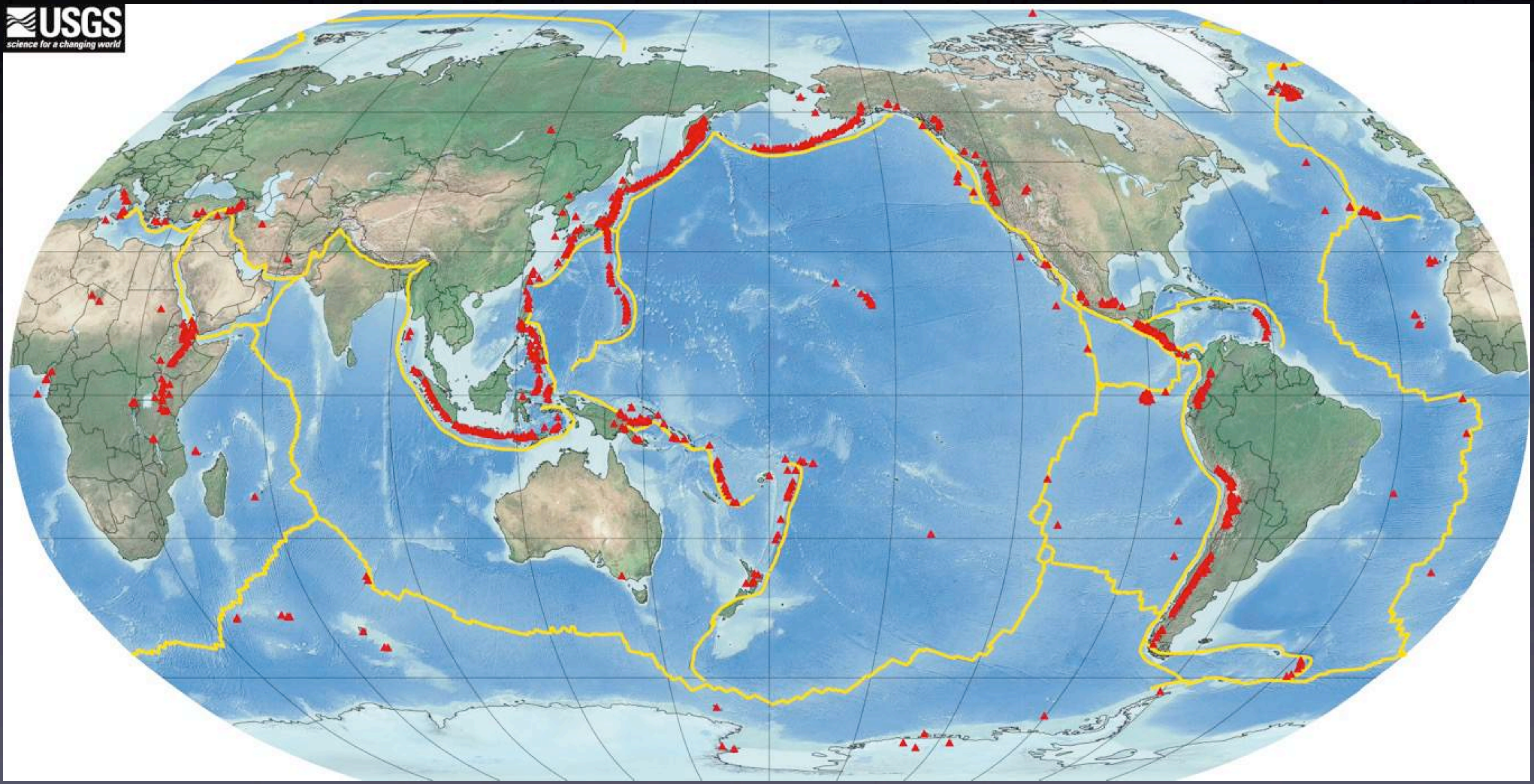

Explosive eruptions: subduction zones

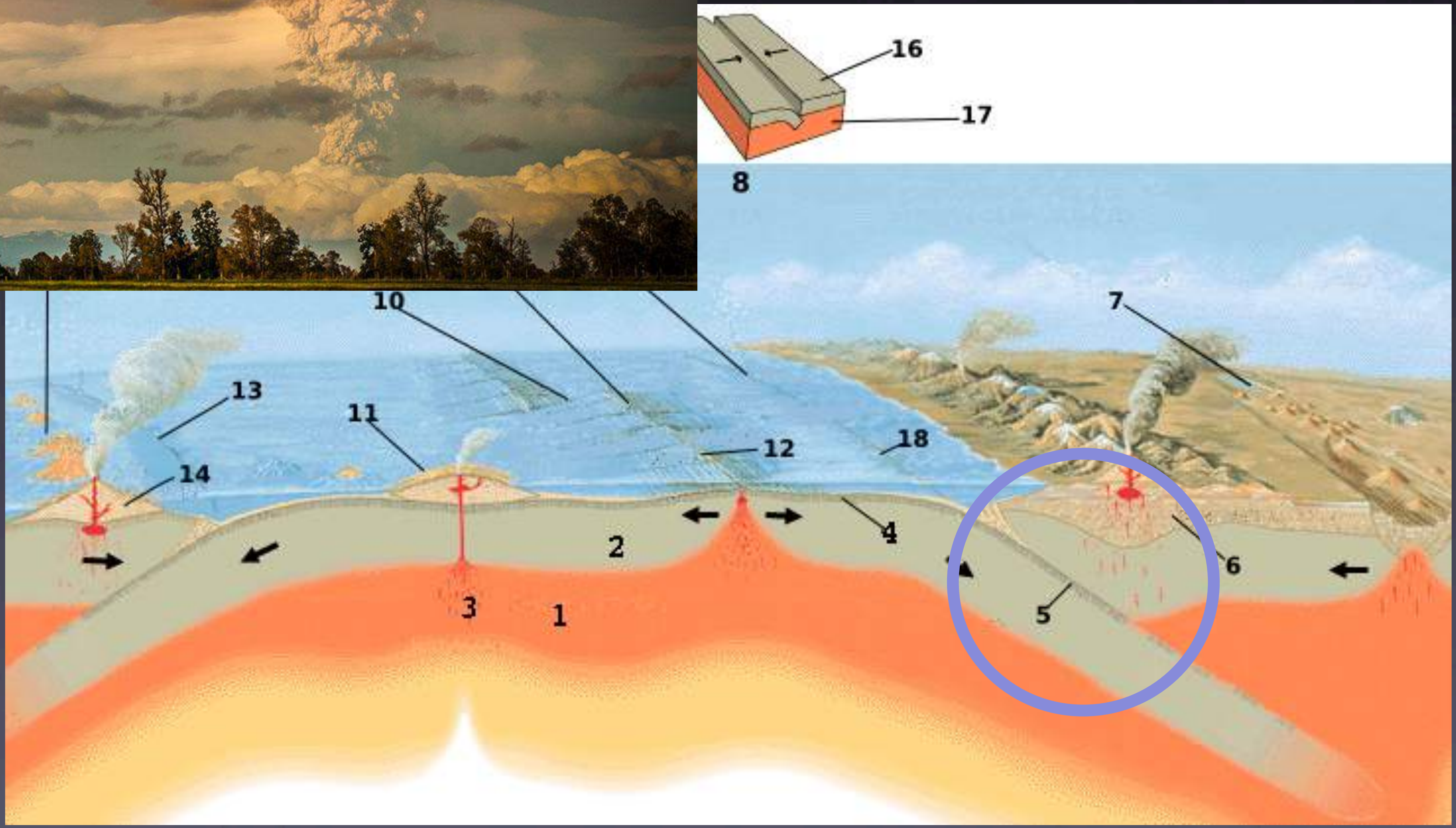

Dome forming eruptions: subduction zones

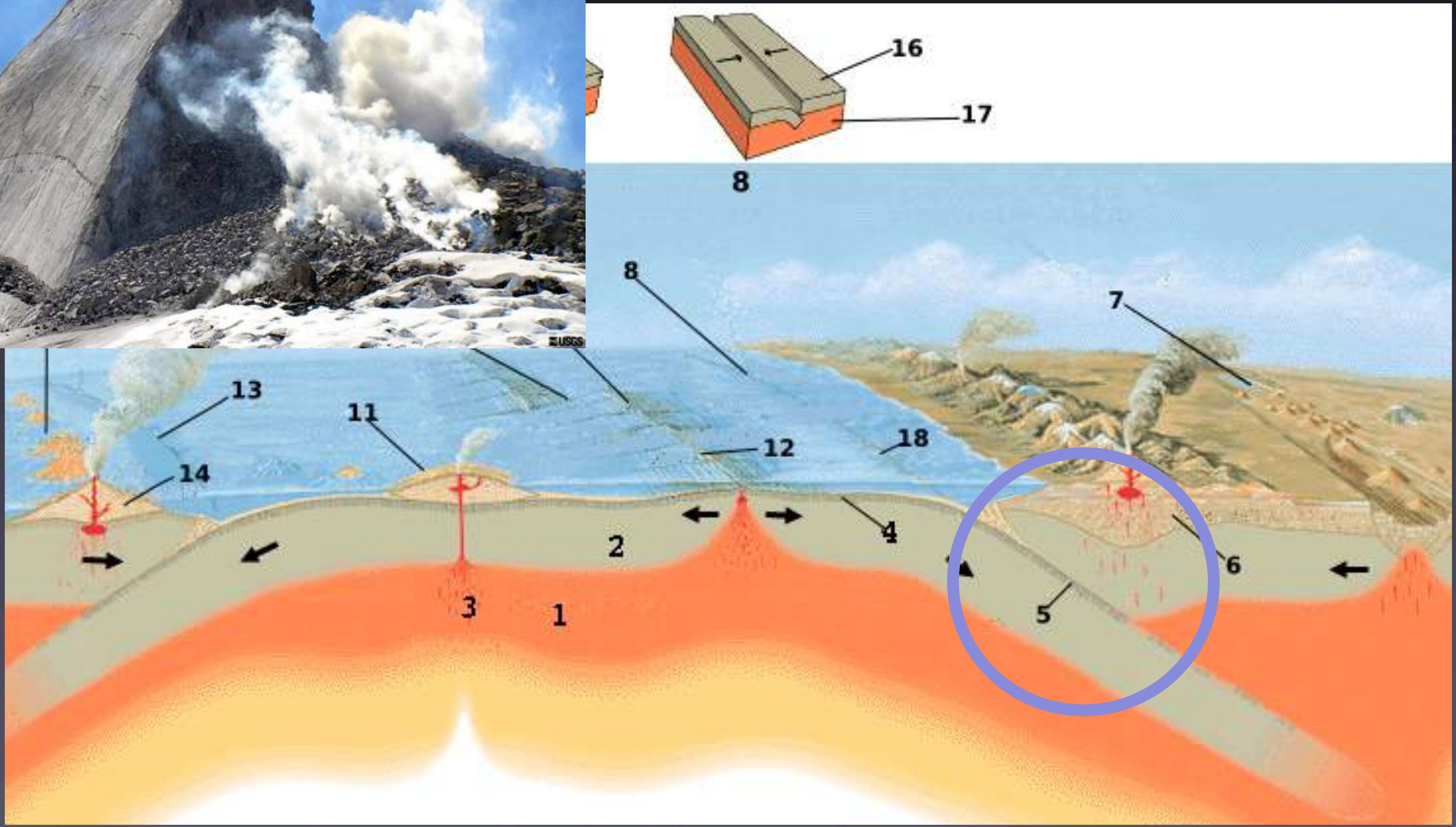

Lava flows: oceanic ridges

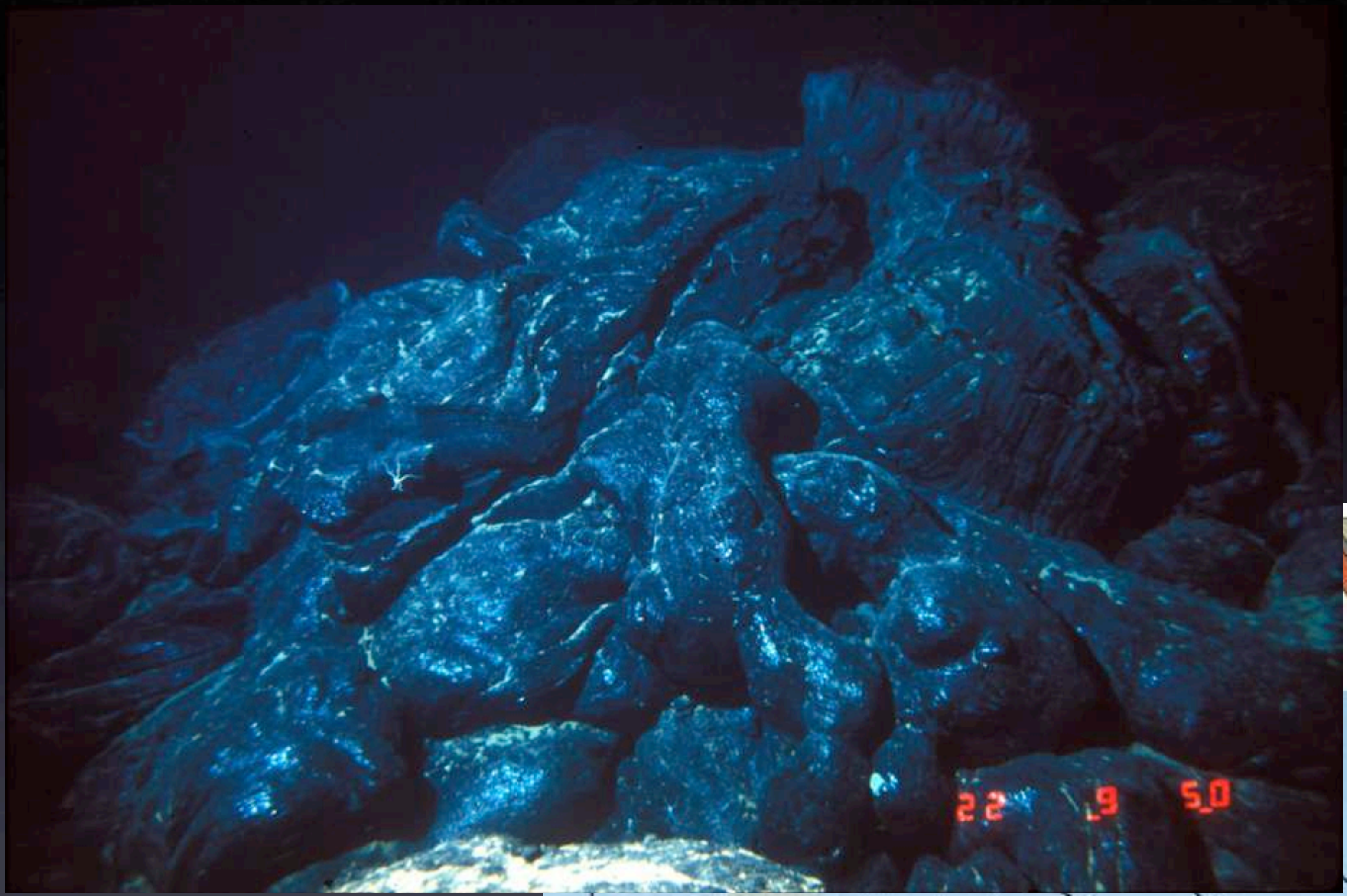

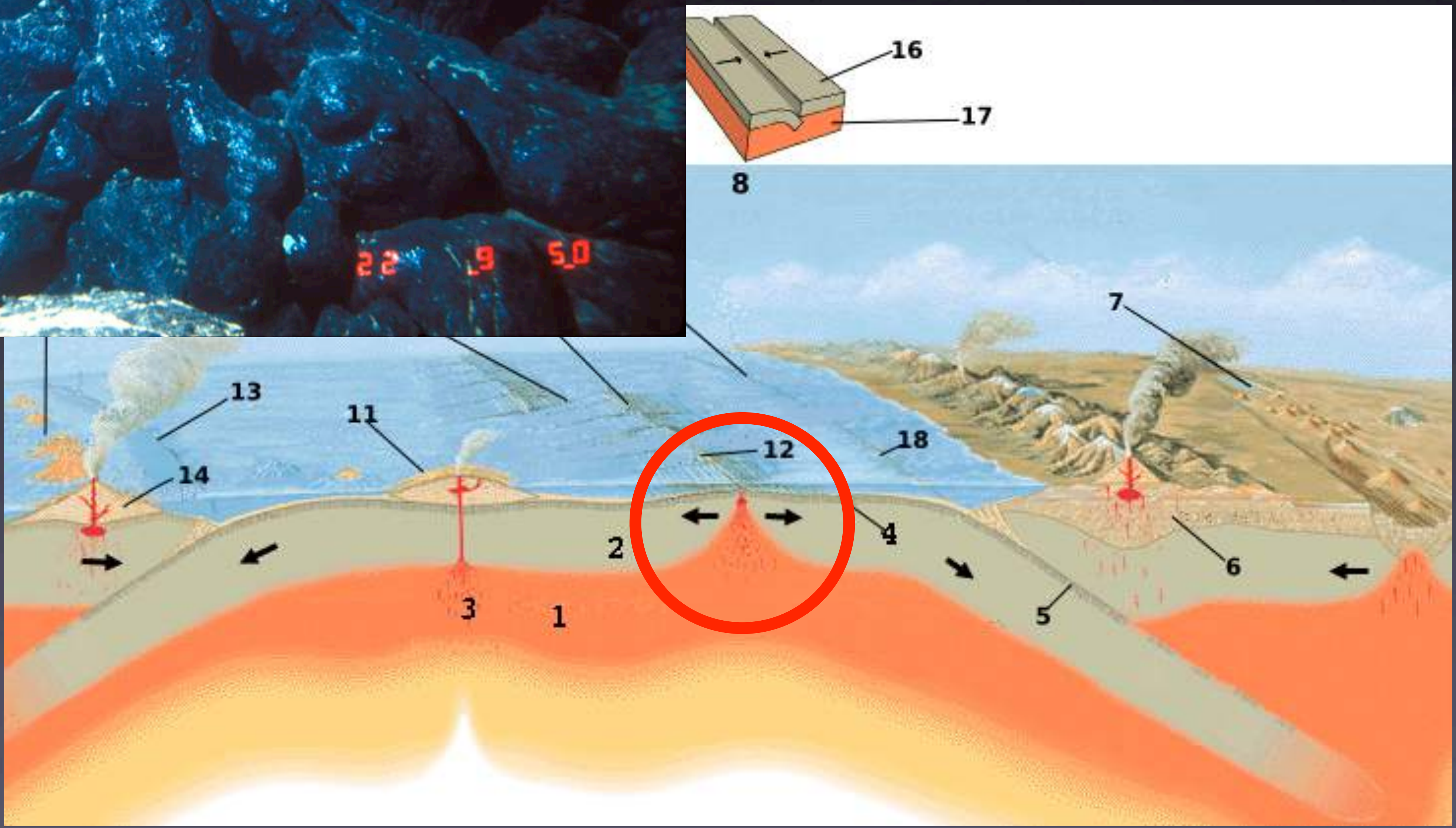

Lava flows: hot spots

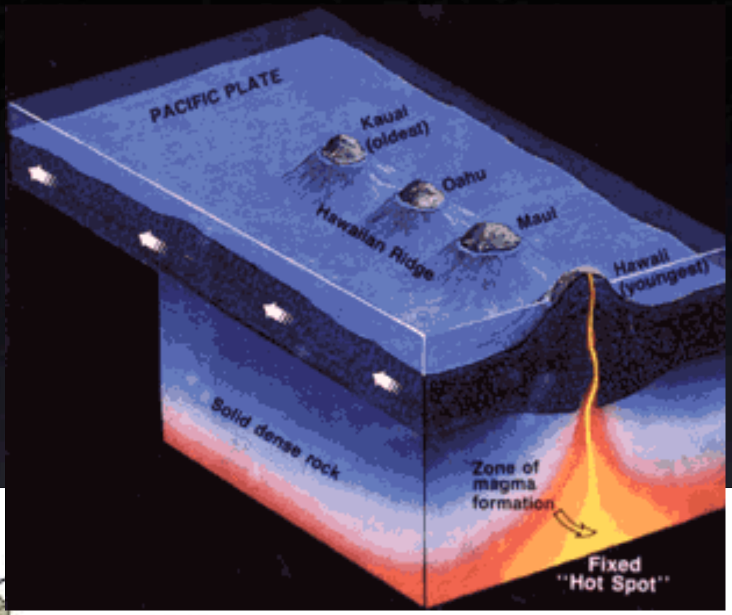

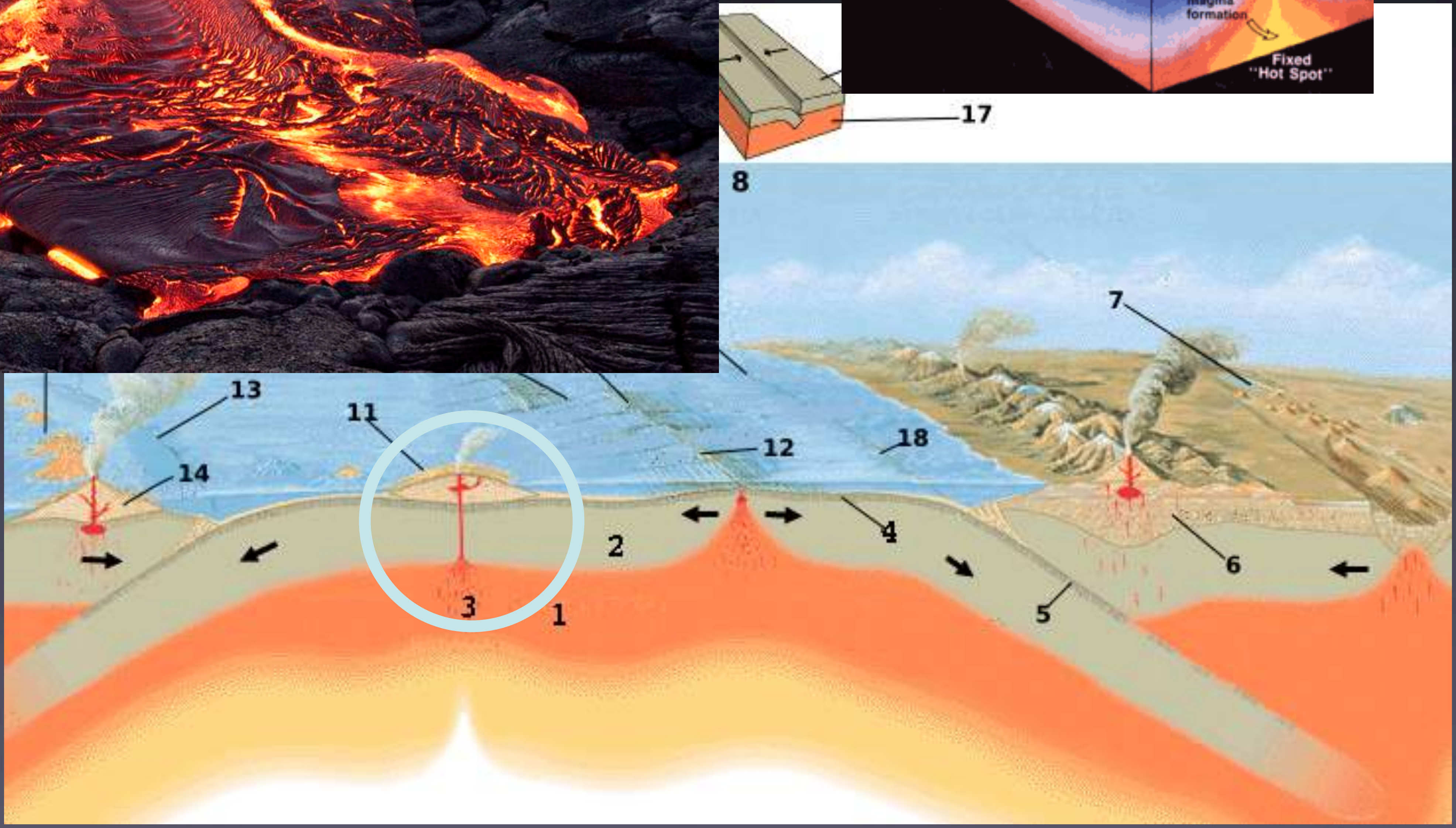

Production of magma in the Earth mantle

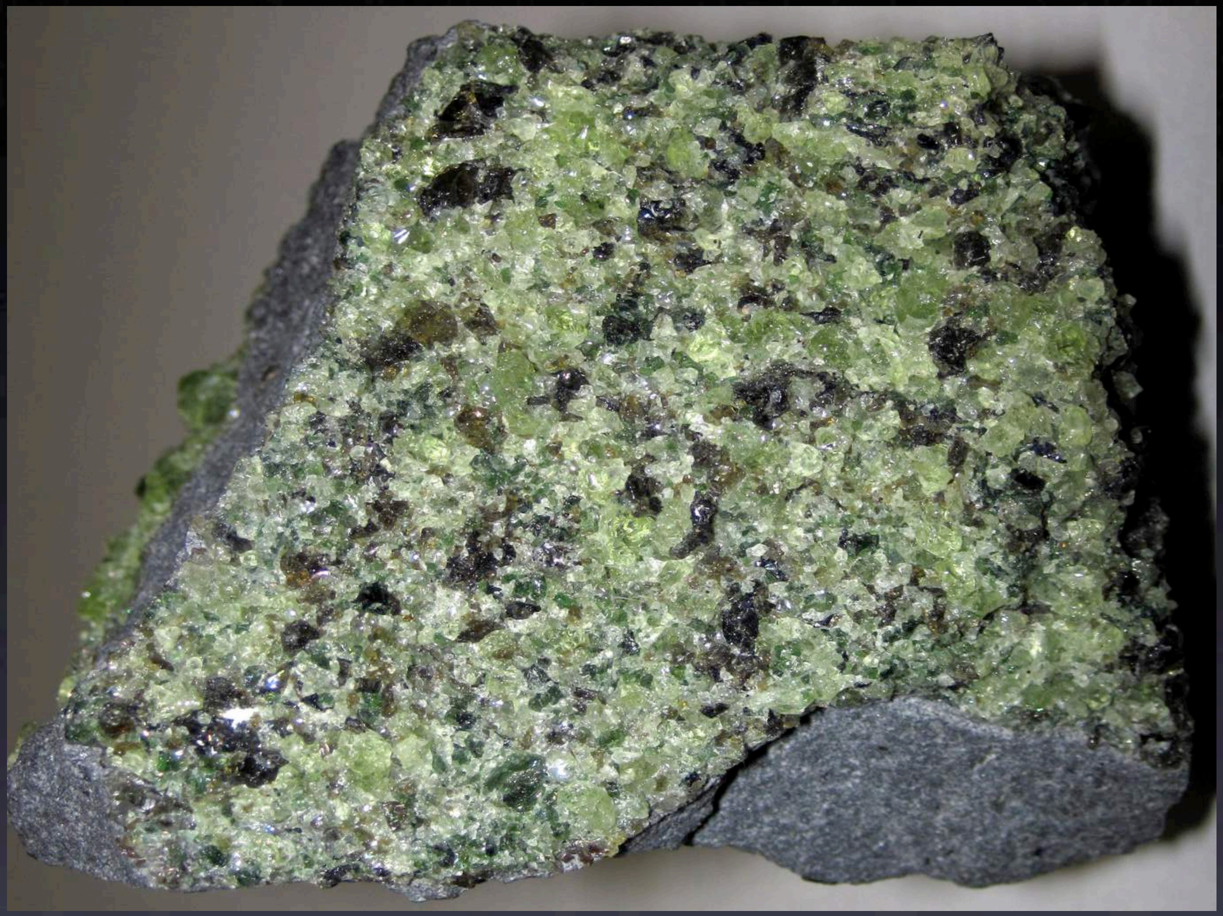

Partial melting: experiments

TABLE 1. Phases, and Their Components, That Are Most Probably Present in the Upper Mantle

Olivine	Clinopyroxene	Orthopyroxene	Spinel	Garnet
Mg_2SiO_4	$CaSiO_3$	$MgSiO_3$	$MgAl_2O_4$	$Mg_3Al_2Si_3O_{12}$
Fe_2SiO_4	$MgSiO_3$	$FeSiO_3$	$FeCr_2O_4$	$Fe_3Al_2Si_3O_{12}$
	$FeSiO_3$	$MgAl_2SiO_6$		$Ca_3Al_2Si_3O_{12}$
	$NaFeSi_2O_6$			
	$NaAlSi_2O_6$			
	$CaTiAl_2O_6$			
	$CaAl_2SiO_6$			

Mantle = peridotite = Fo + Opx + Cpx + Gar



Partial melting: experiments

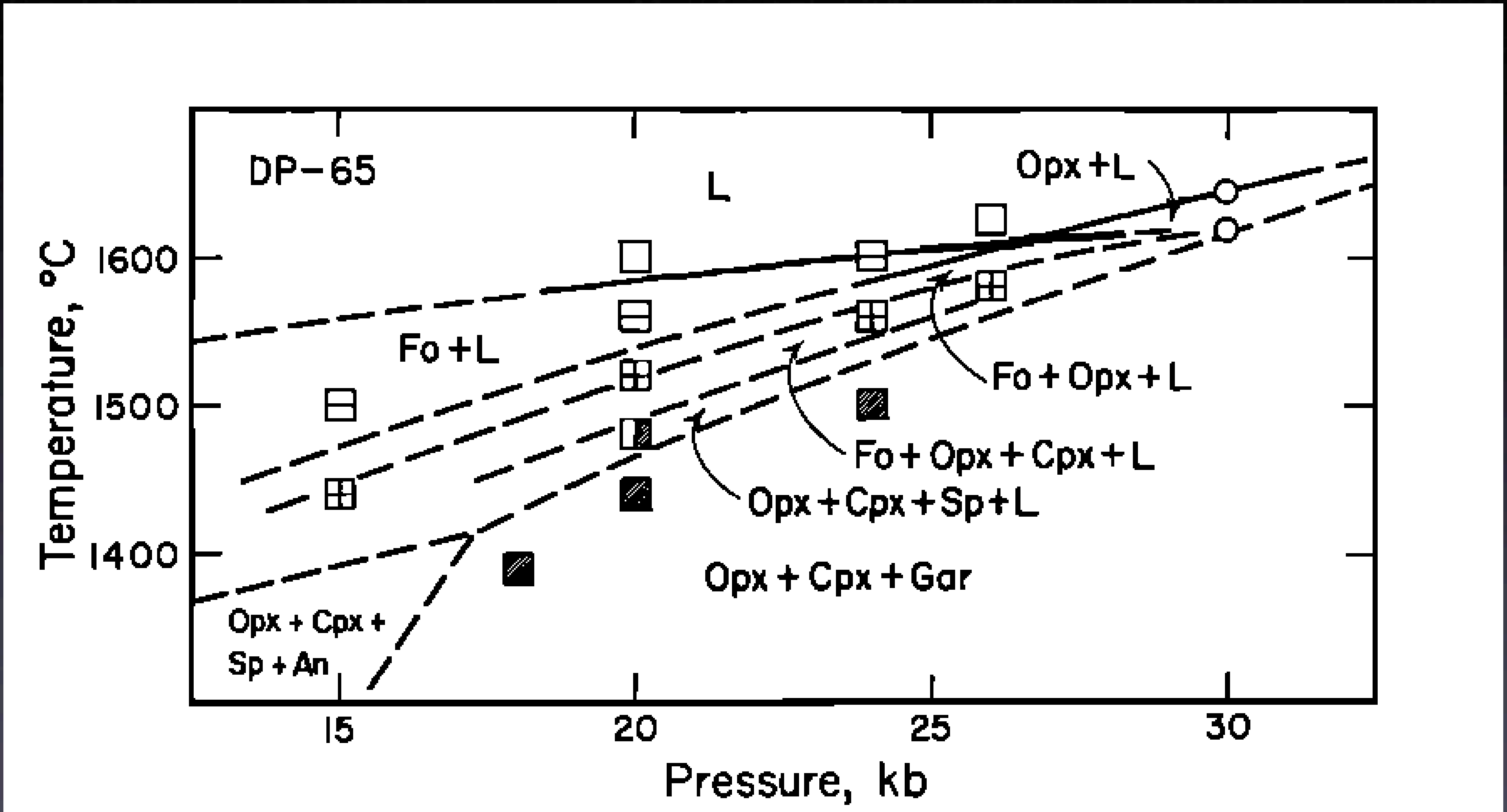

Kushiro

Partial melting: geotherm and solidus

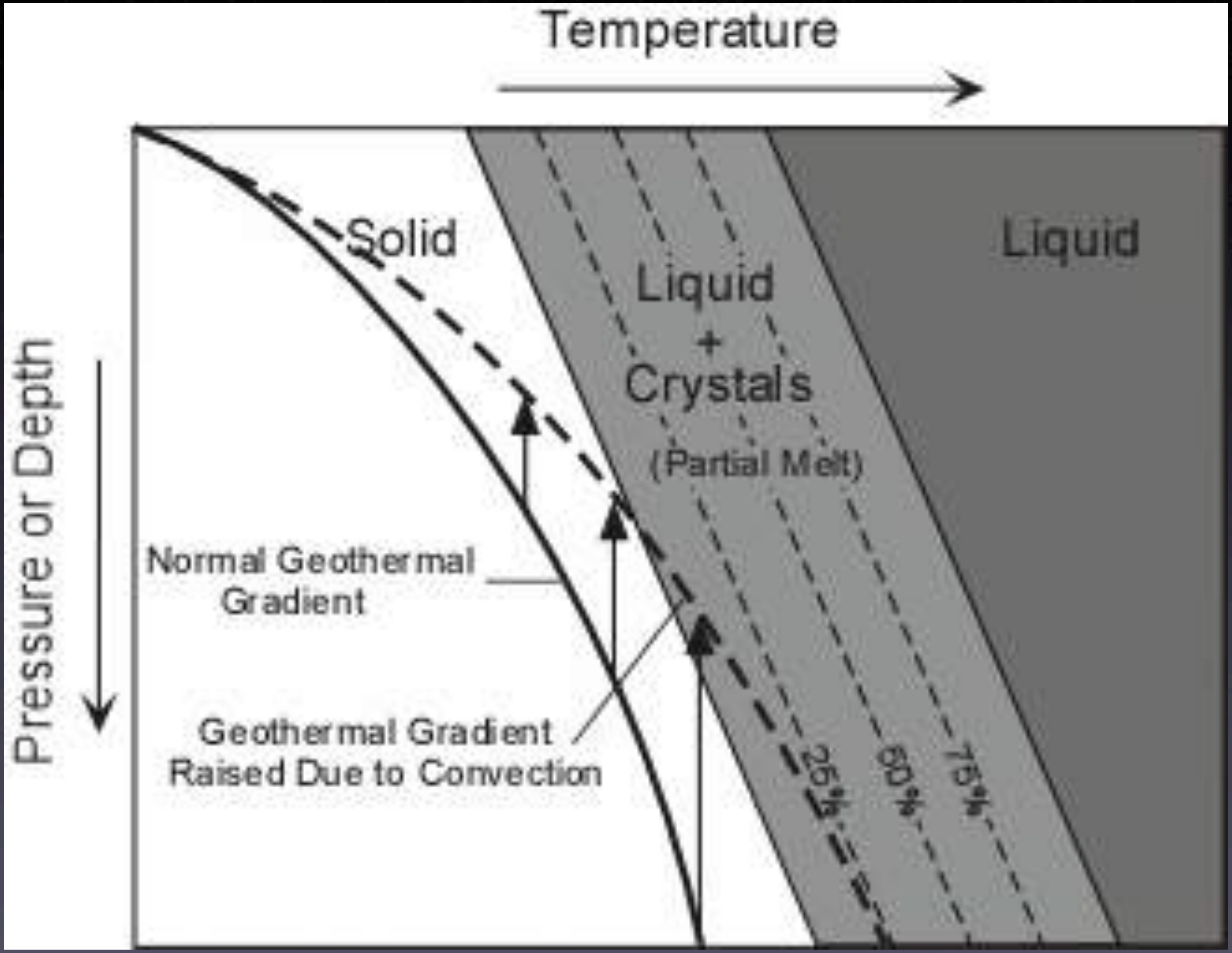

Melting by decompression

Partial melting: geotherm and solidus

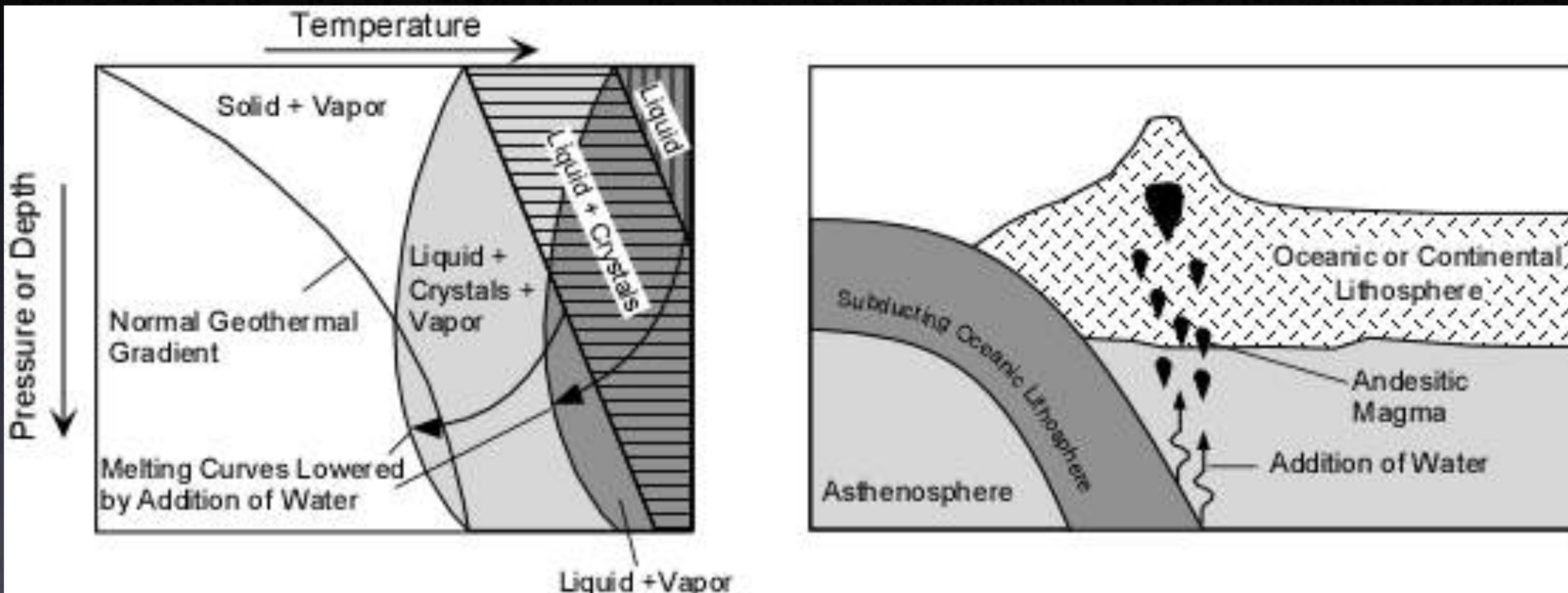

Melting due to addition of water

Partial melting: e.g. under a ridge

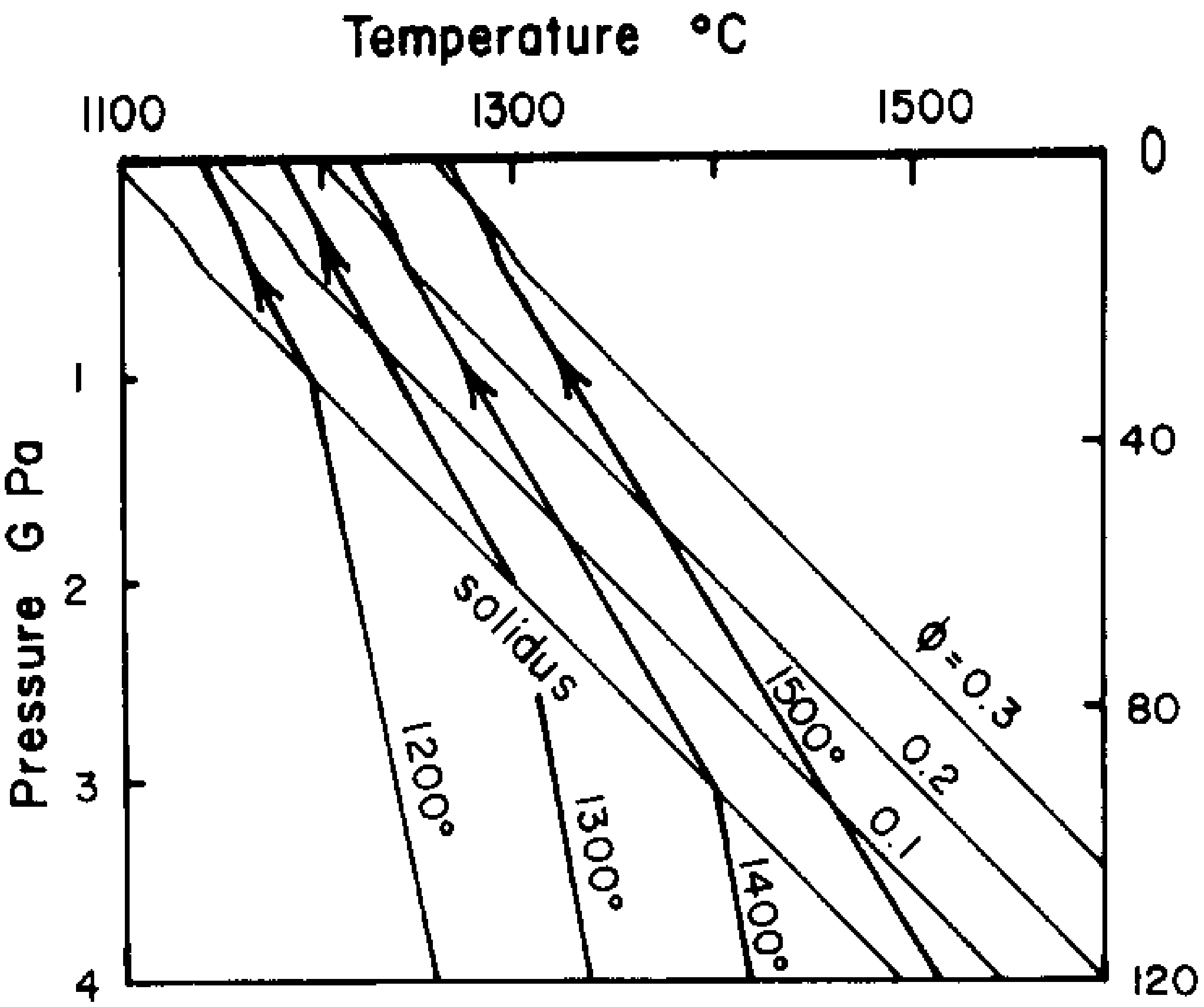

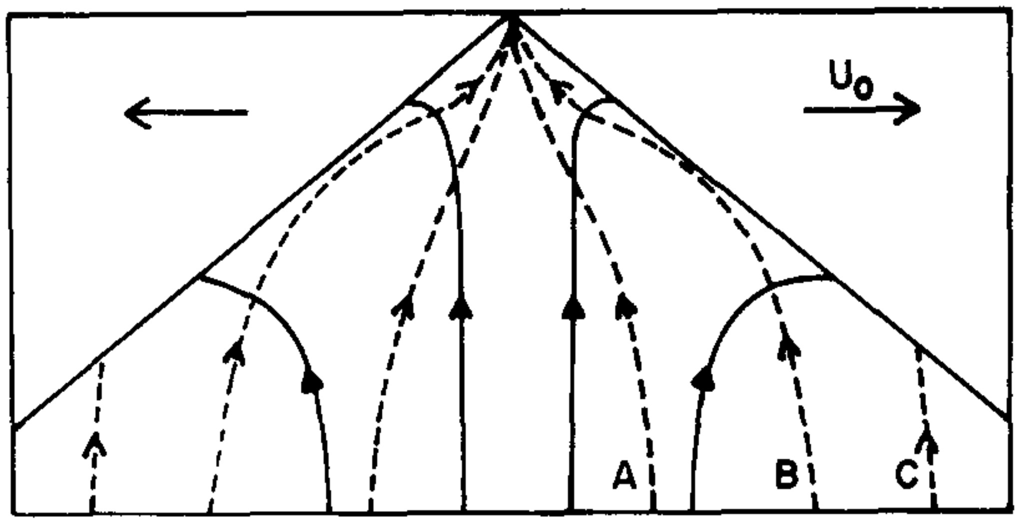

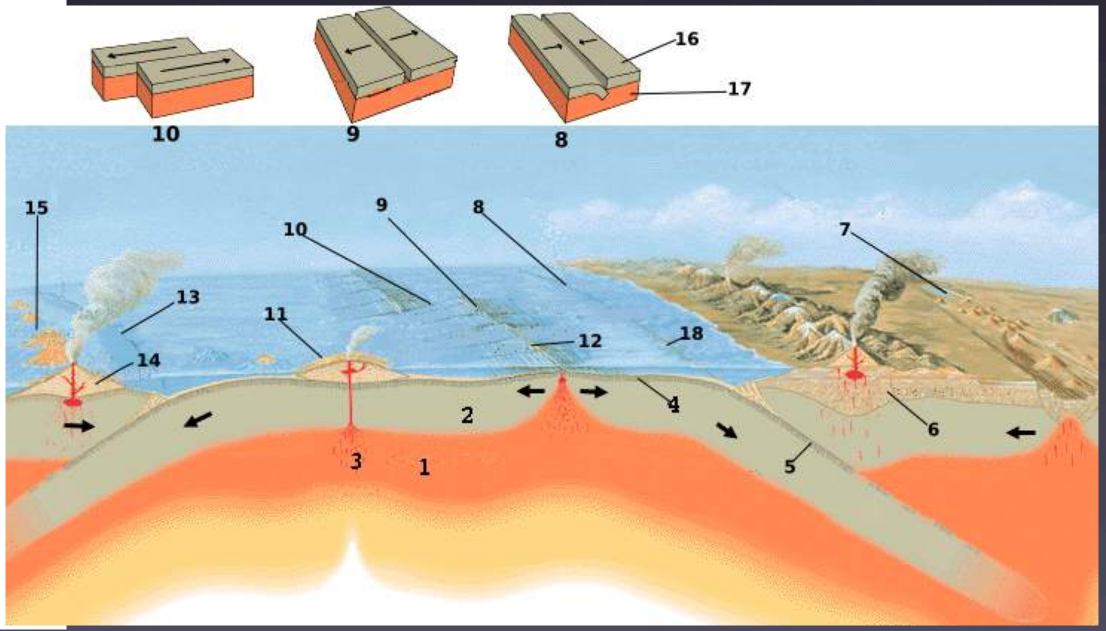

Mc Kenzie

Melt circulation = compaction

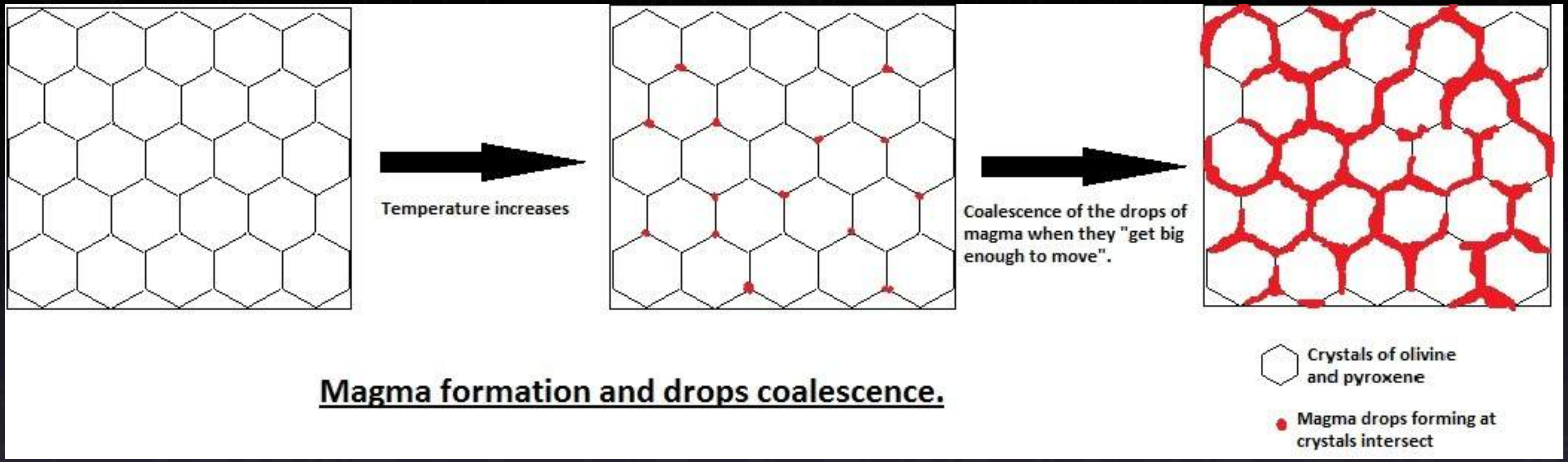

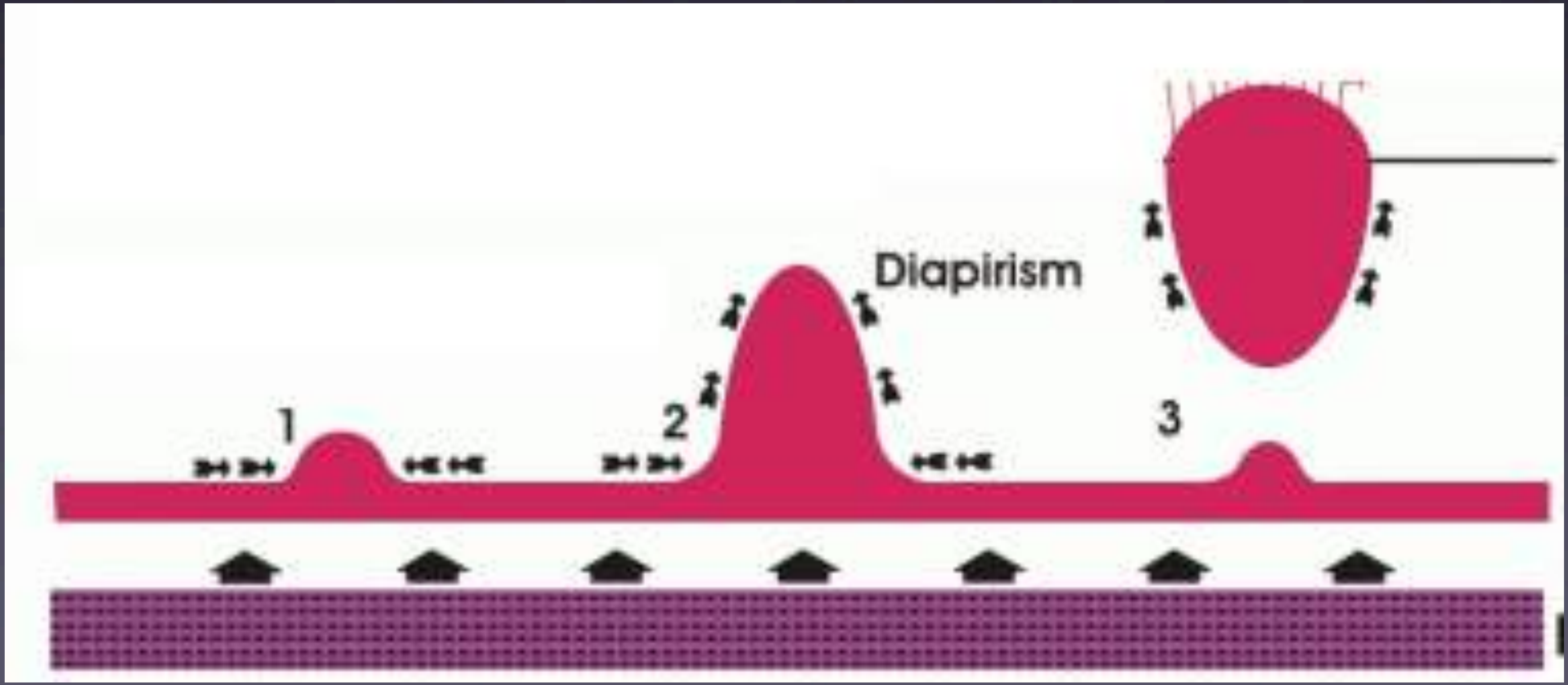

Theory of compaction in viscous mantle

$$0 = -(1-\phi) g \Delta\rho + \frac{\eta_f \phi}{k_\phi}(w - W) + \left(\zeta_s + \frac{4}{3}\eta_s\right)\frac{d^2 W}{dz^2}$$

balance of 3 forces :

relative melt buoyancy

melt viscous resistance to flow

viscous resistance of matrix to deformation

Scaling analysis

$$\phi' = \phi/\phi_0$$

$$z' = z\bigg/\left[\frac{k_0(\zeta_s + 4\eta_s/3)}{\eta_f}\right]^{1/2} \equiv z/\delta_c$$

$$k_0 = Ca^2\phi_0^n$$

Scaling analysis

$$\frac{d^2\phi}{dz^2} + \frac{1-\phi}{\phi^n} = R$$

$$R = \frac{k_0 g \Delta\rho}{\phi_0 U_0 \eta_{\mathrm{f}}}$$

Model prediction

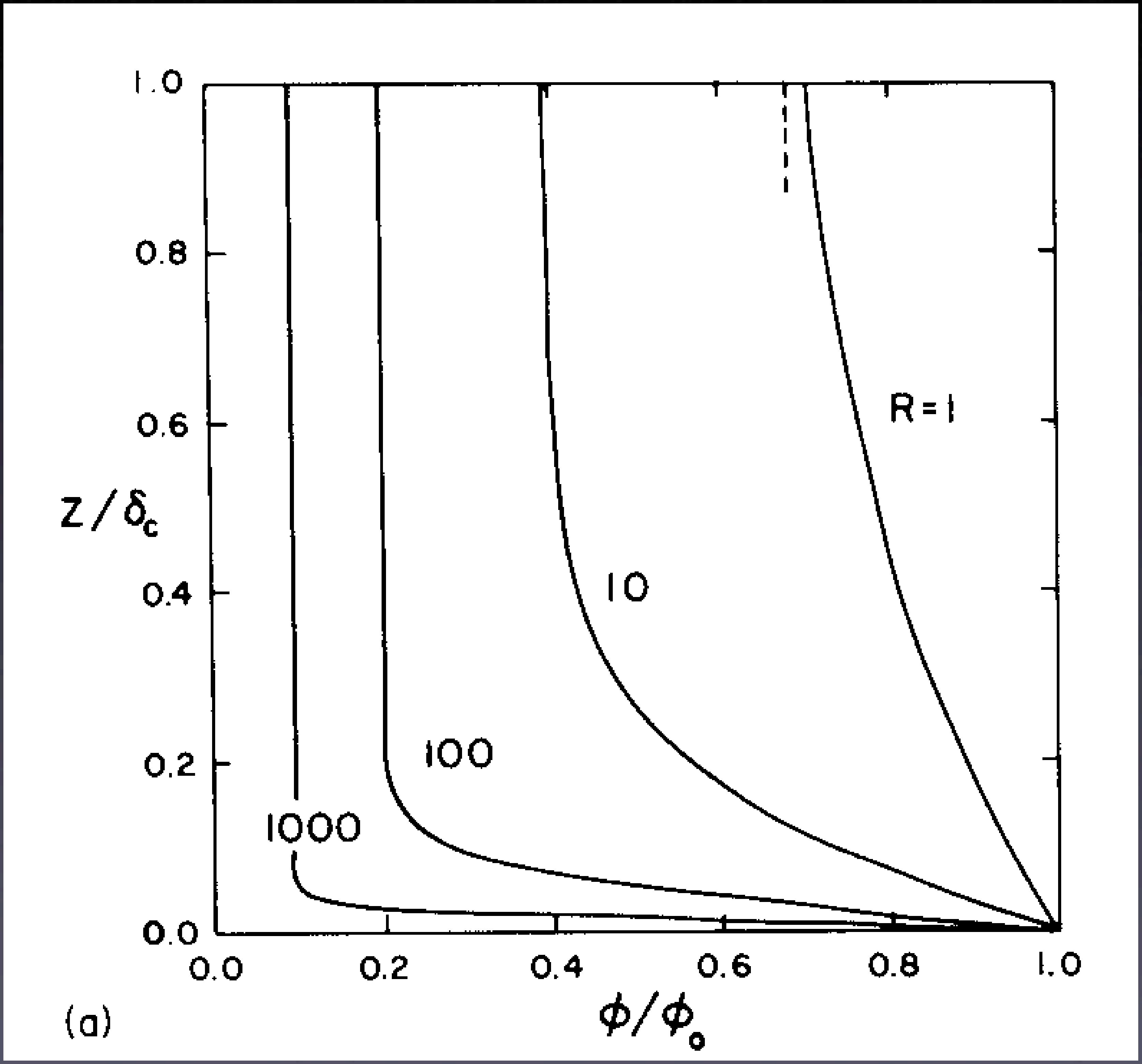

Ribe

Model prediction

$$\delta_R = R^{-1/2}\delta_c = \left[\frac{\phi_0 U_0(\zeta_s + 4\eta_s/3)}{g\Delta\rho}\right]^{1/2}$$

Compaction occurs over a length ≈ 0.1/1 km

then melt flows according to Darcy’s law

$$\boldsymbol{u}-\boldsymbol{U}=\frac{k_\phi g \Delta\rho}{\eta_f \phi}$$

Model refinement: chemistry

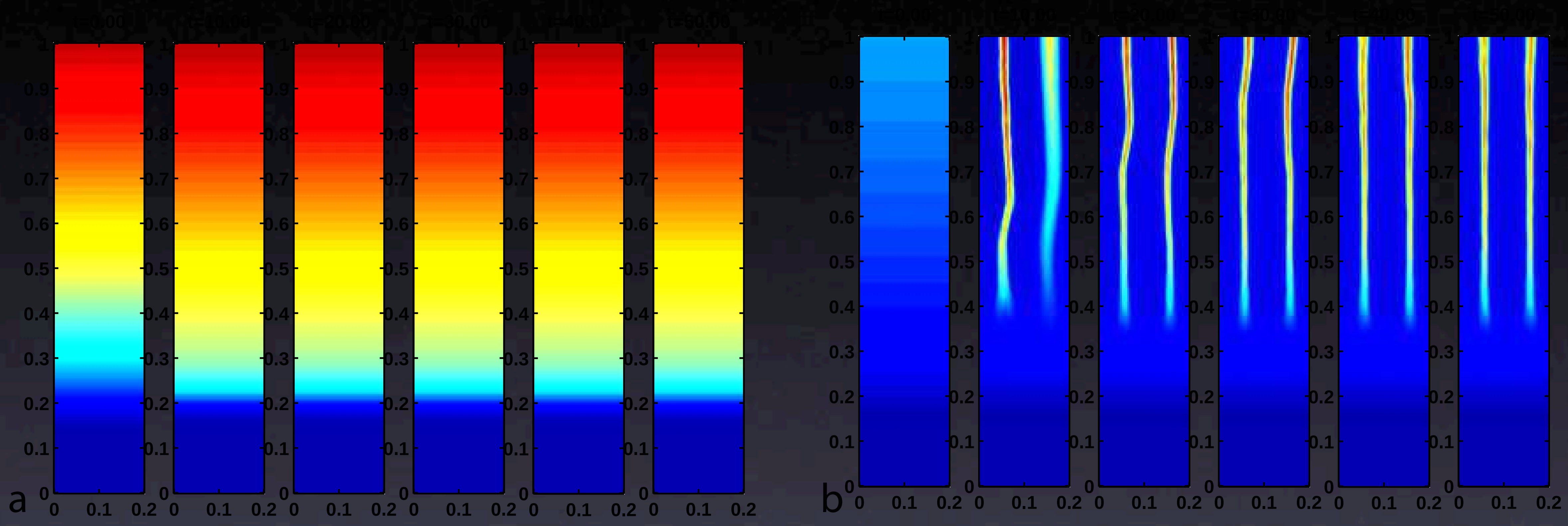

Spiegelman & Kelemen

Chemical reaction (dissolution of cpx) focuses the melt in x10m channels

Melt propagation in the rigid lithosphere

$$0 = -(1-\phi)g\,\Delta\rho + \frac{\eta_f\,\phi}{k_\phi}(w - W) + \cancel{\left(\zeta_s + \frac{4}{3}\eta_s\right)\frac{d^2 W}{dz^2}}$$

non viscous deformation of matrix

balance of 3 forces :

relative melt buoyancy (ρ decreases upward)

(non viscous) resistance of rocks
to deformation

melt viscous resistance to flow

Cooling and crystallization in magmatic reservoirs

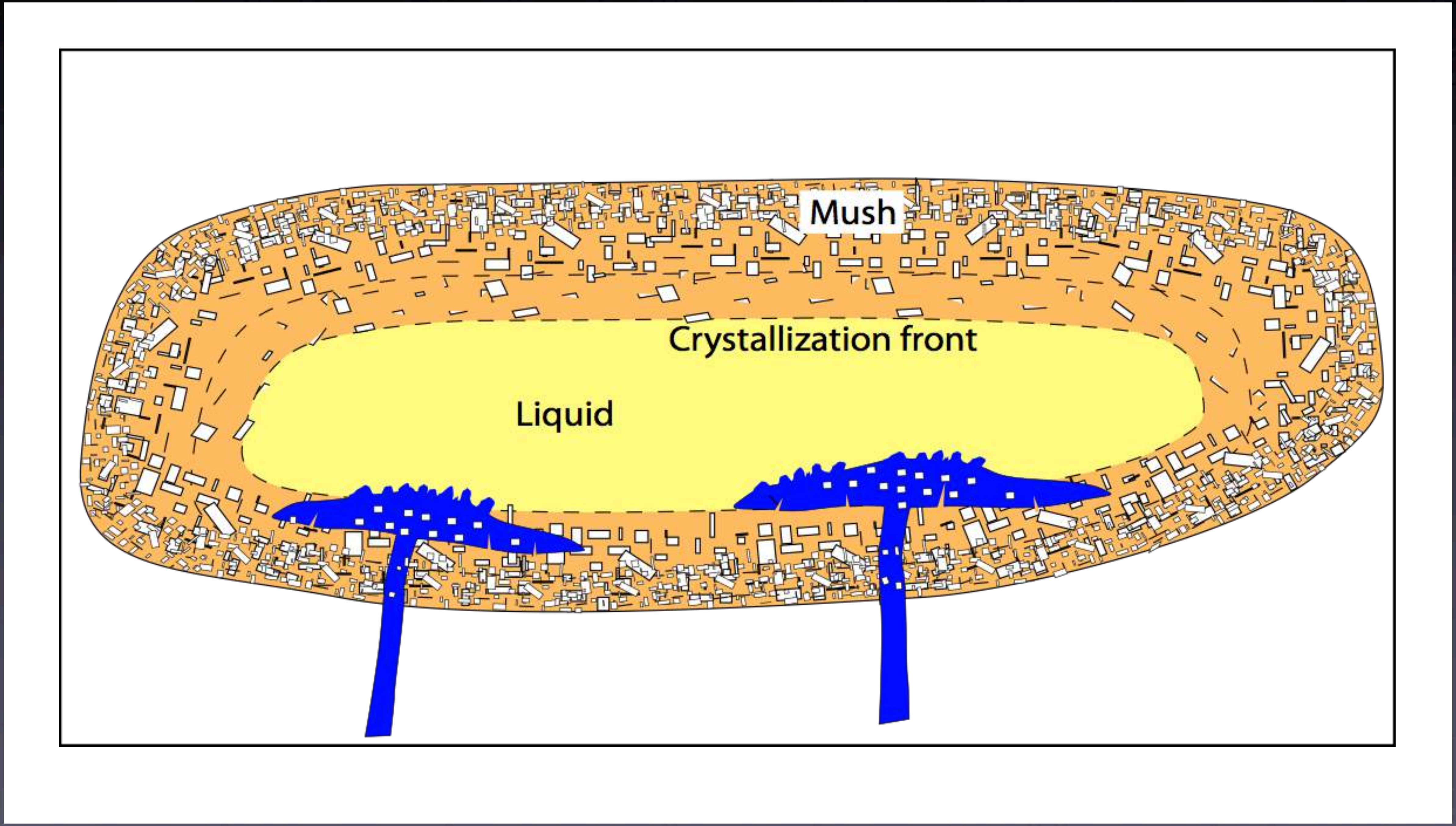

Reminder: Experiments on partial melting

TABLE 1. Phases, and Their Components, That Are Most Probably Present in the Upper Mantle

Olivine	Clinopyroxene	Orthopyroxene	Spinel	Garnet
Mg_2SiO_4	$CaSiO_3$	$MgSiO_3$	$MgAl_2O_4$	$Mg_3Al_2Si_3O_{12}$
Fe_2SiO_4	$MgSiO_3$	$FeSiO_3$	$FeCr_2O_4$	$Fe_3Al_2Si_3O_{12}$
	$FeSiO_3$	$MgAl_2SiO_6$		$Ca_3Al_2Si_3O_{12}$
	$NaFeSi_2O_6$			
	$NaAlSi_2O_6$			
	$CaTiAl_2O_6$			
	$CaAl_2SiO_6$			

plagioclase

Peridotite = Olivine + Pyroxene + Plagioclase

Partial melting: experiments

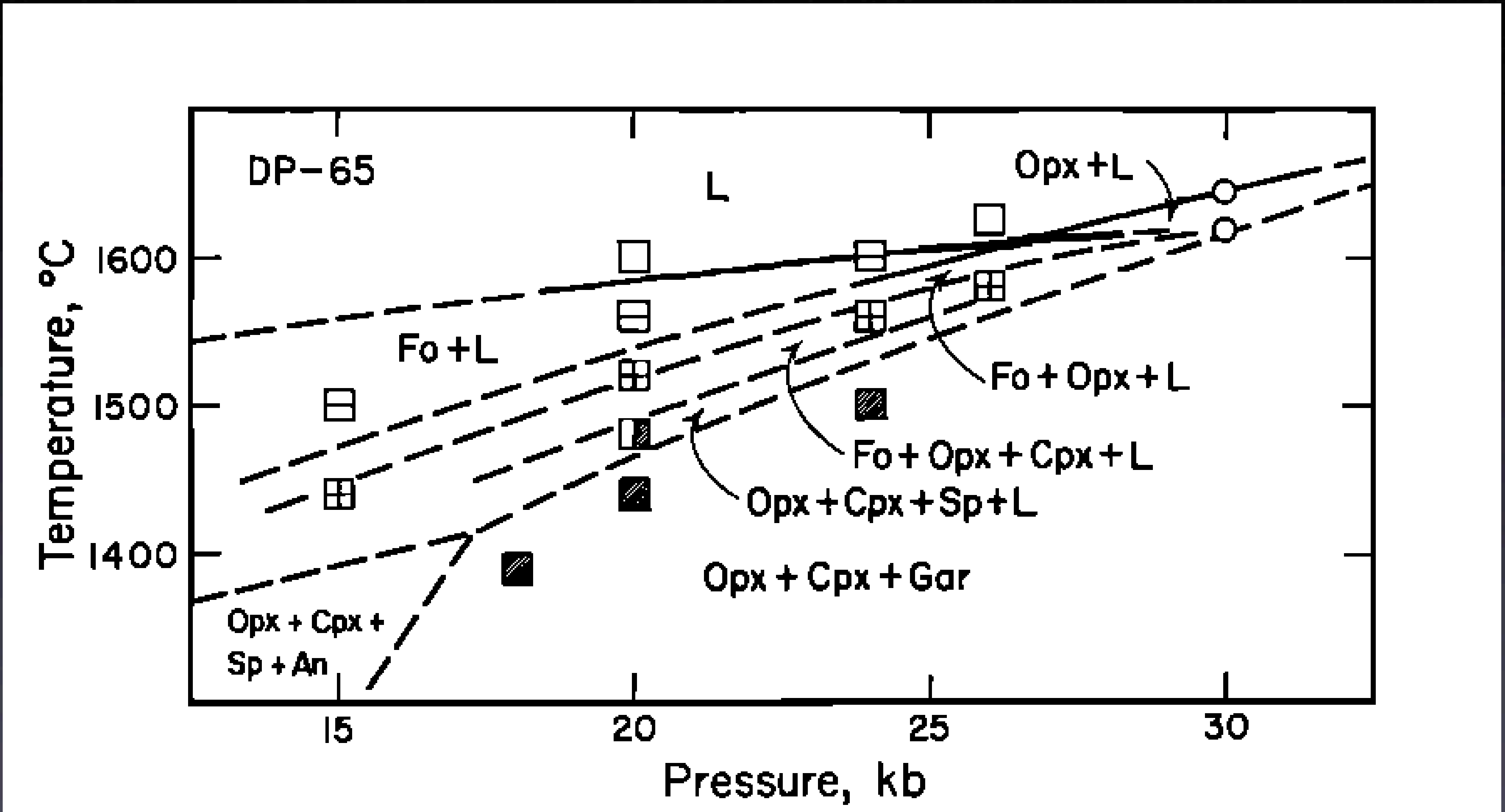

Kushiro

Chemical evolution in magmatic reservoirs

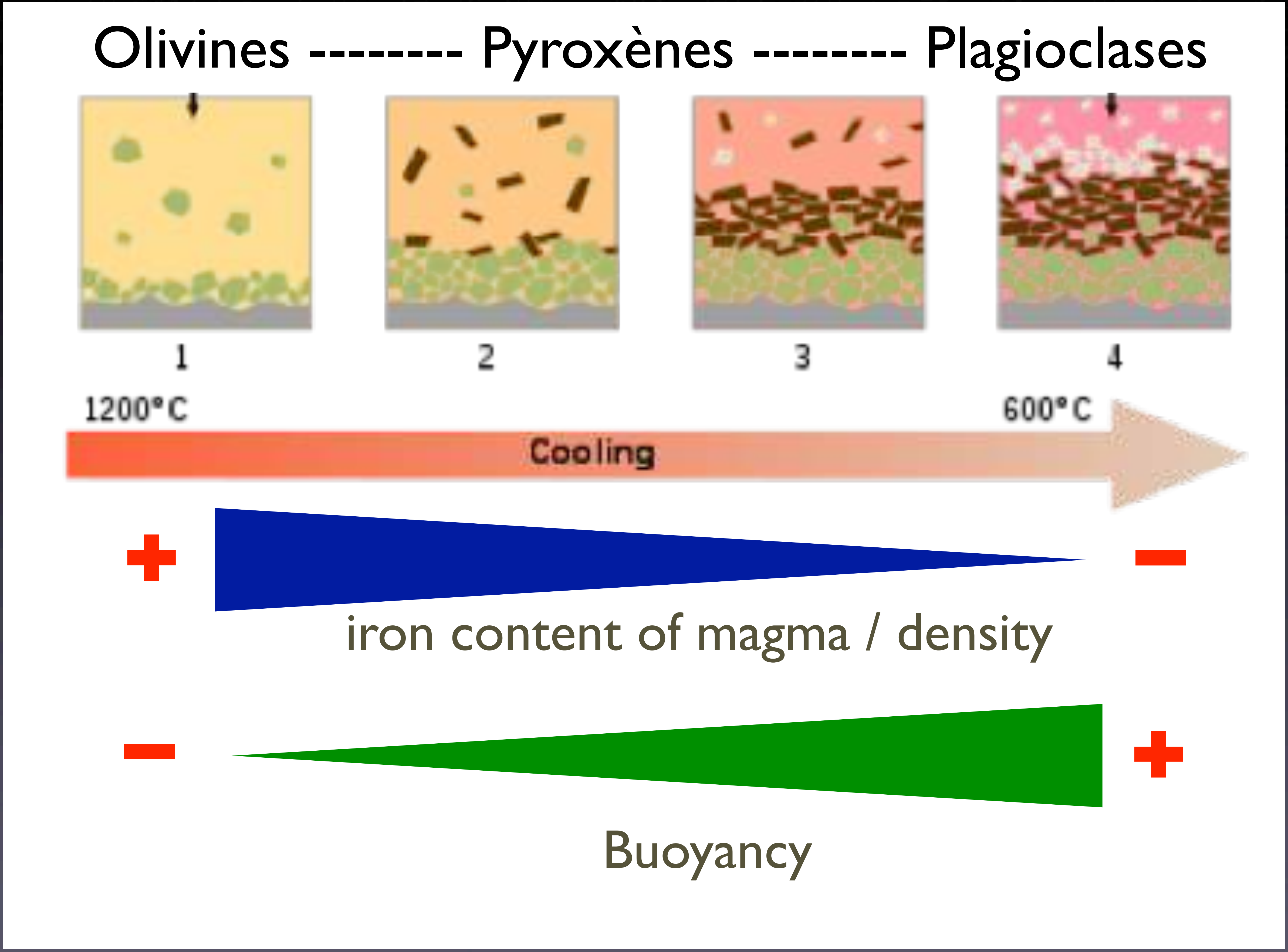

Dike propagation → open conduit

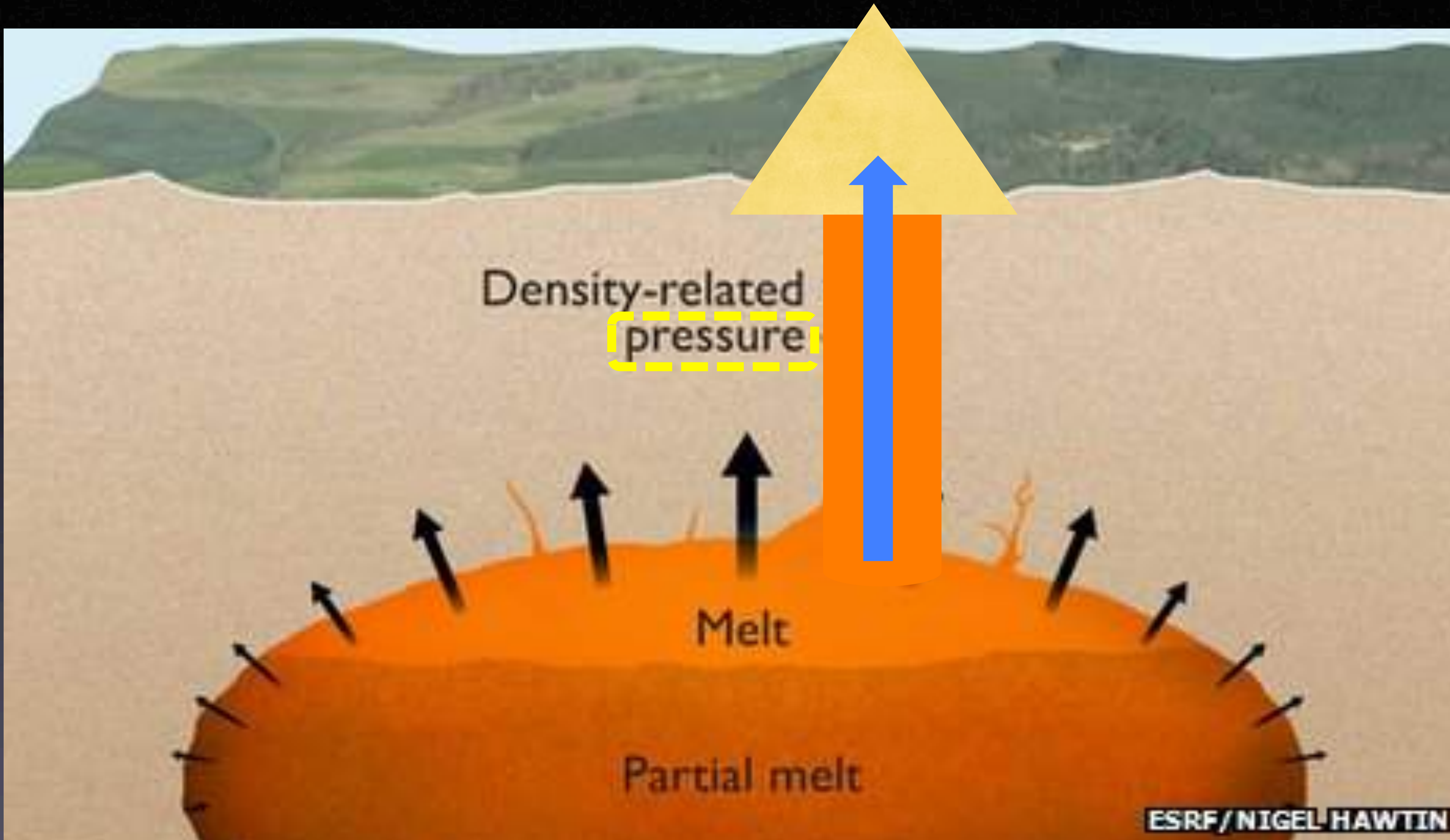

Flow in volcanic conduit and relation with eruption regimes





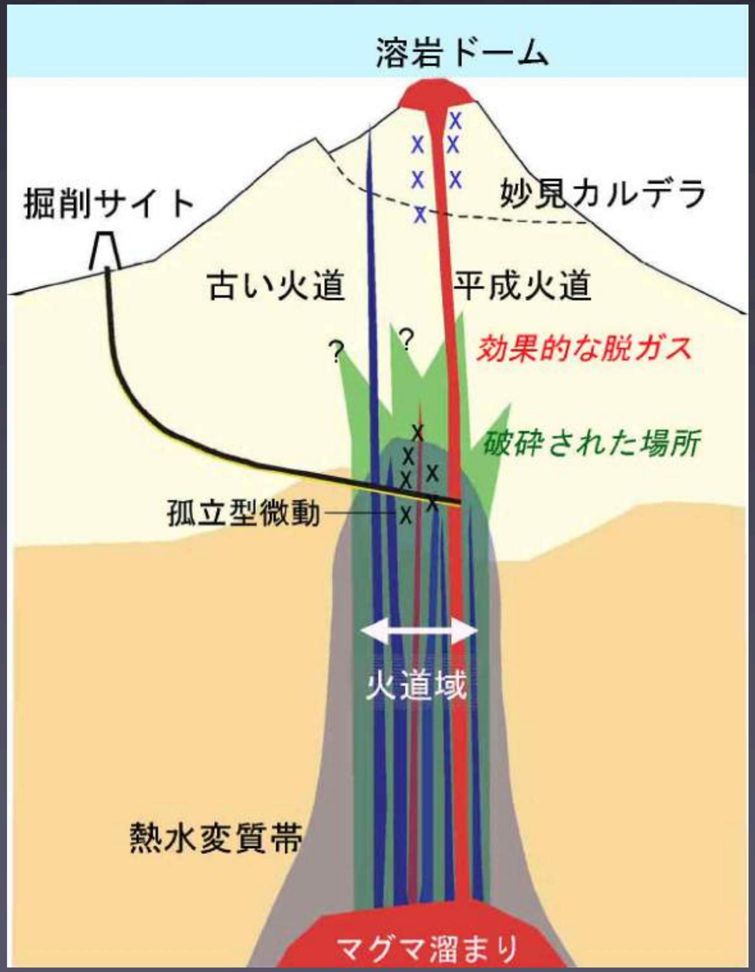



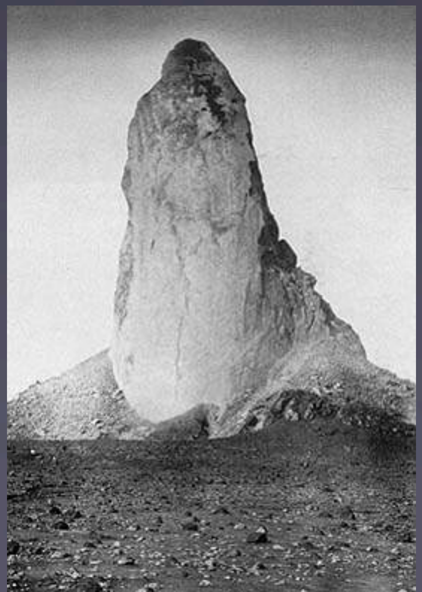

Differential motion between gas and magma

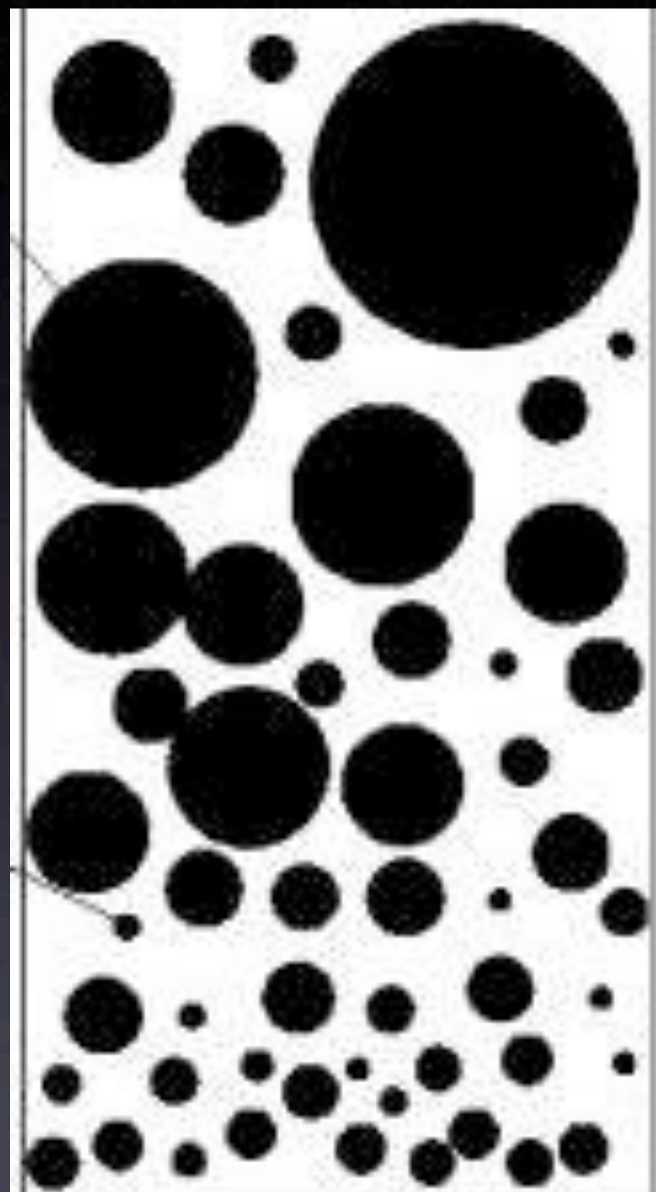

above
exsolution level

$$W_{magma} = Q / \pi a^2 \rho$$

$$W_{bubble} = 2 \Delta\rho g r^2 / 9 \mu$$

$$\frac{1}{\rho} = \frac{nRT}{p} + \frac{1-n}{\sigma}$$

$$n_s = sp^{\beta}$$

Differential motion between gas and magma

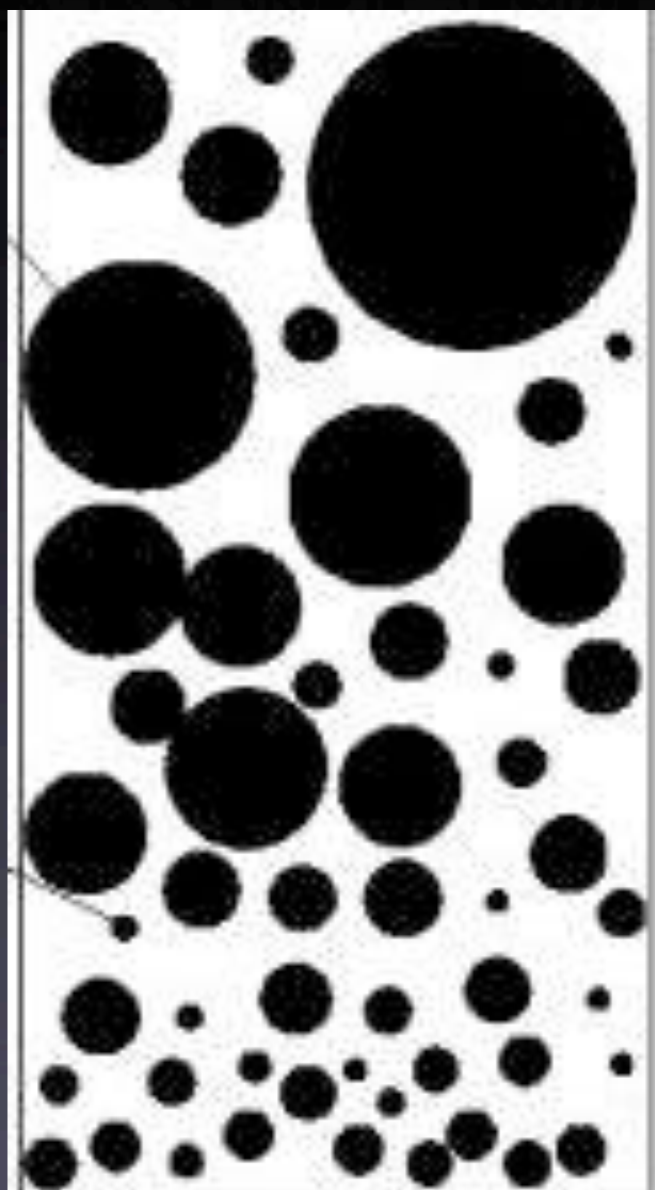

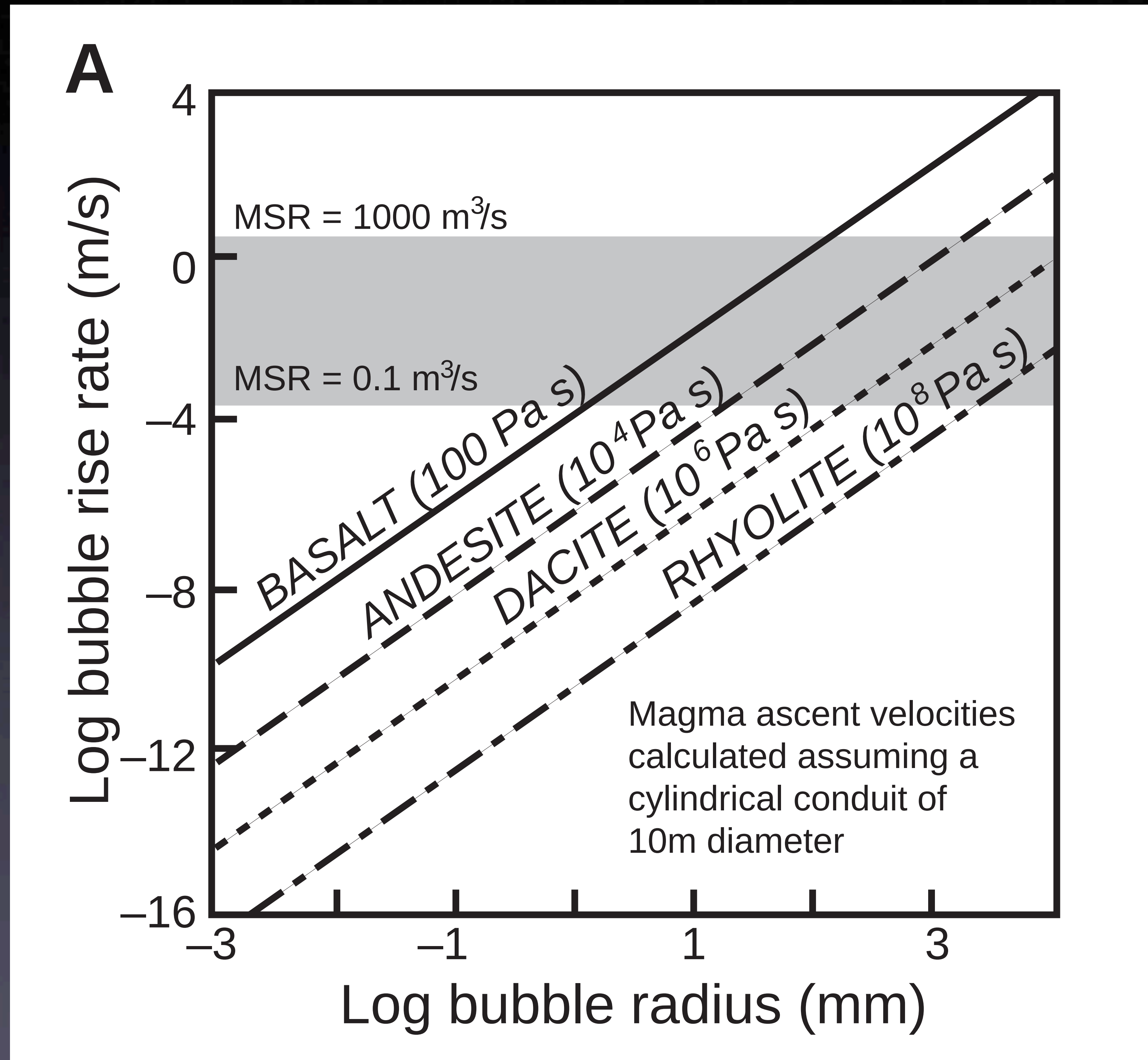

Cashman & Sparks, 2013

Basaltic magma – low viscosity

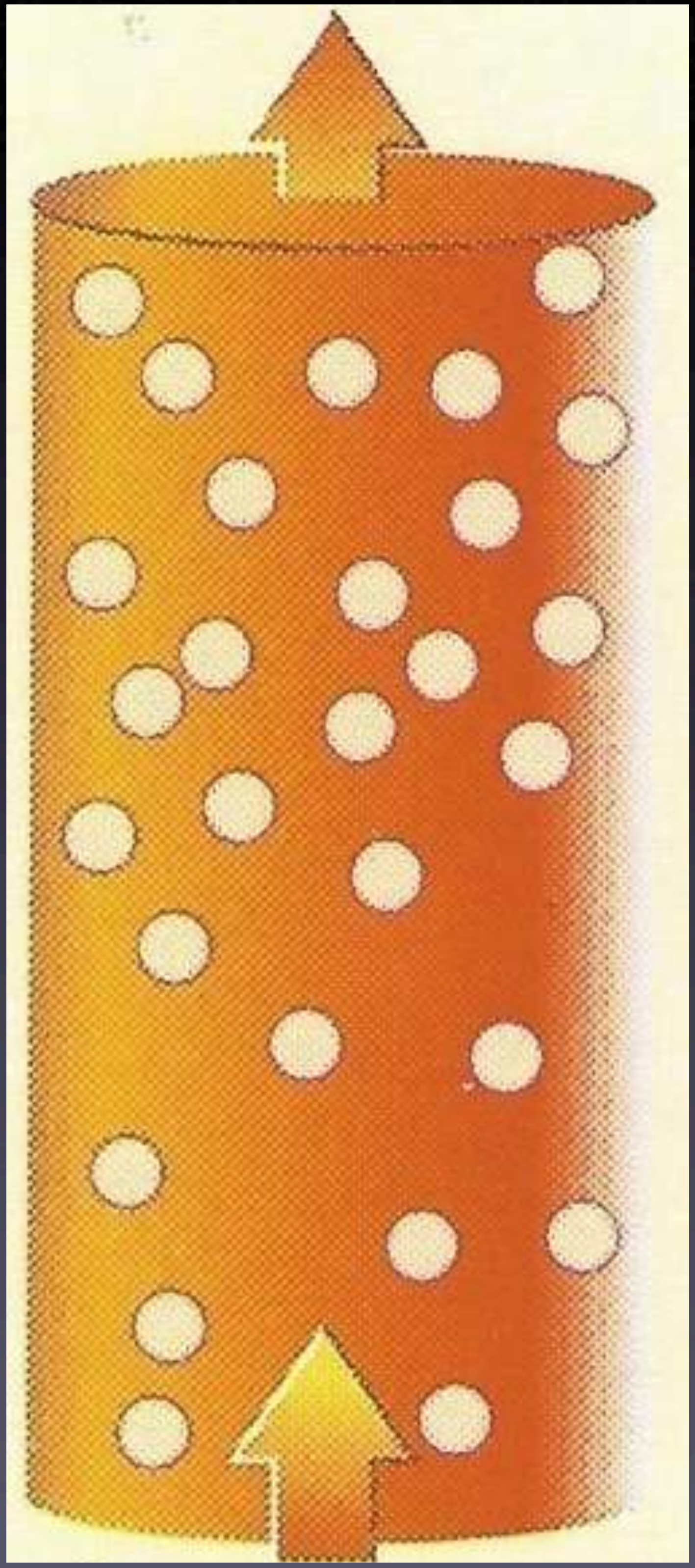

Basaltic magma – higher gas flux

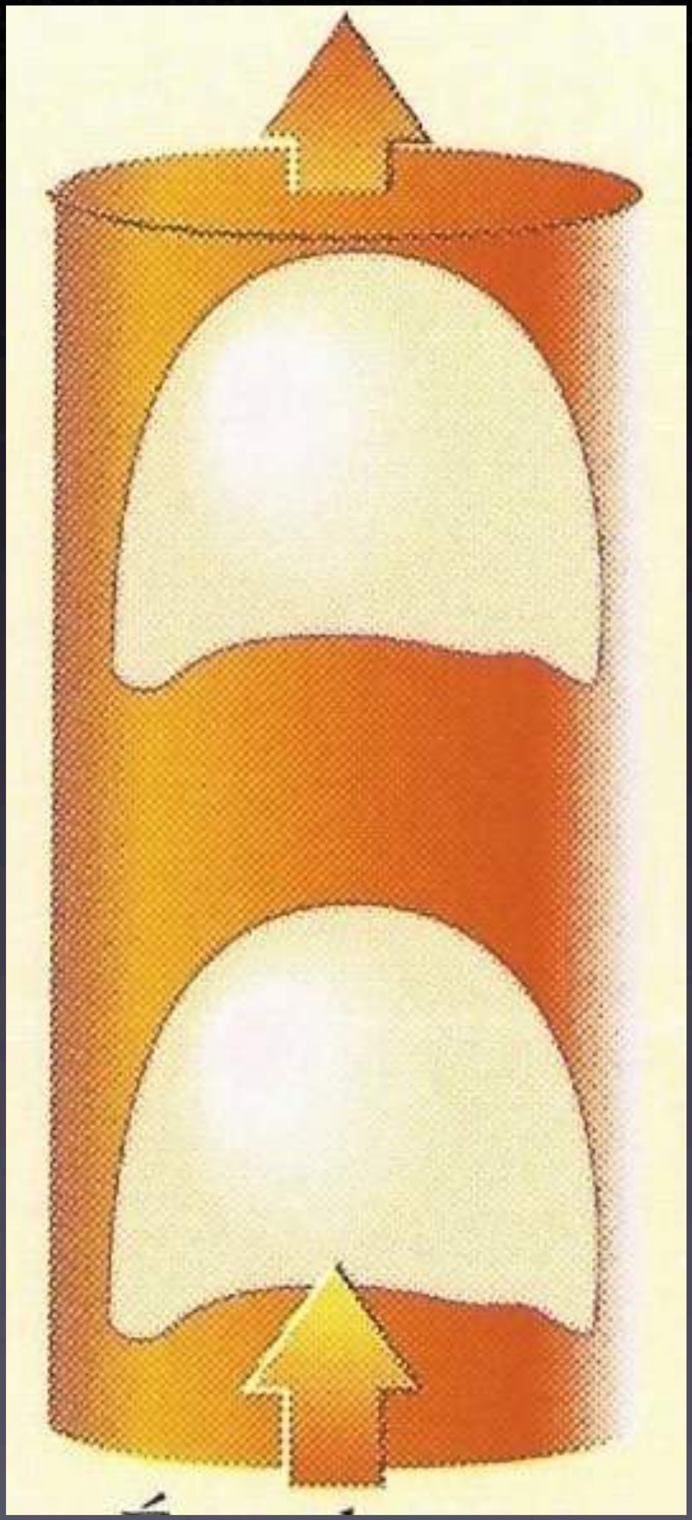

Movie ETNA

Basaltic magma – higher gas flux

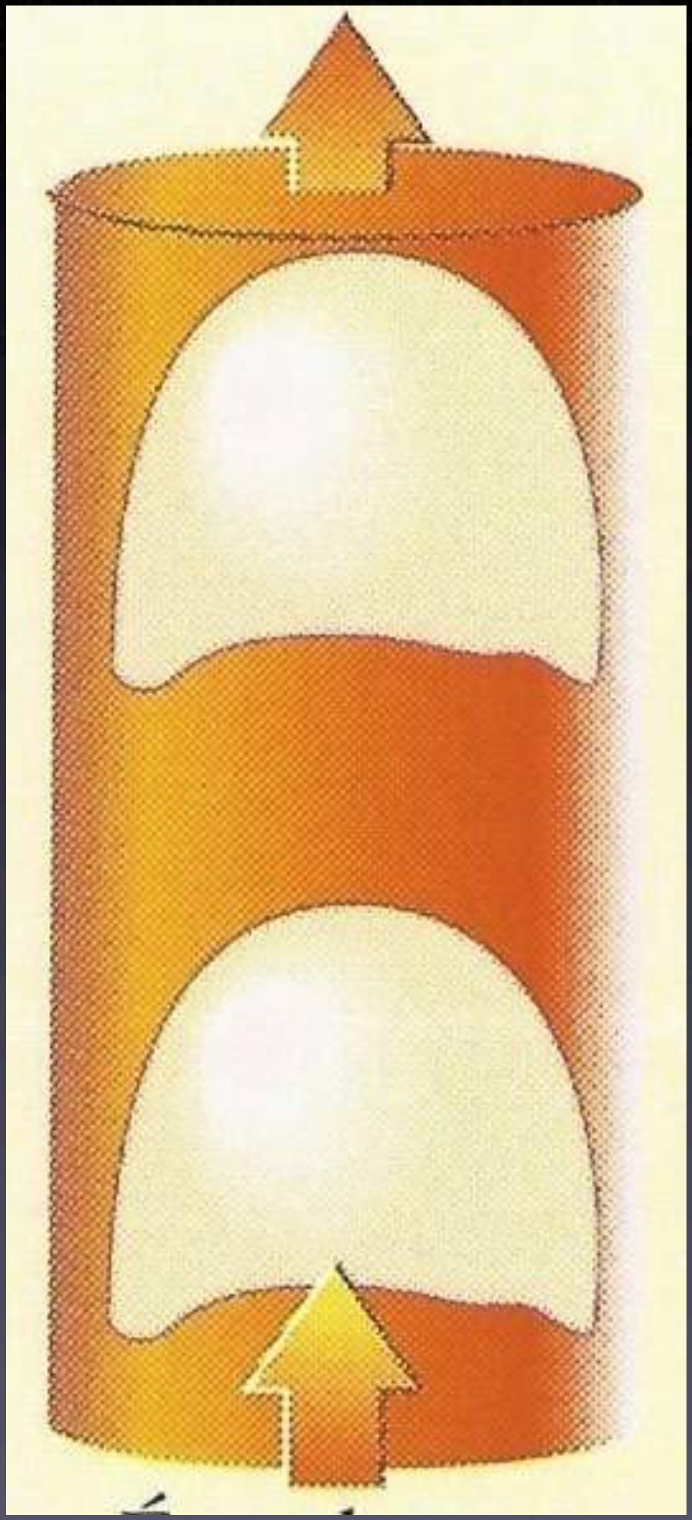

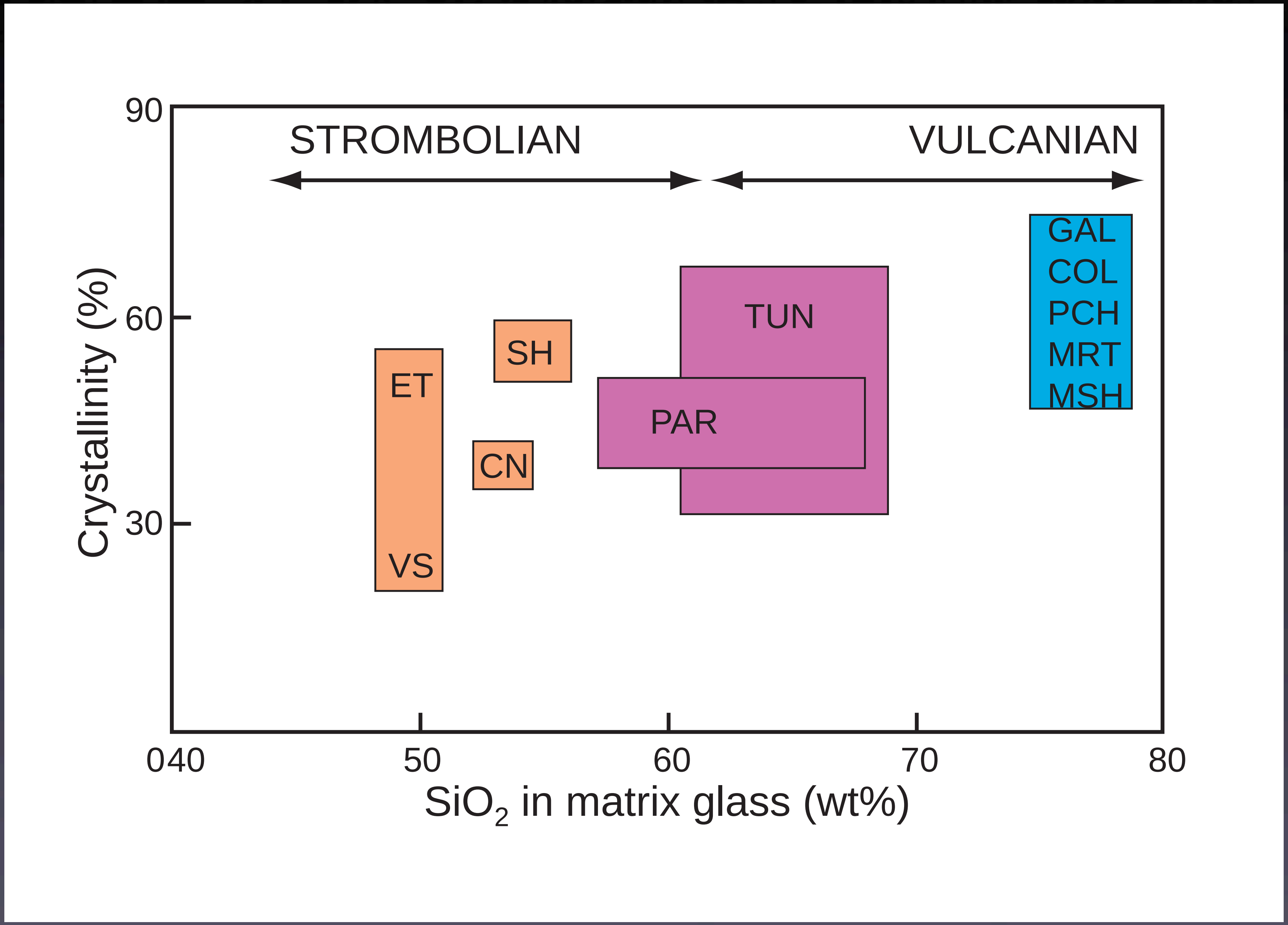

Cashman & Sparks, 2013

Basaltic magma – fire fountains

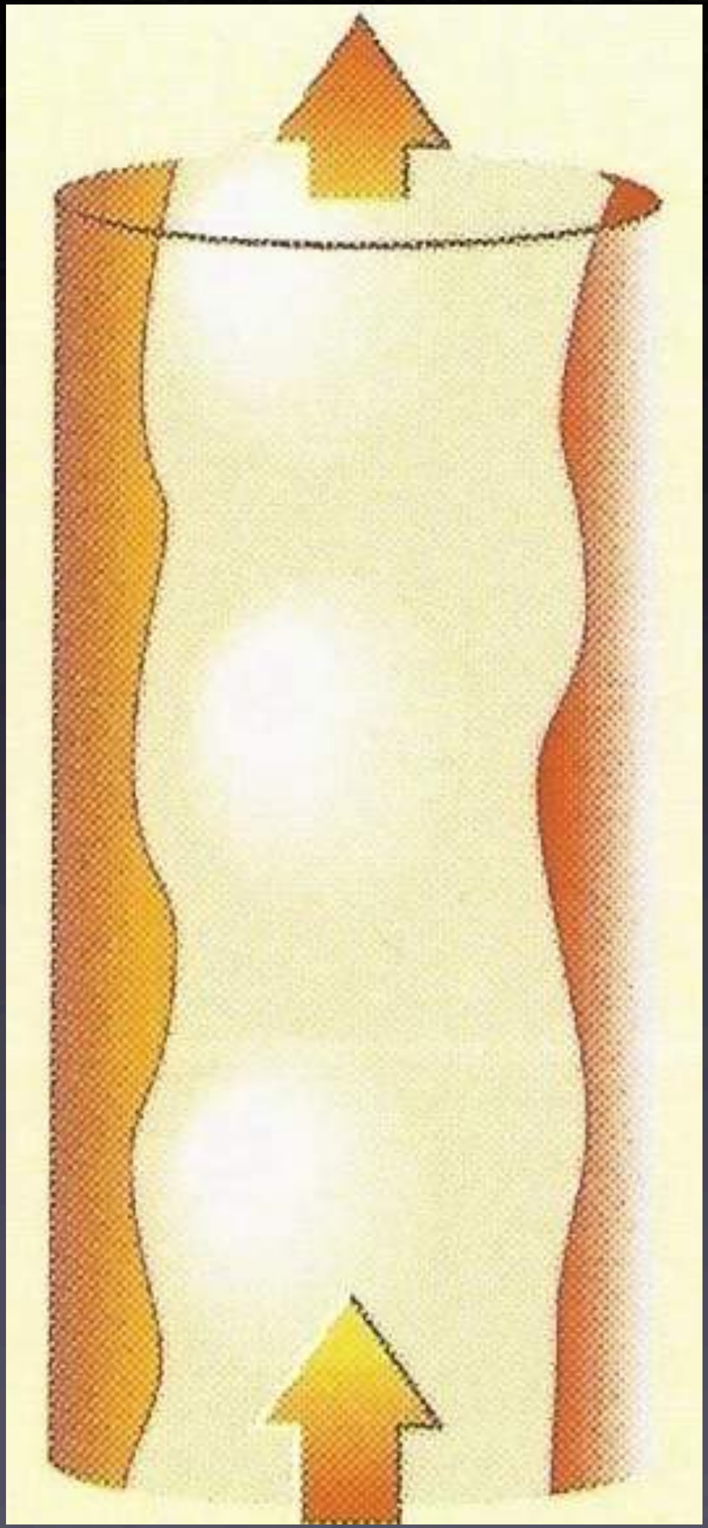

Viscous magma

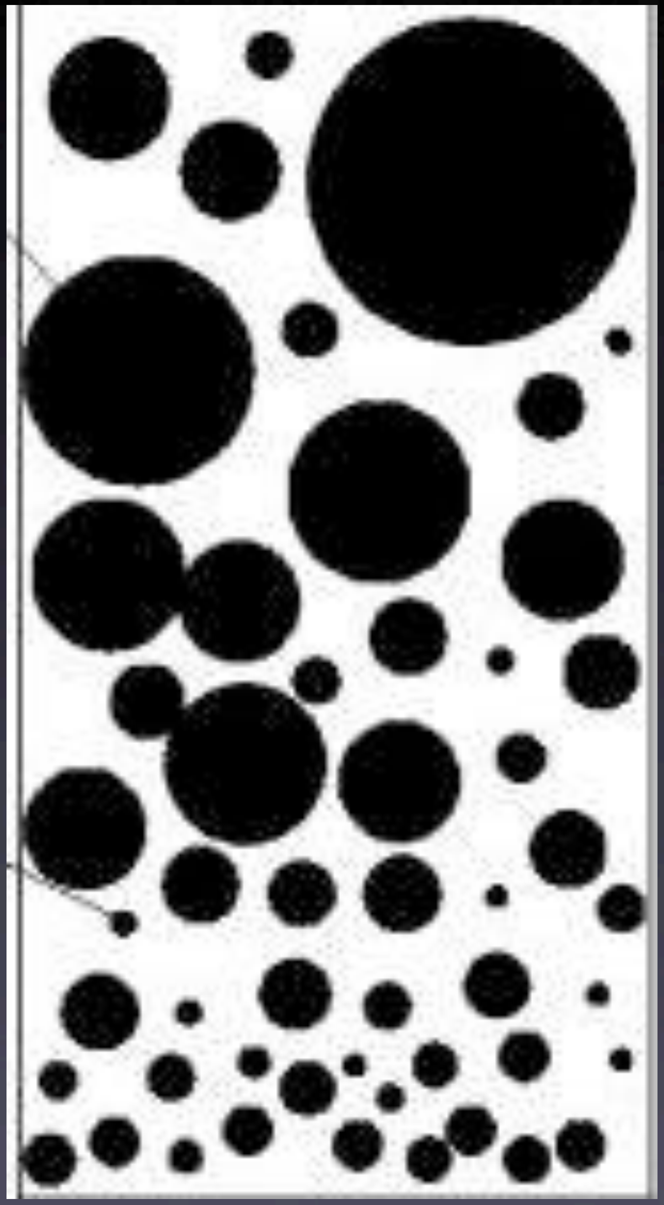

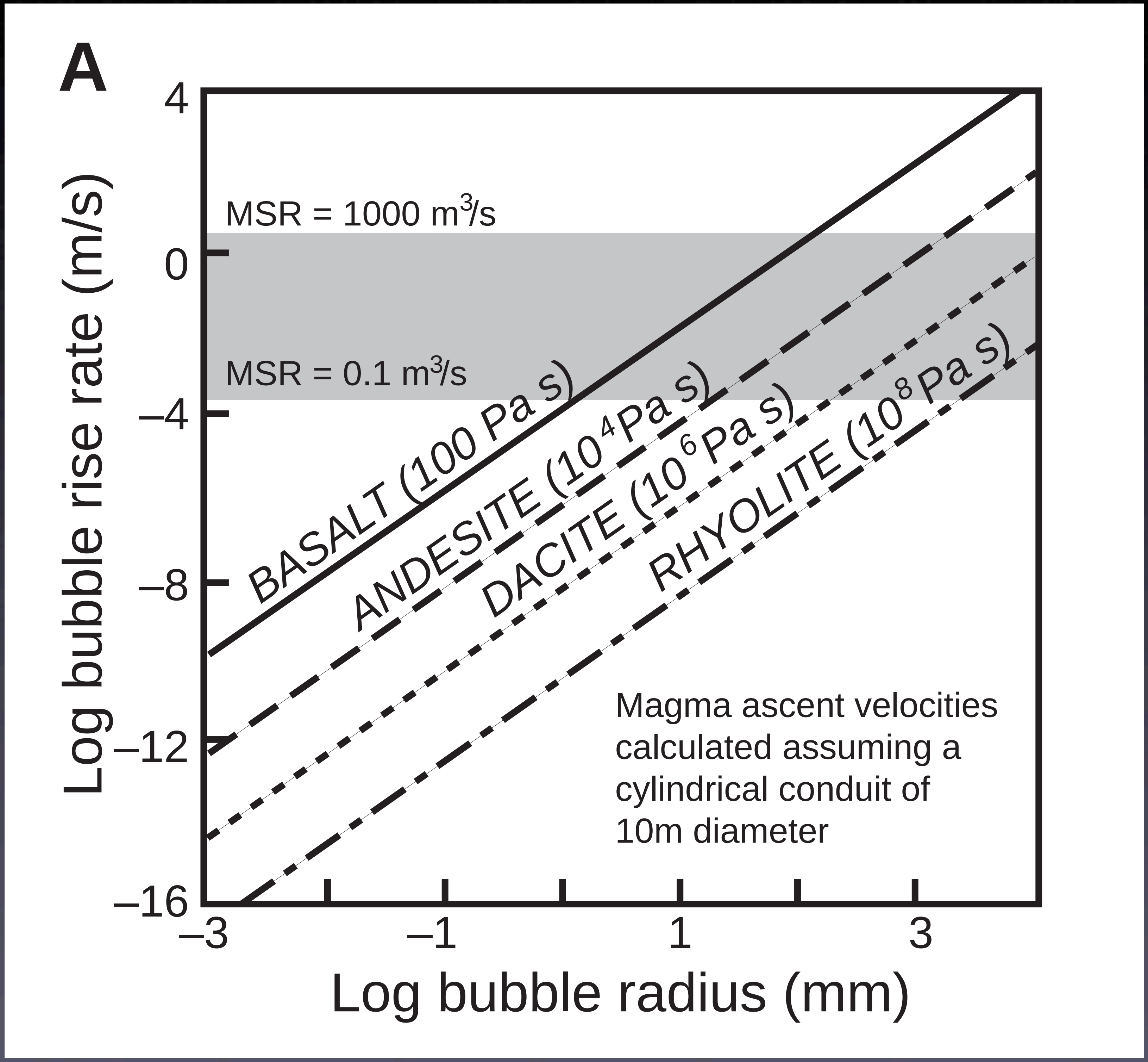

Bubbly viscous flow

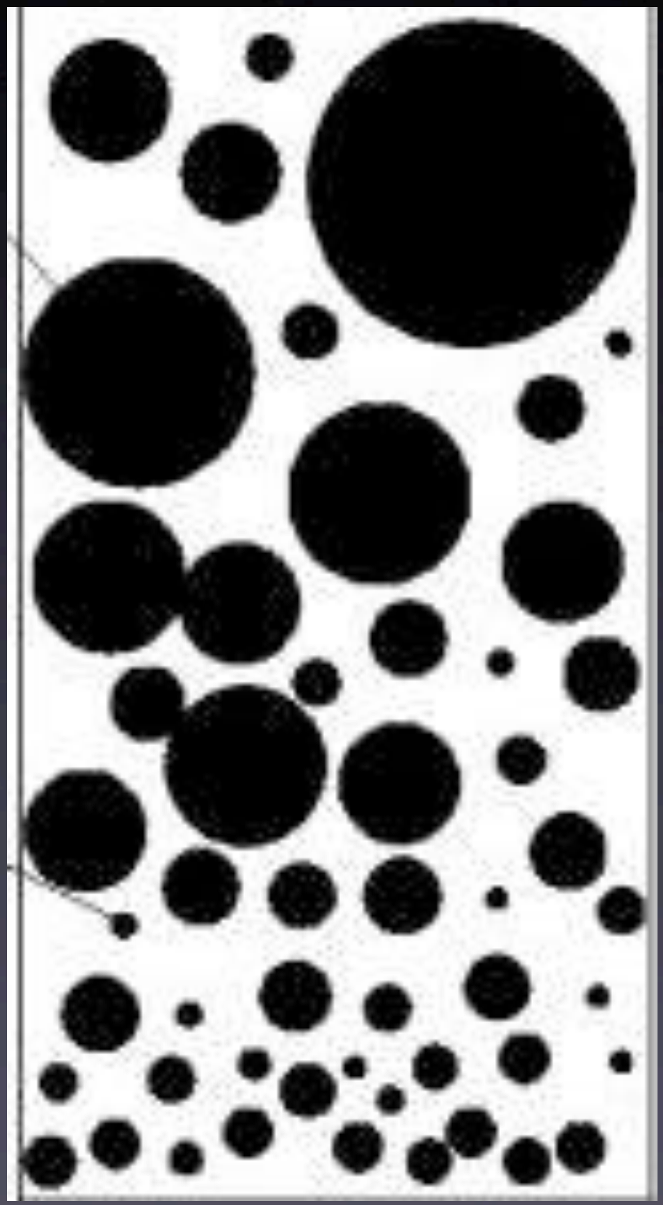

$$\rho u A = Q$$

$$\rho u \frac{du}{dz} = -\frac{dp}{dz} - \rho g - f$$

$$f = \frac{3\boxed{\mu_0}[\exp(5 - 100 n_0)](1 - \phi)^{-5/2}}{2r^2}$$

Woods, 1995

Fragmentation threshold

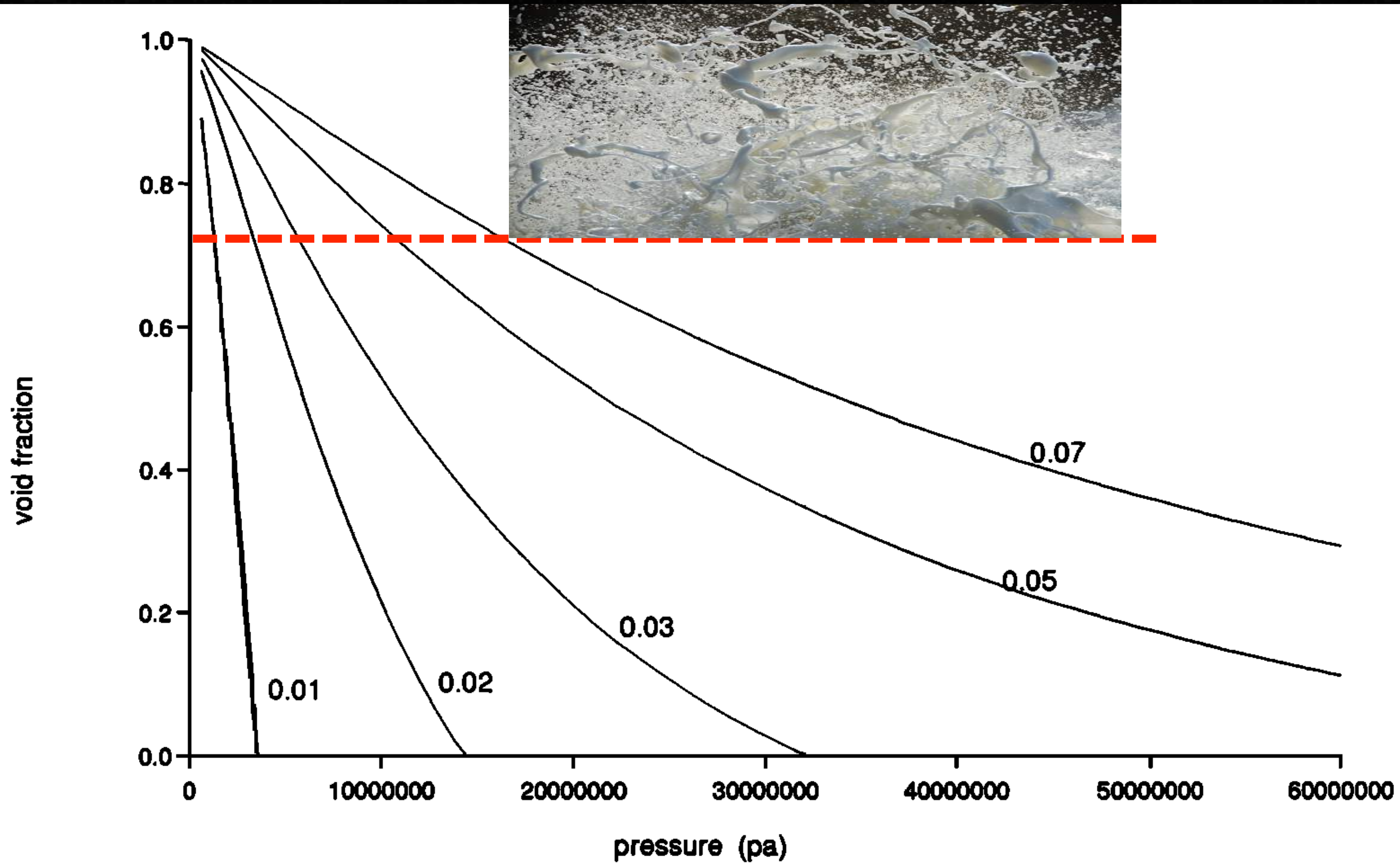

Figure 3. Variation of the void fraction with pressure for magma-volatile mixtures at high pressure, and in which the volatile content initially has values 1, 2, 3, 5, and 7 wt. %.

Turbulent dusty gas

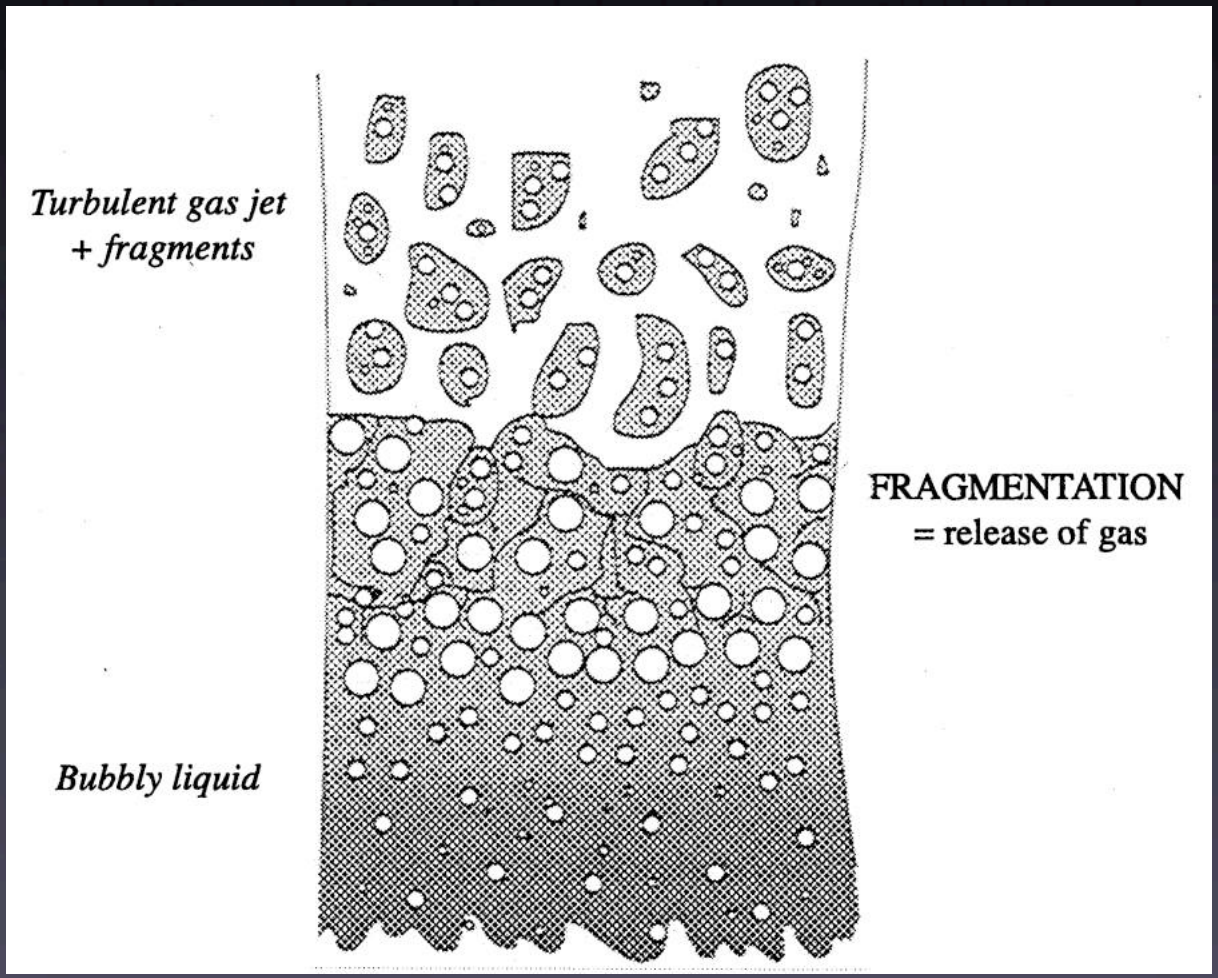

$$\rho u A = Q$$

$$\rho u \frac{du}{dz} = -\frac{dp}{dz} - \rho g - f$$

$$\boxed{f = 0.0025 \frac{\rho u^2}{r}}$$

Flow acceleration and pressure evolution

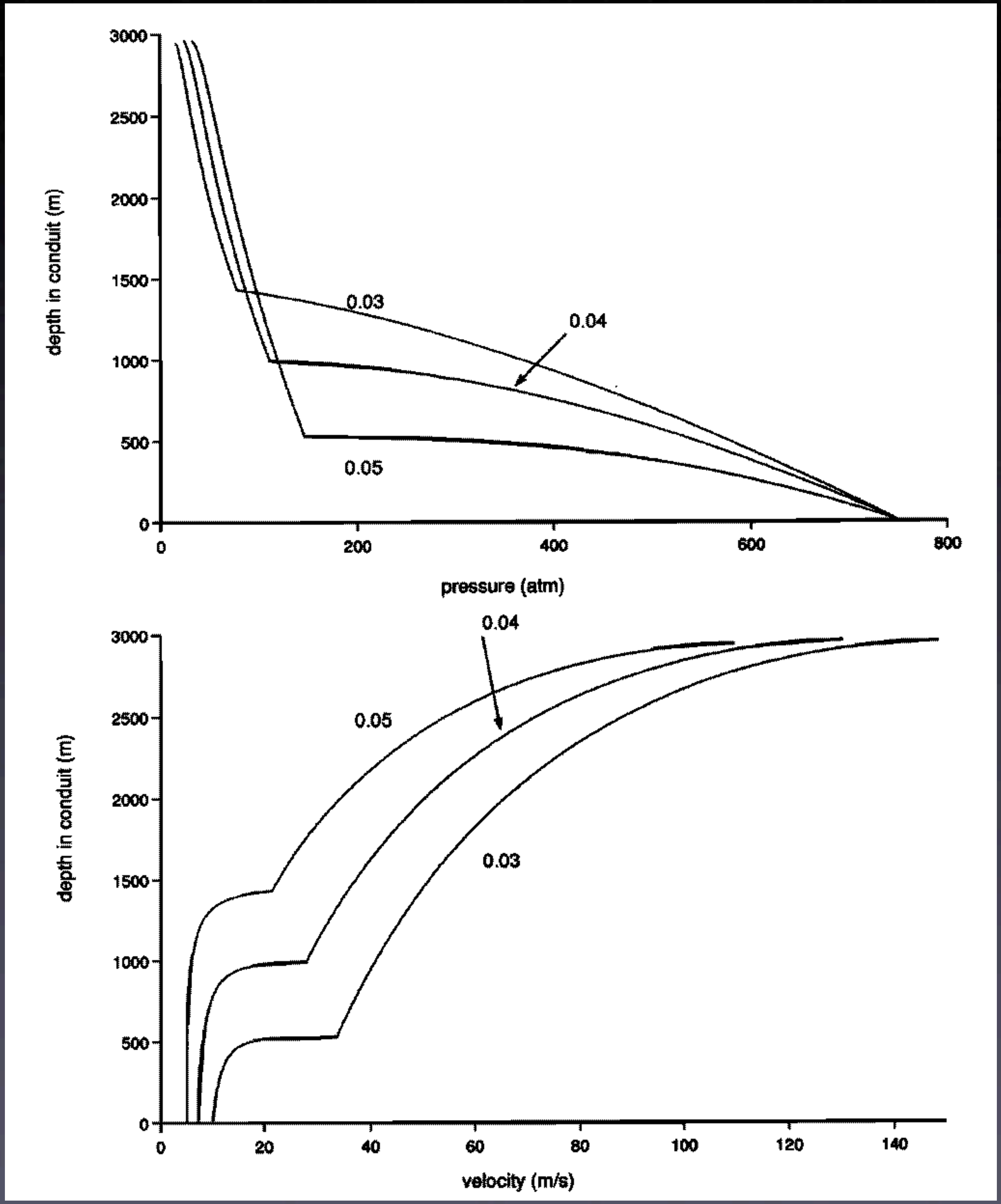

$$\frac{dp}{dz}\left(1 - \frac{u^2}{u_c^2}\right) = -\rho g - f$$

$$u_c \sim 0.97(n_0 RT)^{1/2}$$

$$U_{exit} \approx 2\ u_c$$

Turbulent particle laden jet

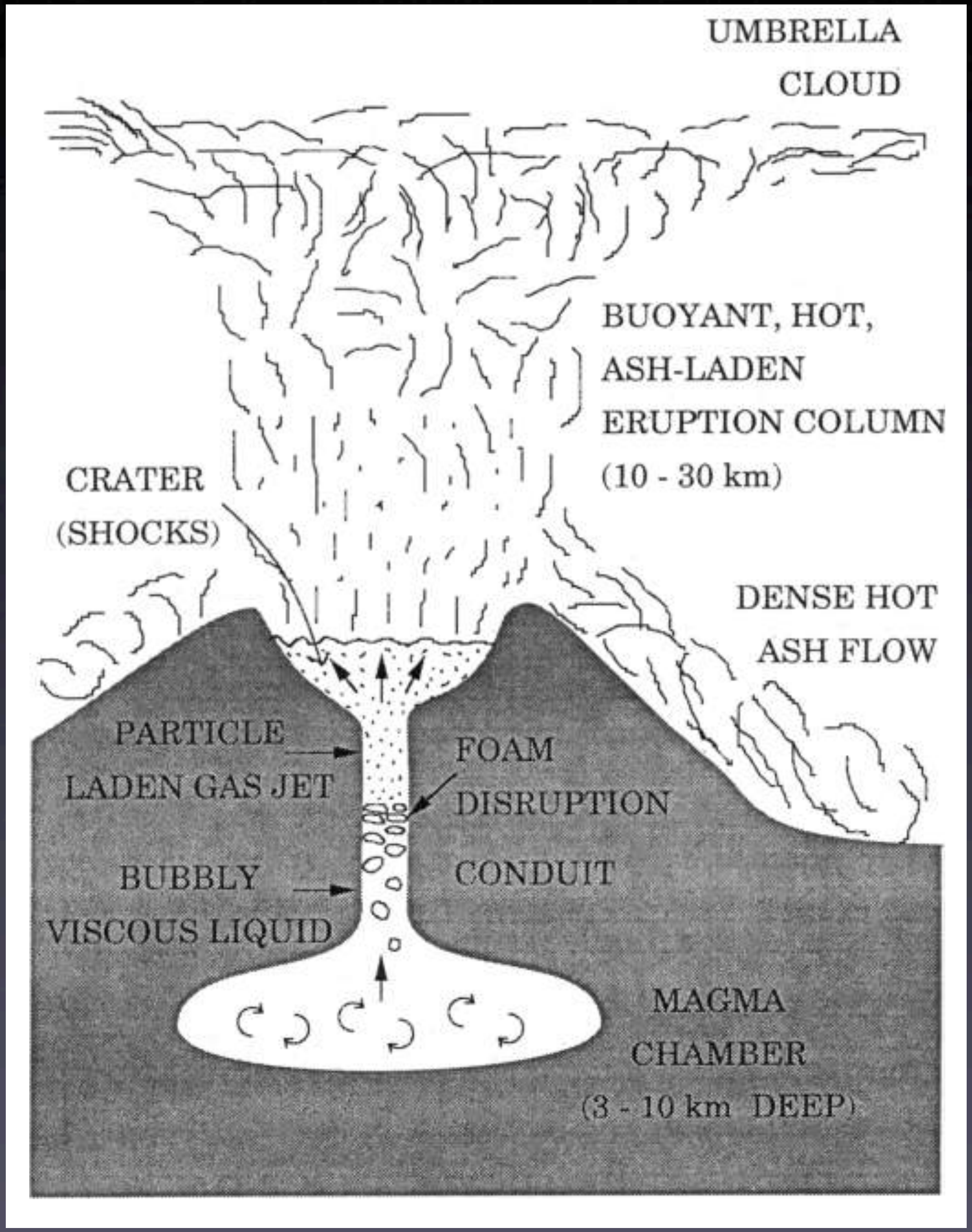

Movie VESUVIUS

An alternative evolution: escape of gas phase

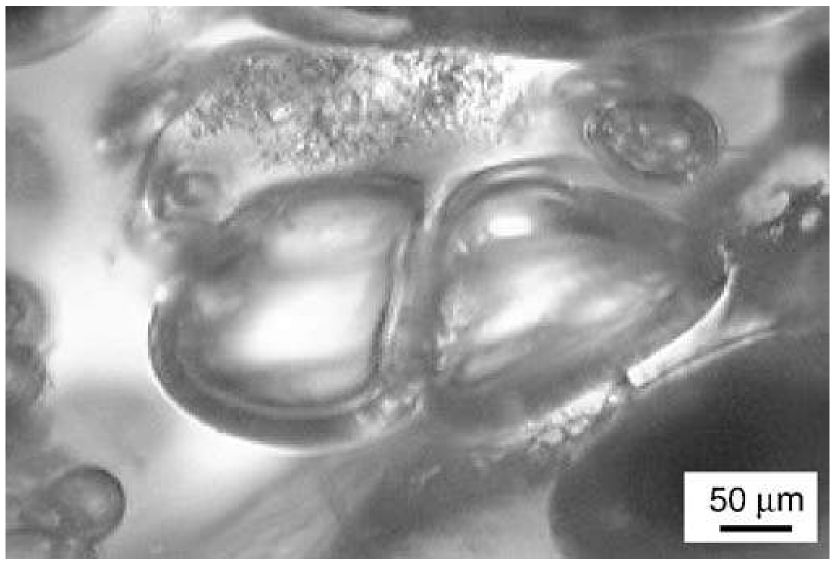

Fig. 10 Typical bubble pair shortly before coalescence. Note the planar shape of the thin separation wall between the bubbles (G303, Table 2)

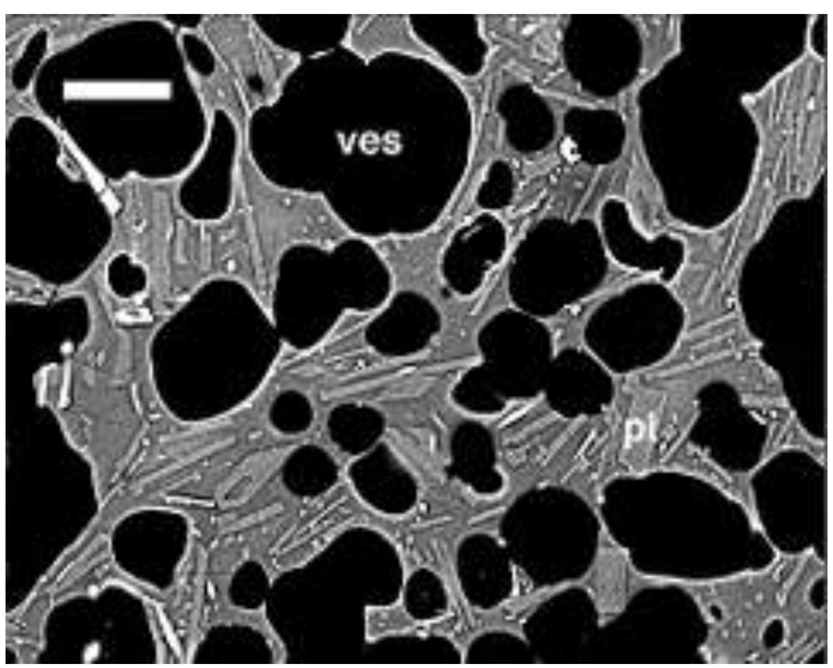

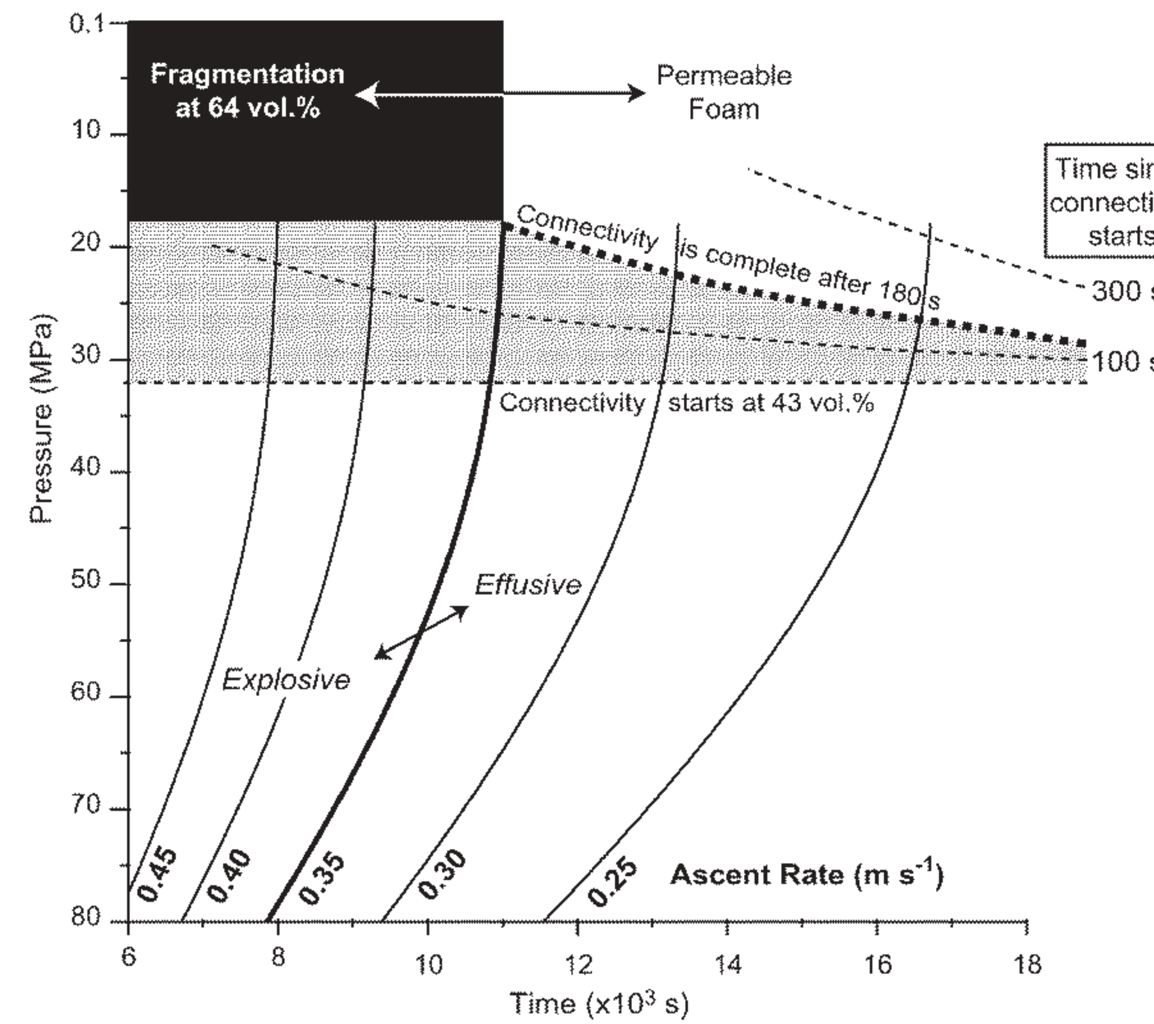

Burgisser &. Gardner, 2005

Gas loss through conduit walls

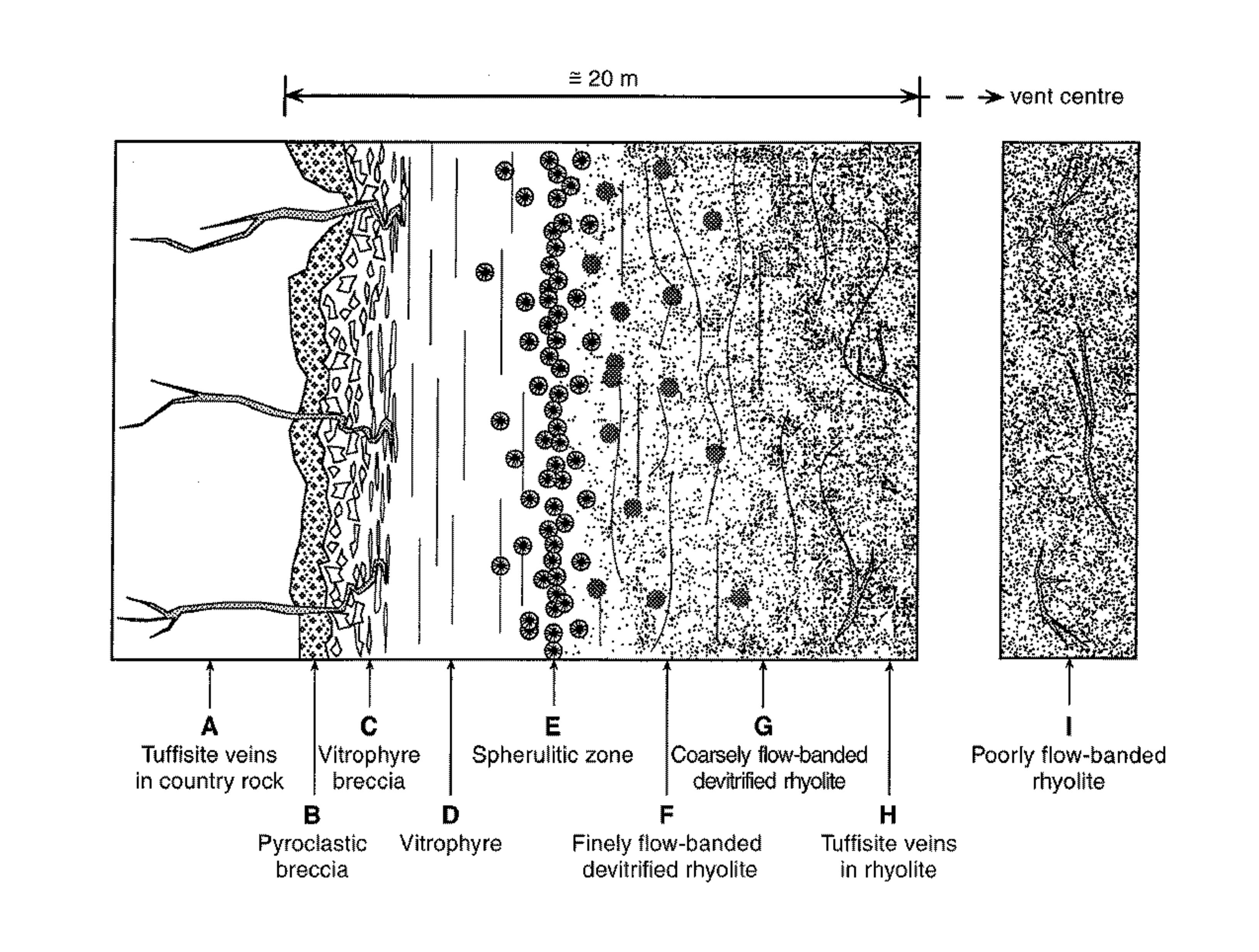

Stasiuk et al, 1996

https://youtu.be/3foeTjsFesY

Quantitative modeling

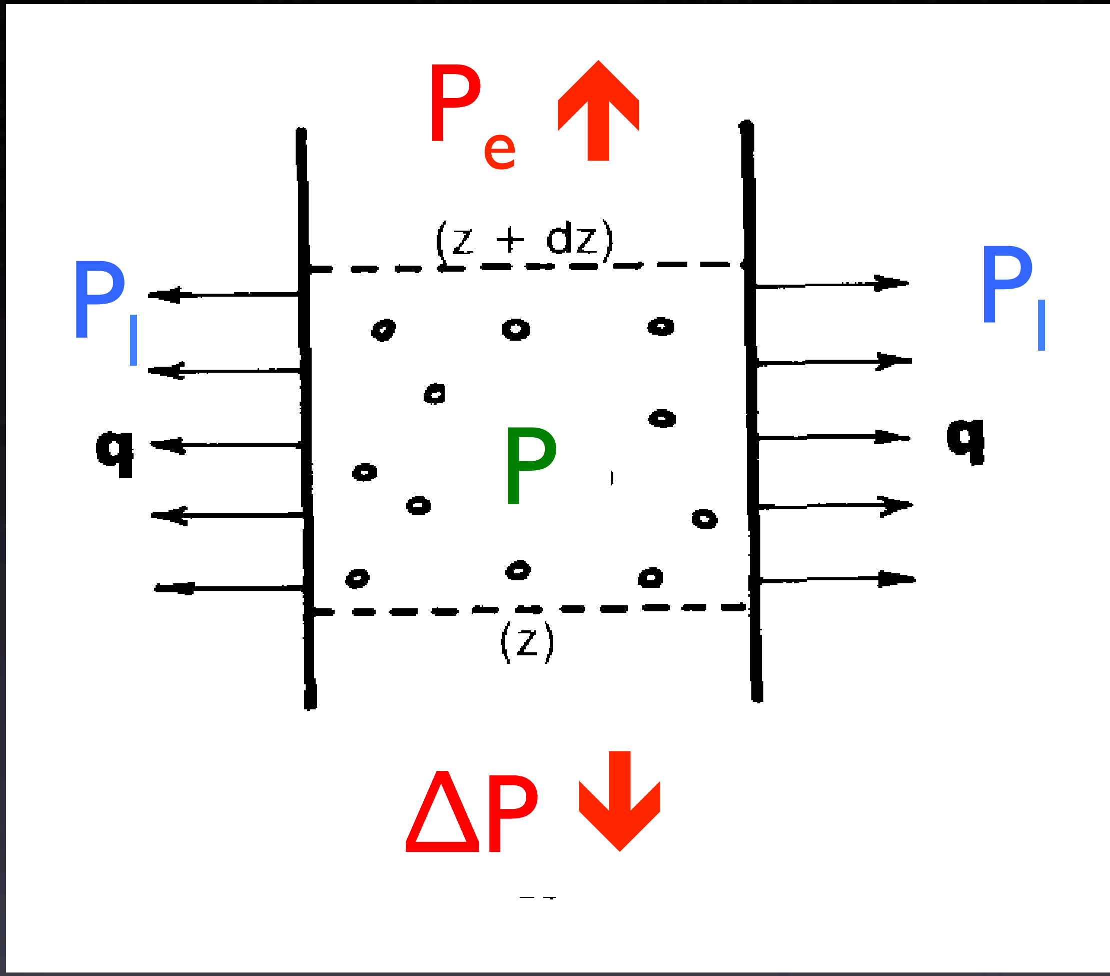

$$\rho_l \frac{a^4}{\mu} \frac{\Delta P - P_e}{H}$$

mass flux of liquid (along z)

$$q = \rho_g \alpha k (P - P_l)$$

gas loss (through conduit walls)

$$C = \frac{k \mu H^2}{a^3} \frac{\Delta P}{\Delta P - P_e}$$

Jaupart & Allègre, 1991

Gas loss can lead to dome formation

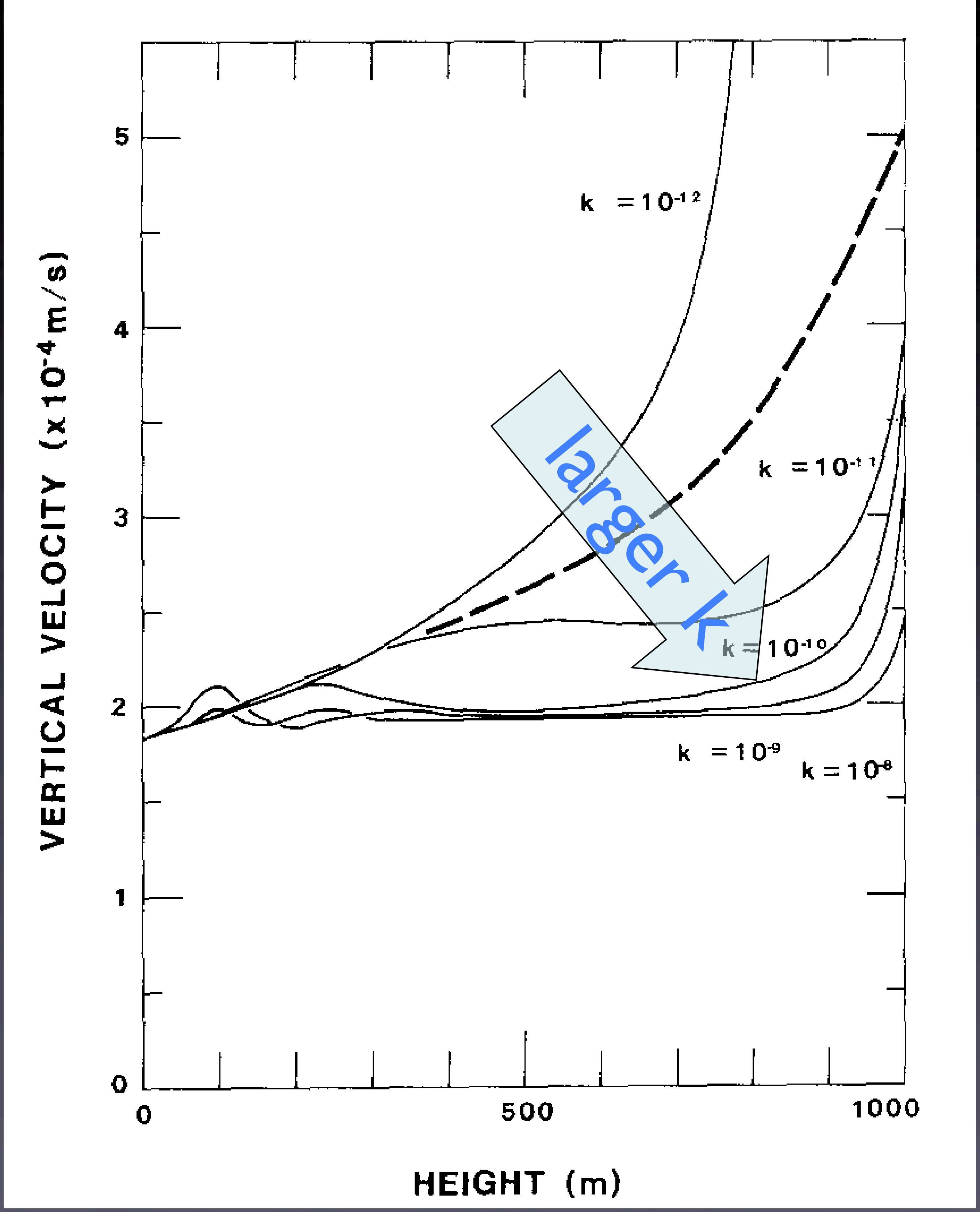

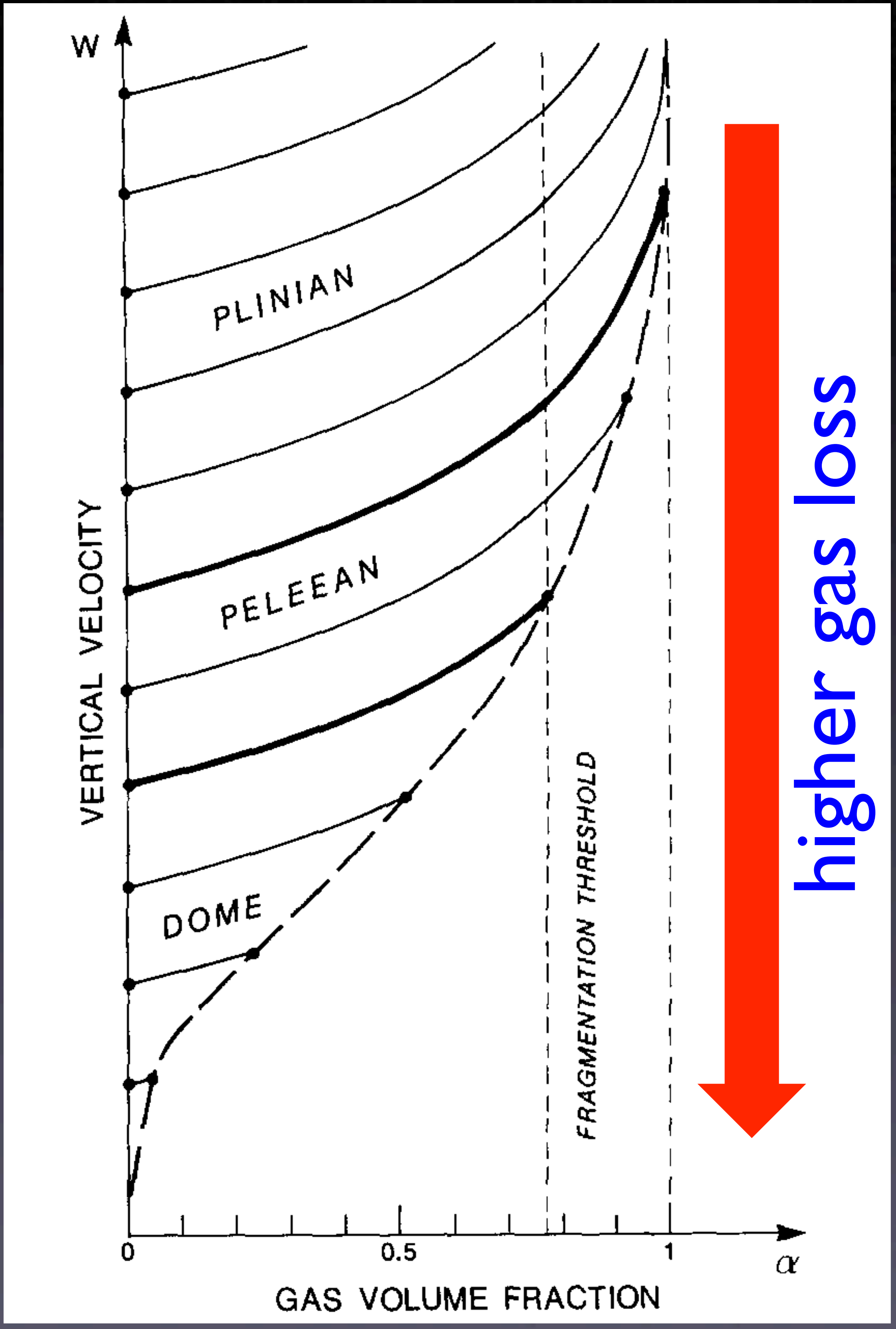

Dome/reservoir coupling

Increasing mass flux

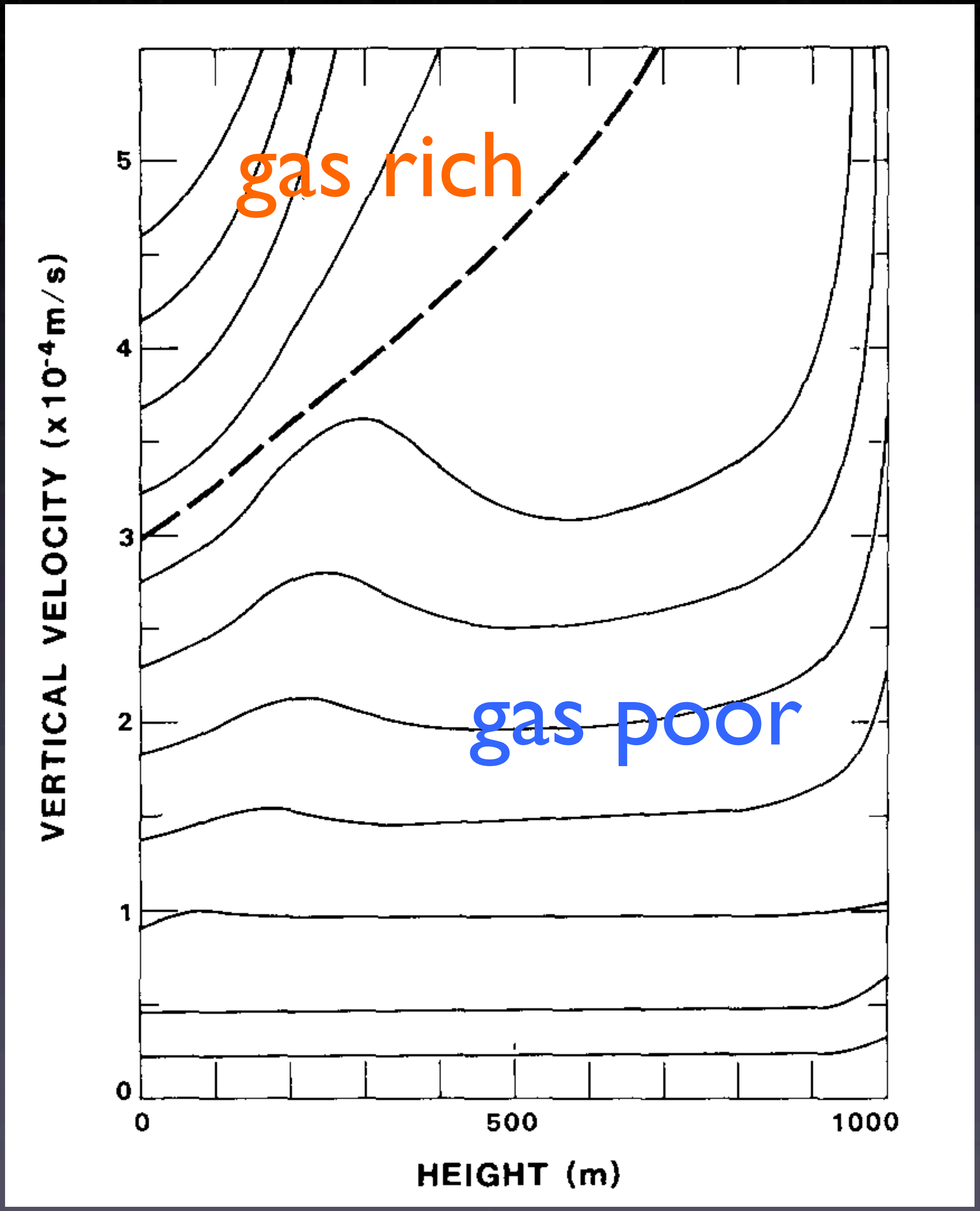

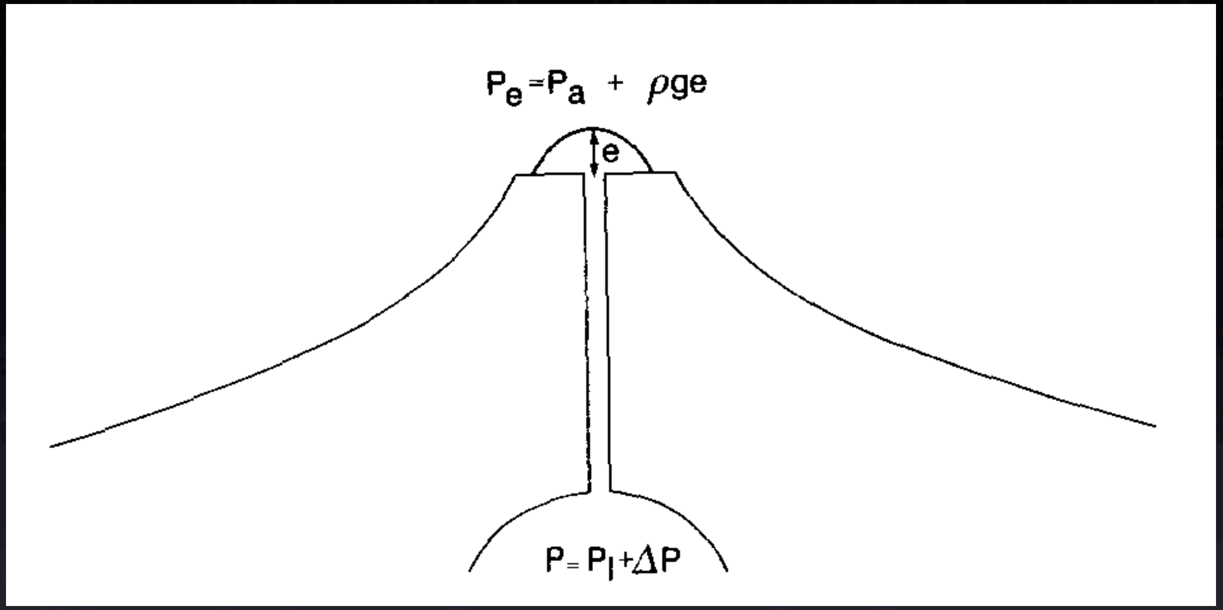

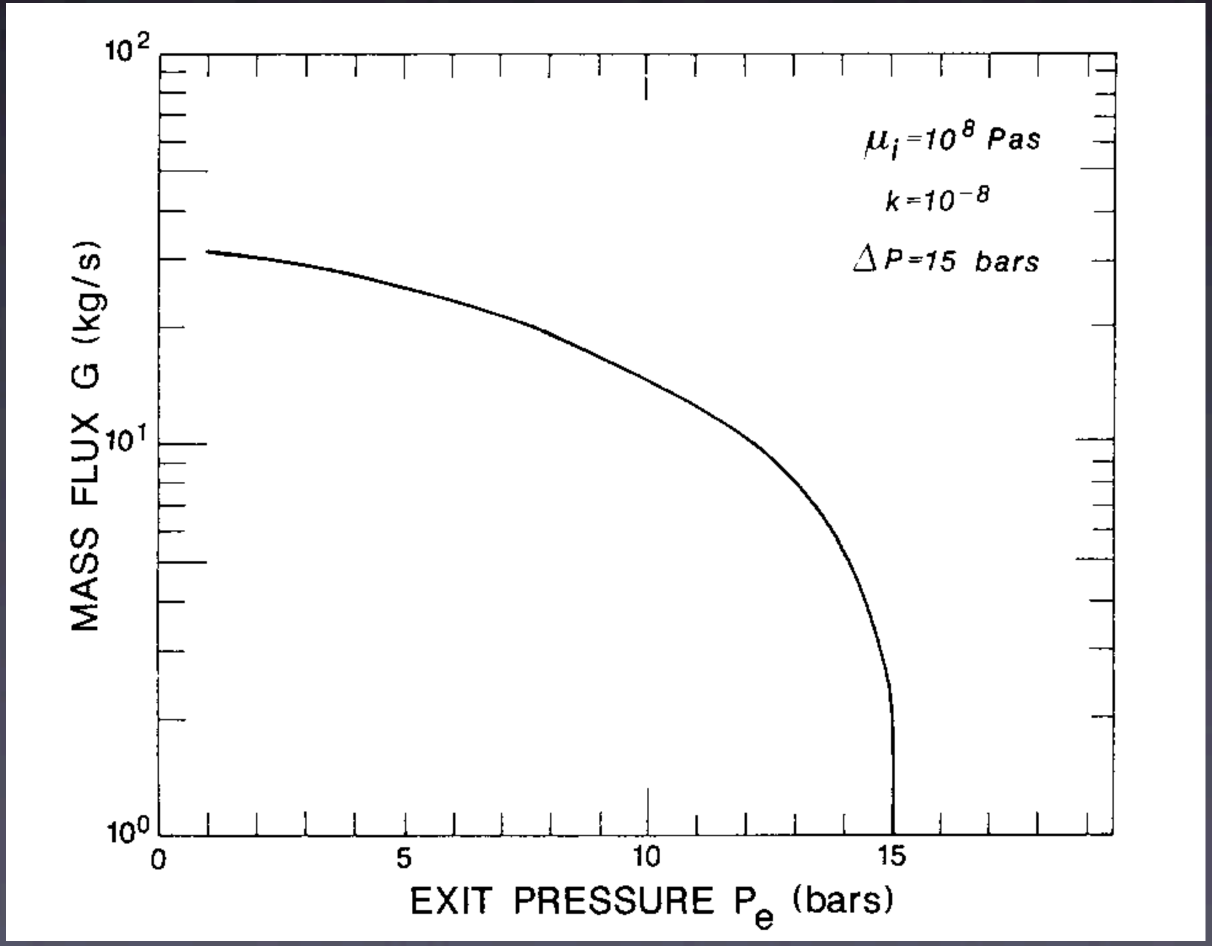

SUMMARY:
key players for explosive vs effusive eruption regime

- properties of magma:
  - (i) total amount of dissolved gas
  - (ii) viscosity

- flow dynamics:
  - (i) mass flux / reservoir overpressure
  - (ii) evolution of gas phase (exsolution, expansion and coalescence of bubbles, gas loss...)

Modeling of volcanic plumes

Modeling of volcanic plumes:

1/ generation of pyroclastic flows by the collapse of the volcanic column

From natural flow to theoretical framework: the role of buoyancy

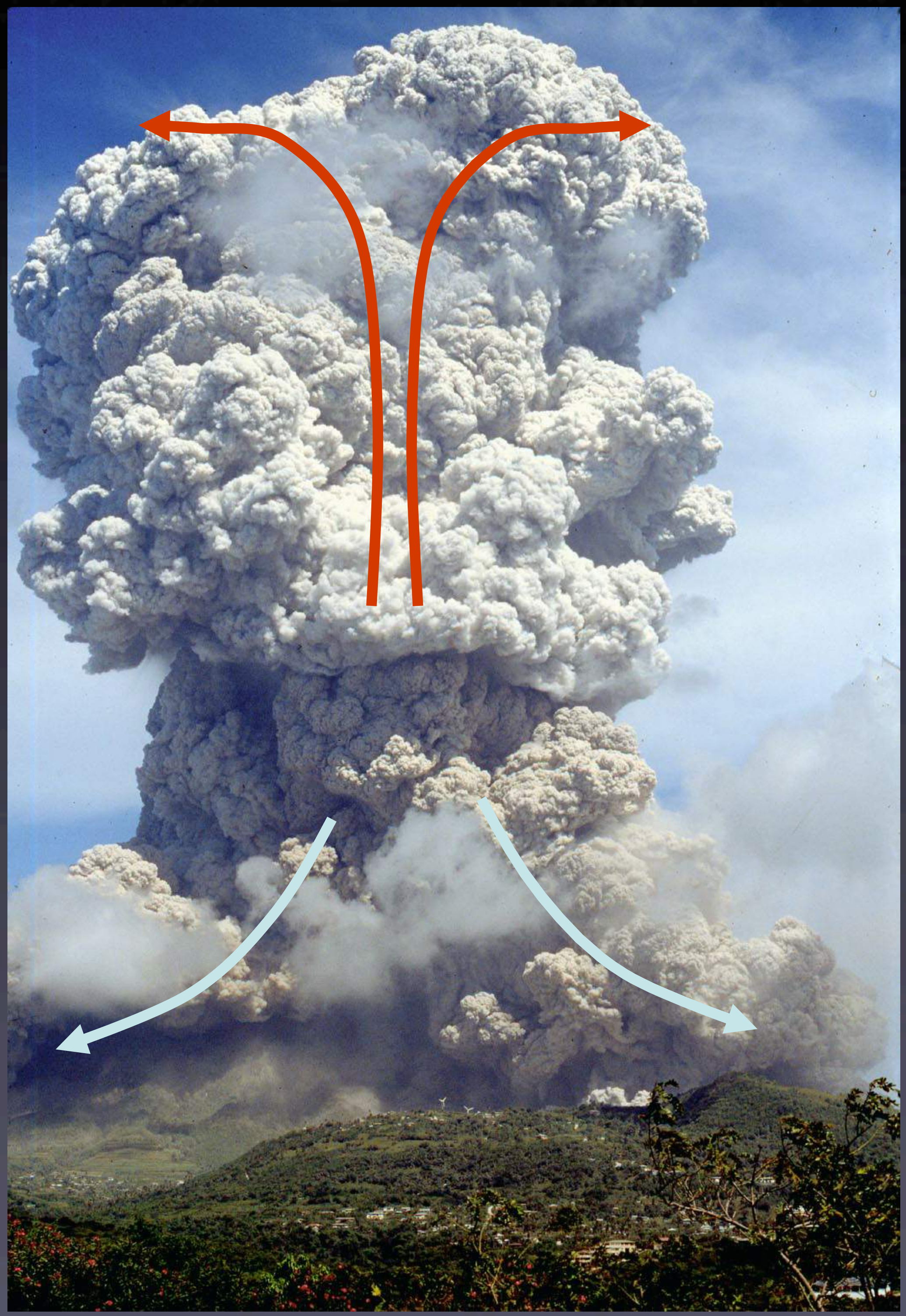

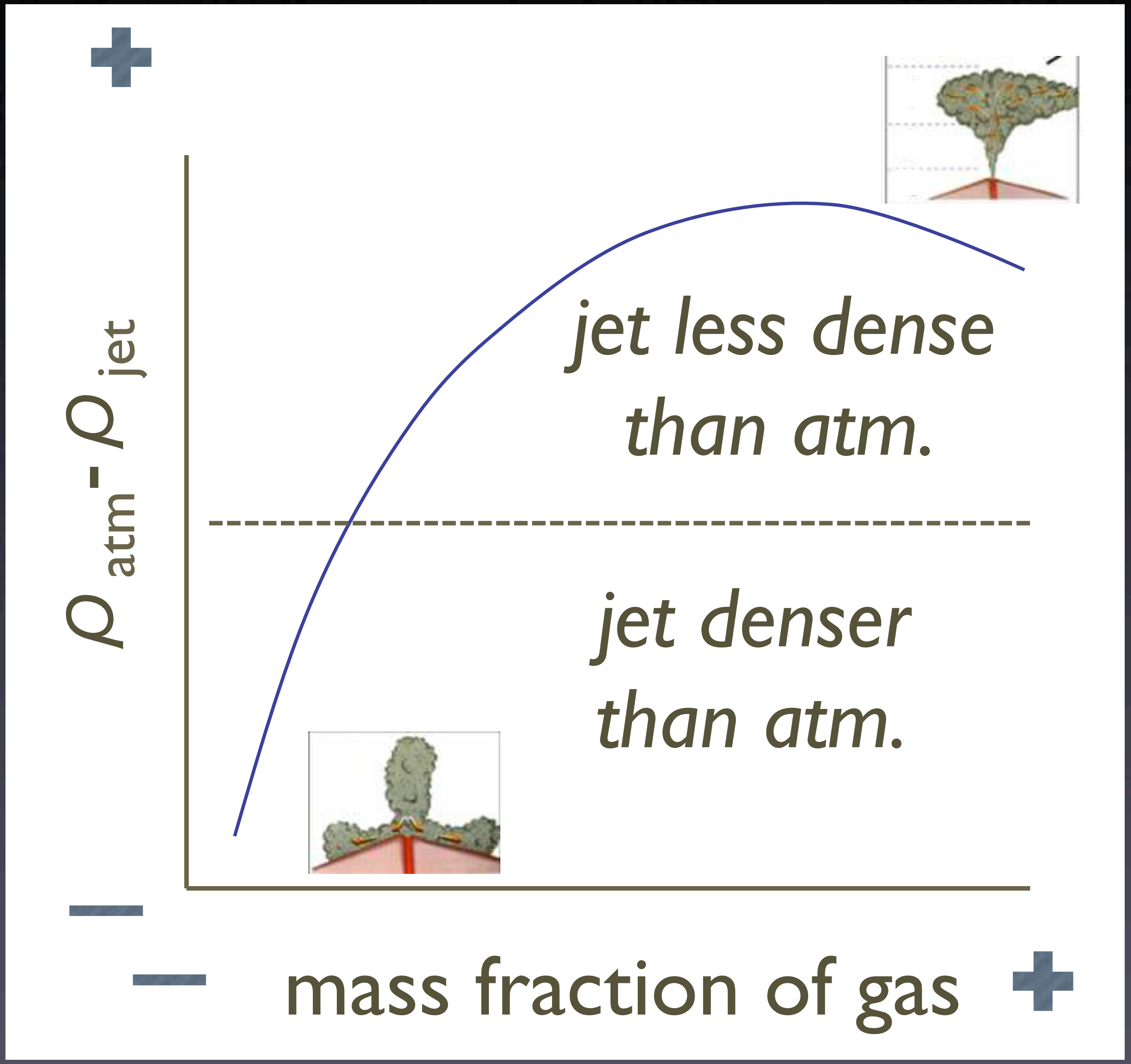

From natural flow to theoretical framework: entrainment and heating of ambient air

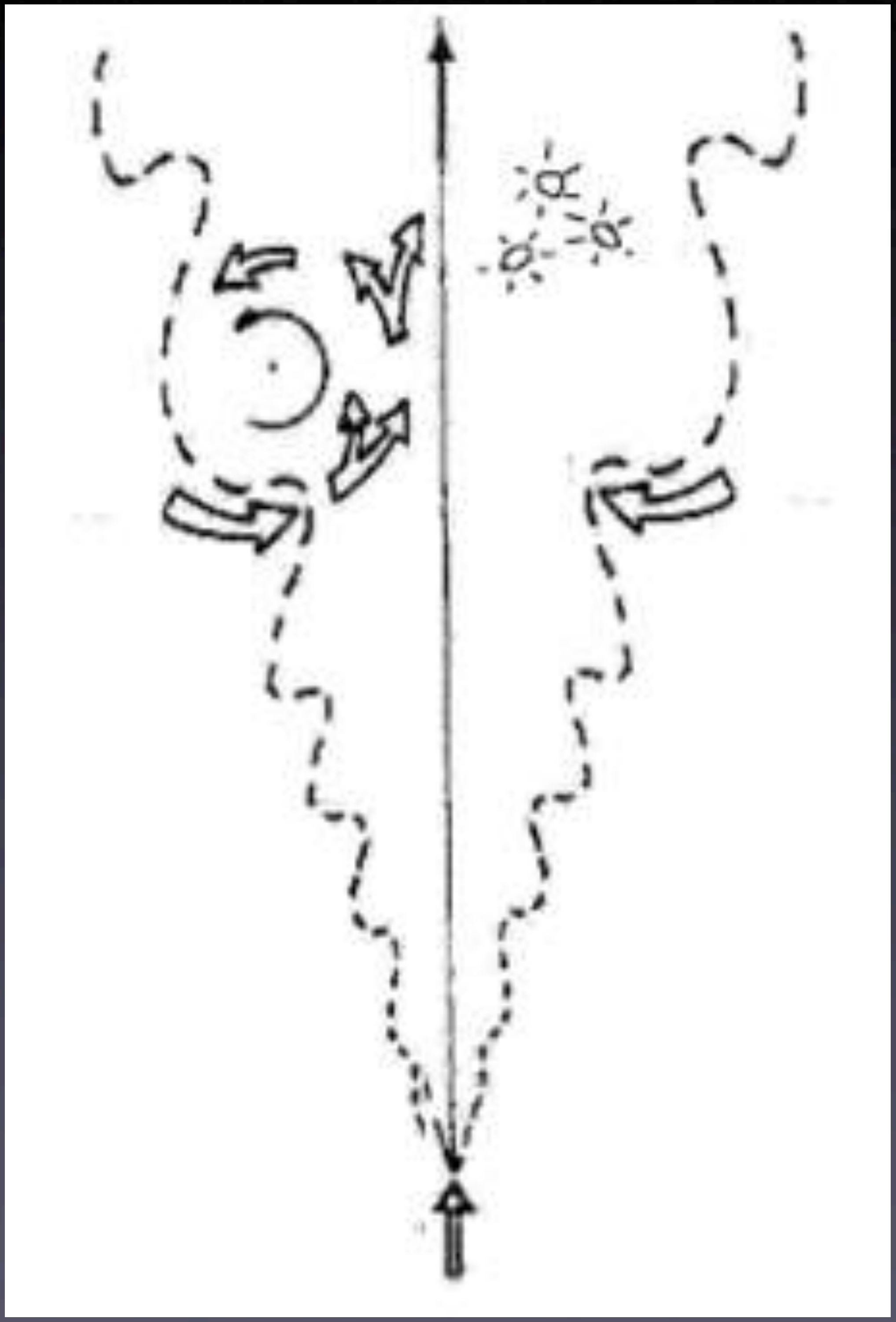

Morton, Turner and Taylor, 1956

From natural flow to theoretical framework: conservation equations (1/4)

mass flux:

$$Q = \pi R^2 W \rho$$

$$dQ/dz = 2\pi R \lambda W \rho_a$$

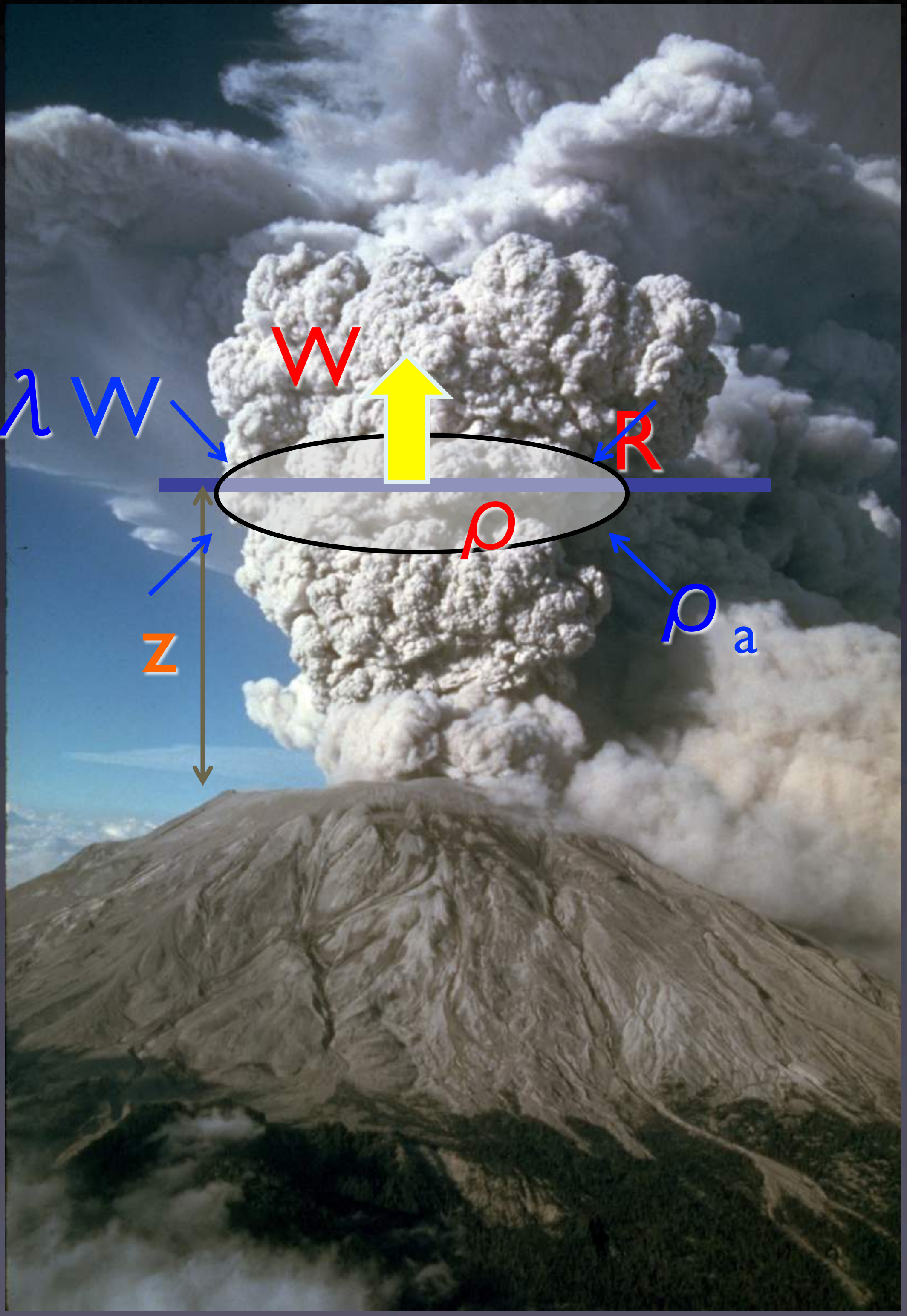

From natural flow to theoretical framework: conservation equations (2/4)

momentum flux:

$$M = \pi R^2 \, W \, \rho W$$

$$dM/dz = \pi R^2 \, (\rho_a - \rho) \, g$$

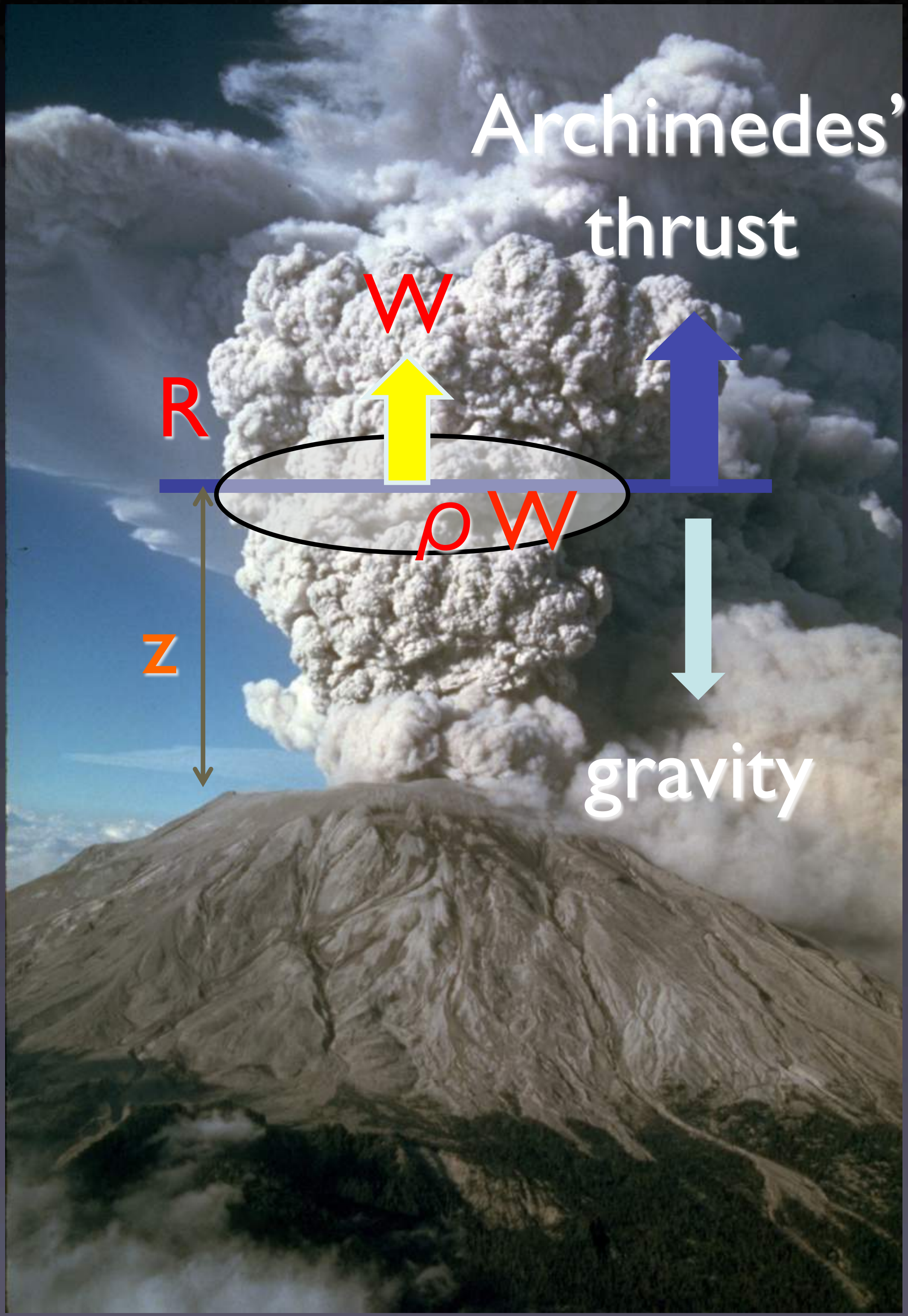

From natural flow to theoretical framework: conservation equations (3/4)

flux of energy:

$$E = \pi R^2 \, W \, \rho C_p (T - T_a)$$

$$dE/dz = 2\pi R \, \lambda W \, \rho_a C_p T_a$$

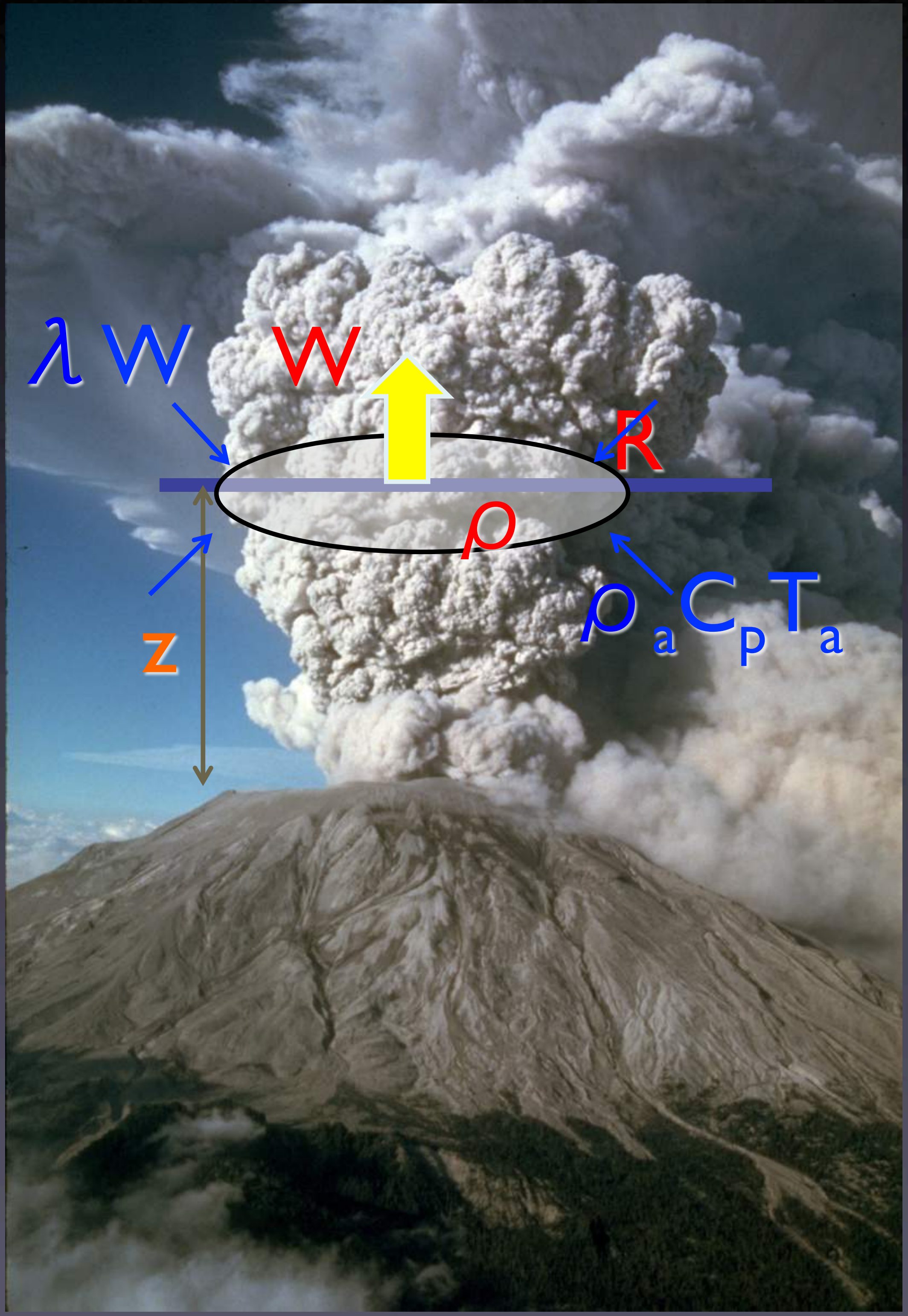

From natural flow to theoretical framework: conservation equations (4/4)

(reduced) buoyancy flux

$$F = \pi R^2\, W\, (\rho-\rho_a)/\rho_0\, g = \pi R^2\, W\, g'$$

equation of state

$$(\rho-\rho_a)/\rho_0 = \alpha\,(T-T_a)$$

$$dF/dz = \pi R^2\, W\, g/\rho_0\, d\rho_a/dz$$

$$dF/dz = \pi R^2\, W\, N^2$$

Numerical solution of the equations (1/2)

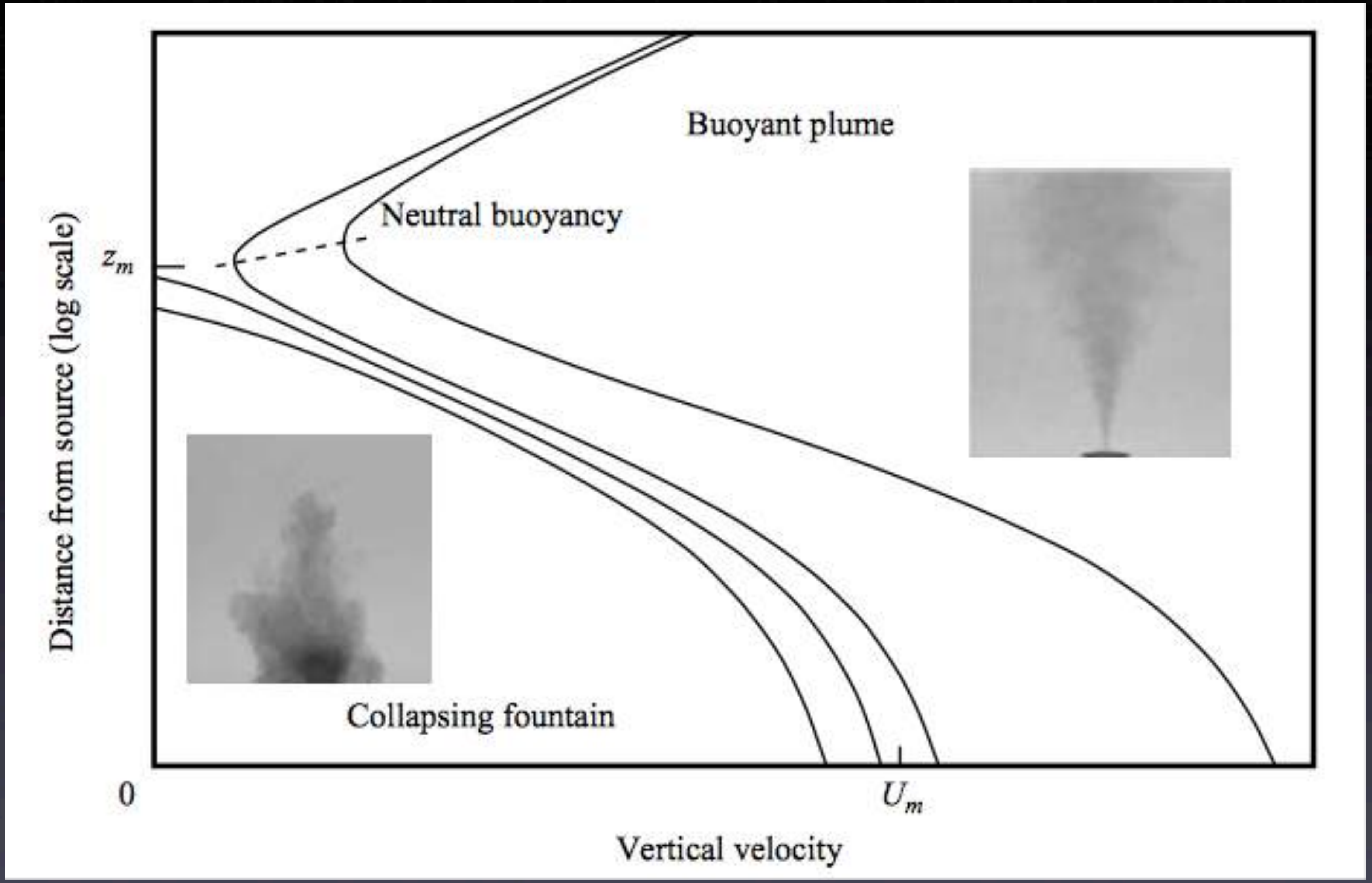

For a given mass flux: collapse depends on U_{exit}

$$U_{exit} \approx 2\ (n\ R\ T)^{0.5}$$

Numerical solution of the equations (2/2)

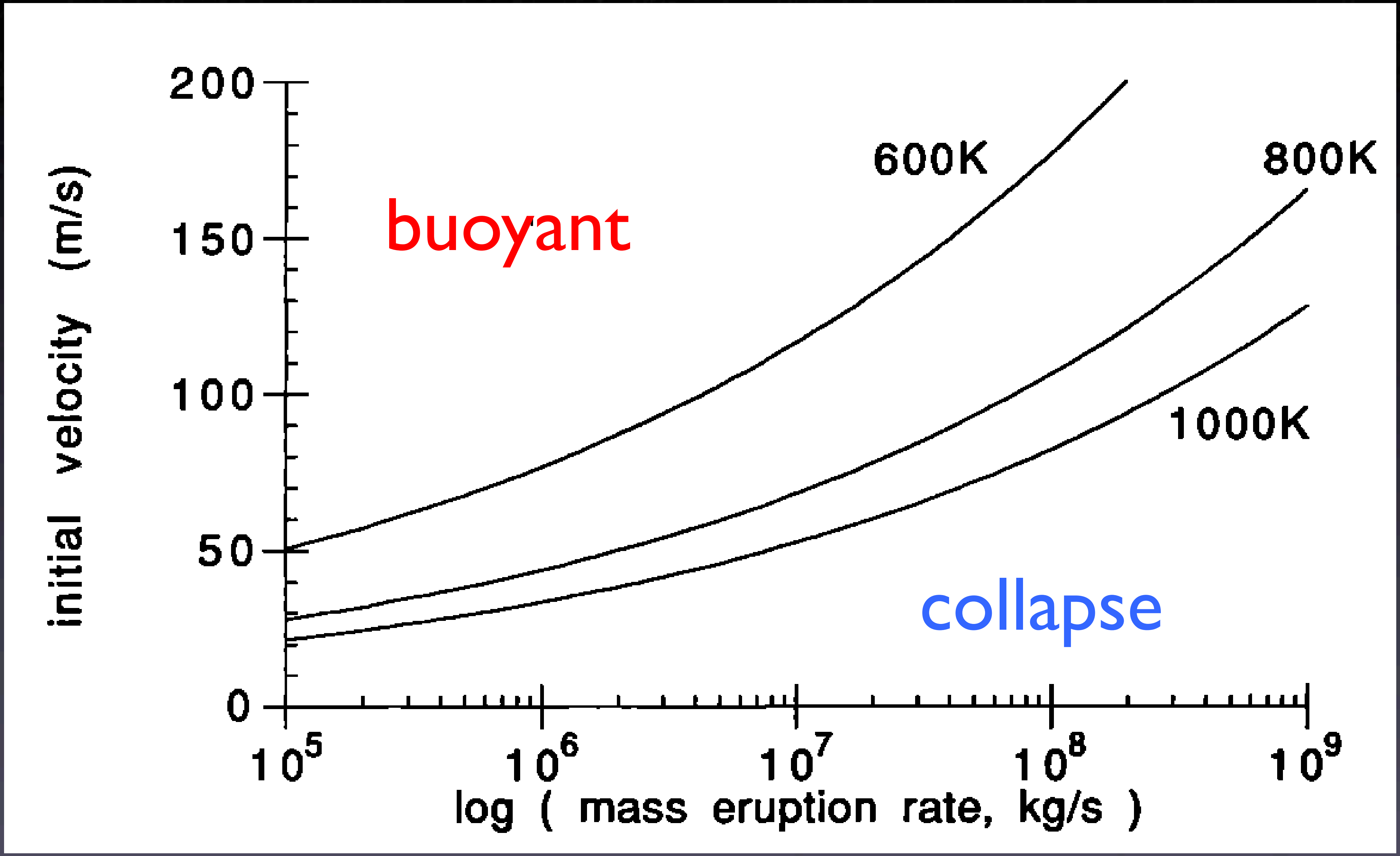

The larger the mass flux, the larger the threshold velocity

Woods, 1995

Comparison between model predictions and field data

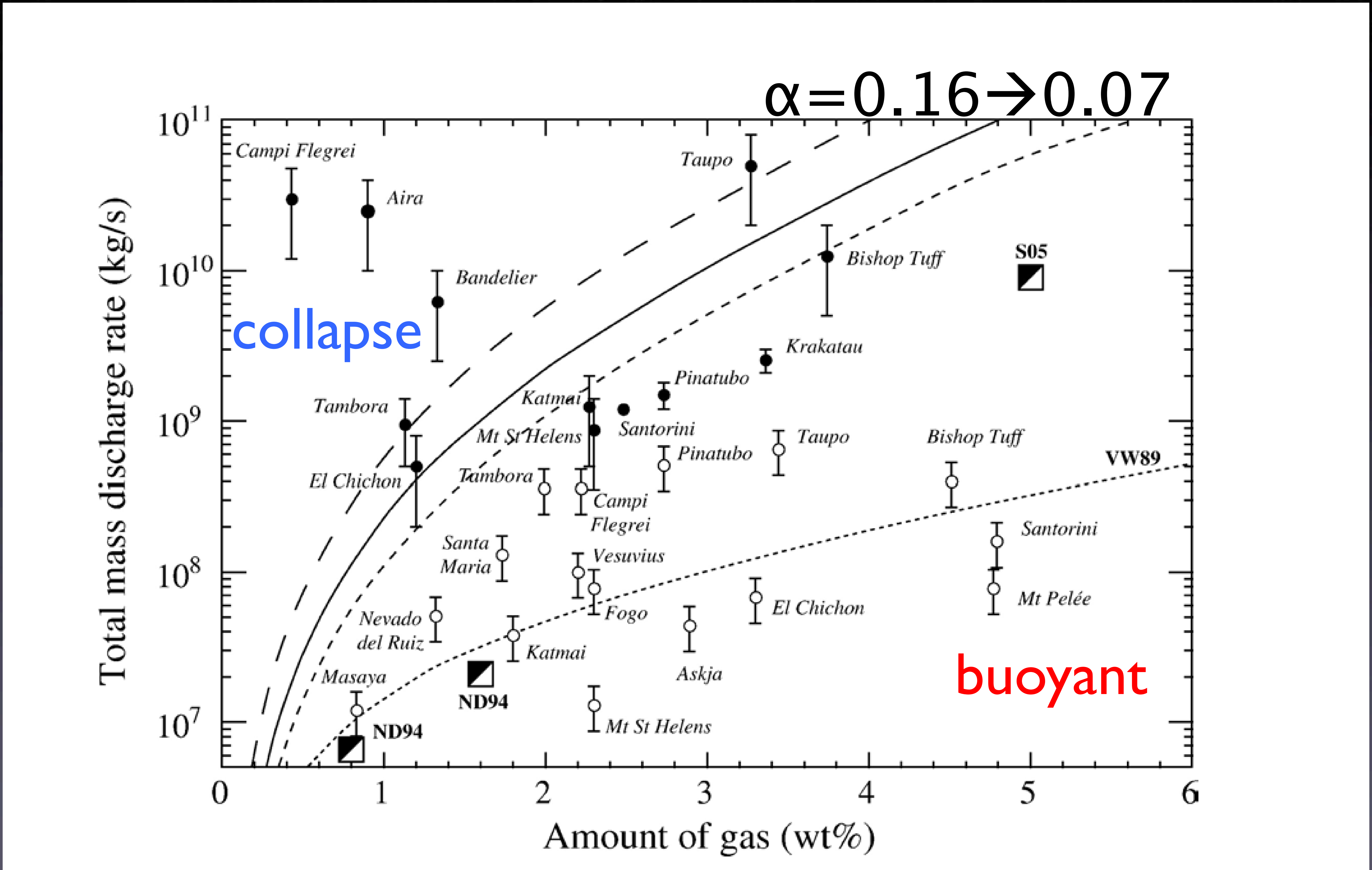

Refined model of turbulent entrainment

$$\lambda = \lambda_{jet} + \color{blue}{b}\, R^2\, \color{red}{g'}/W$$

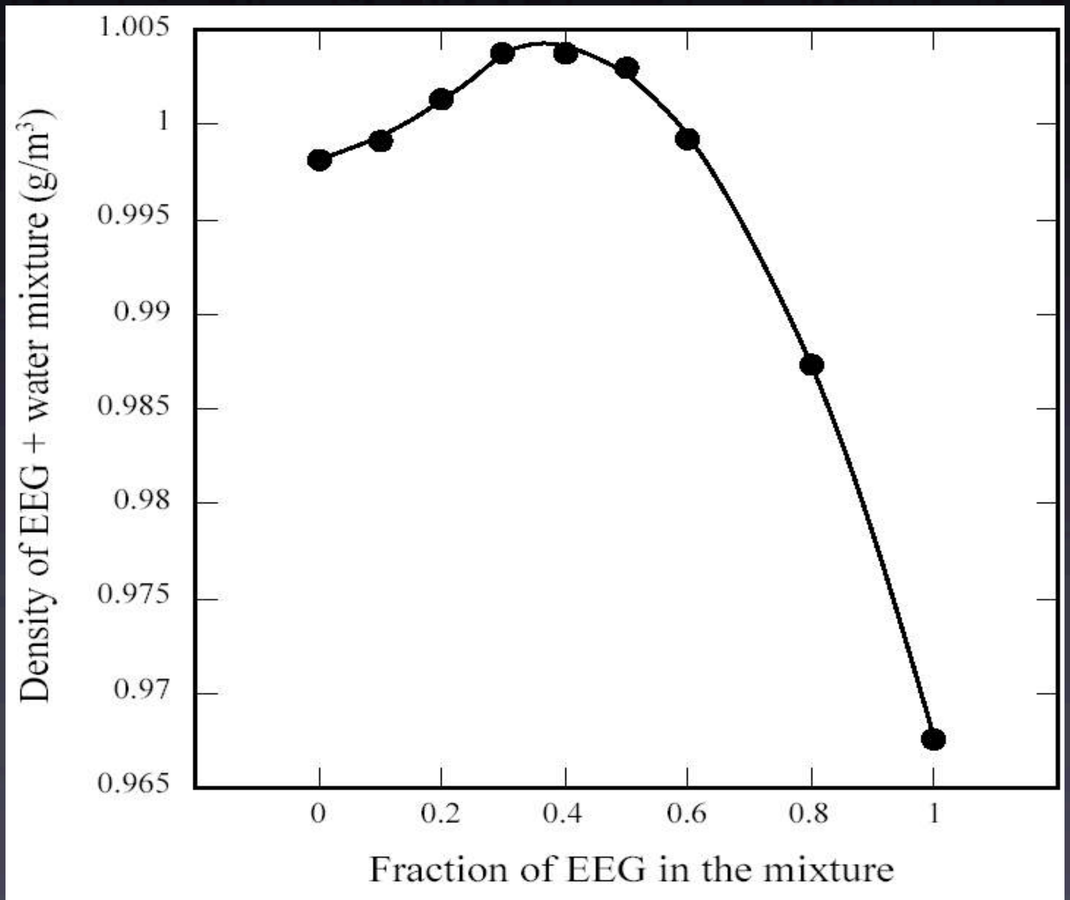

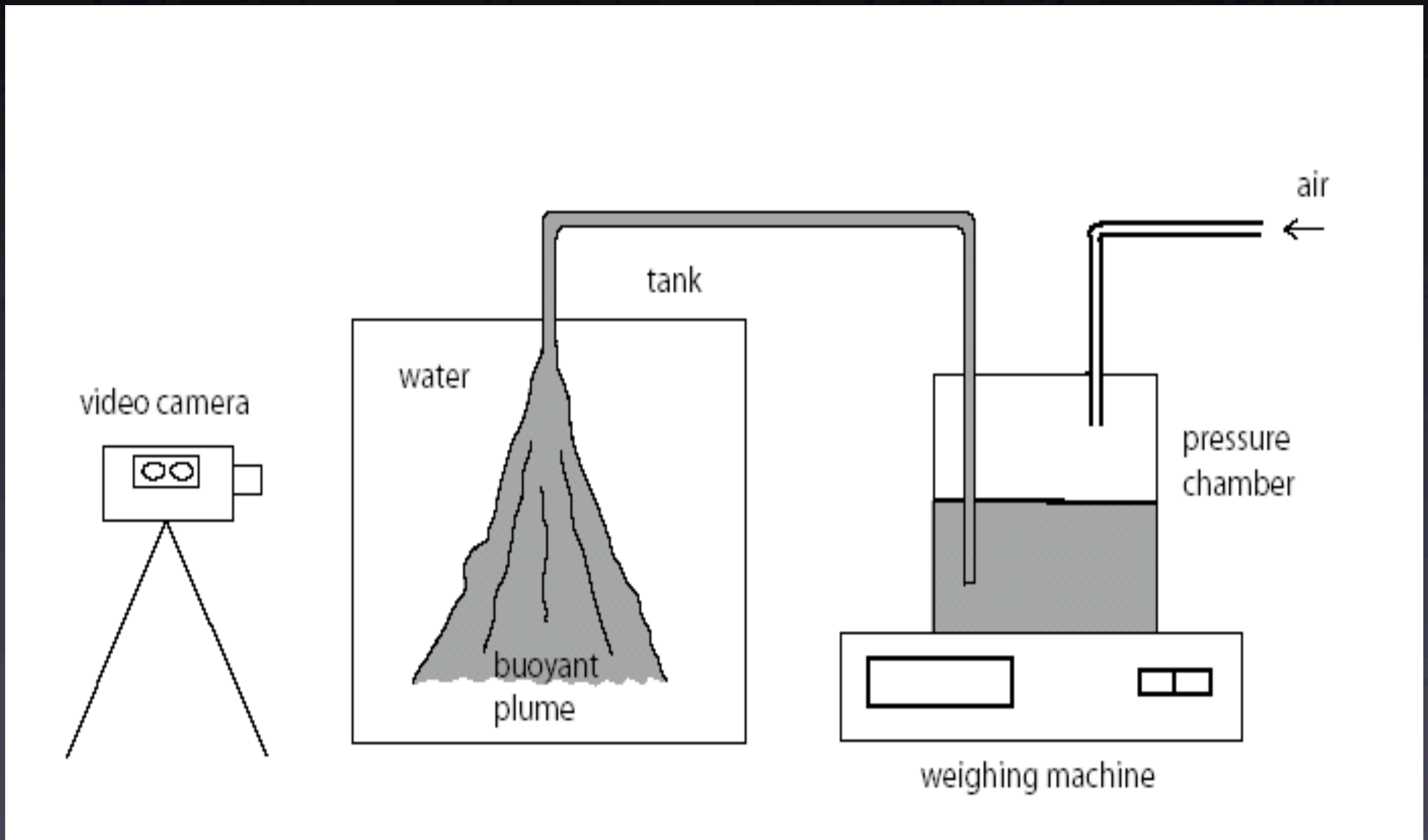

Lab-scale experiments used to constrain the model parameters

Kaminski et al., 2005

Experiments

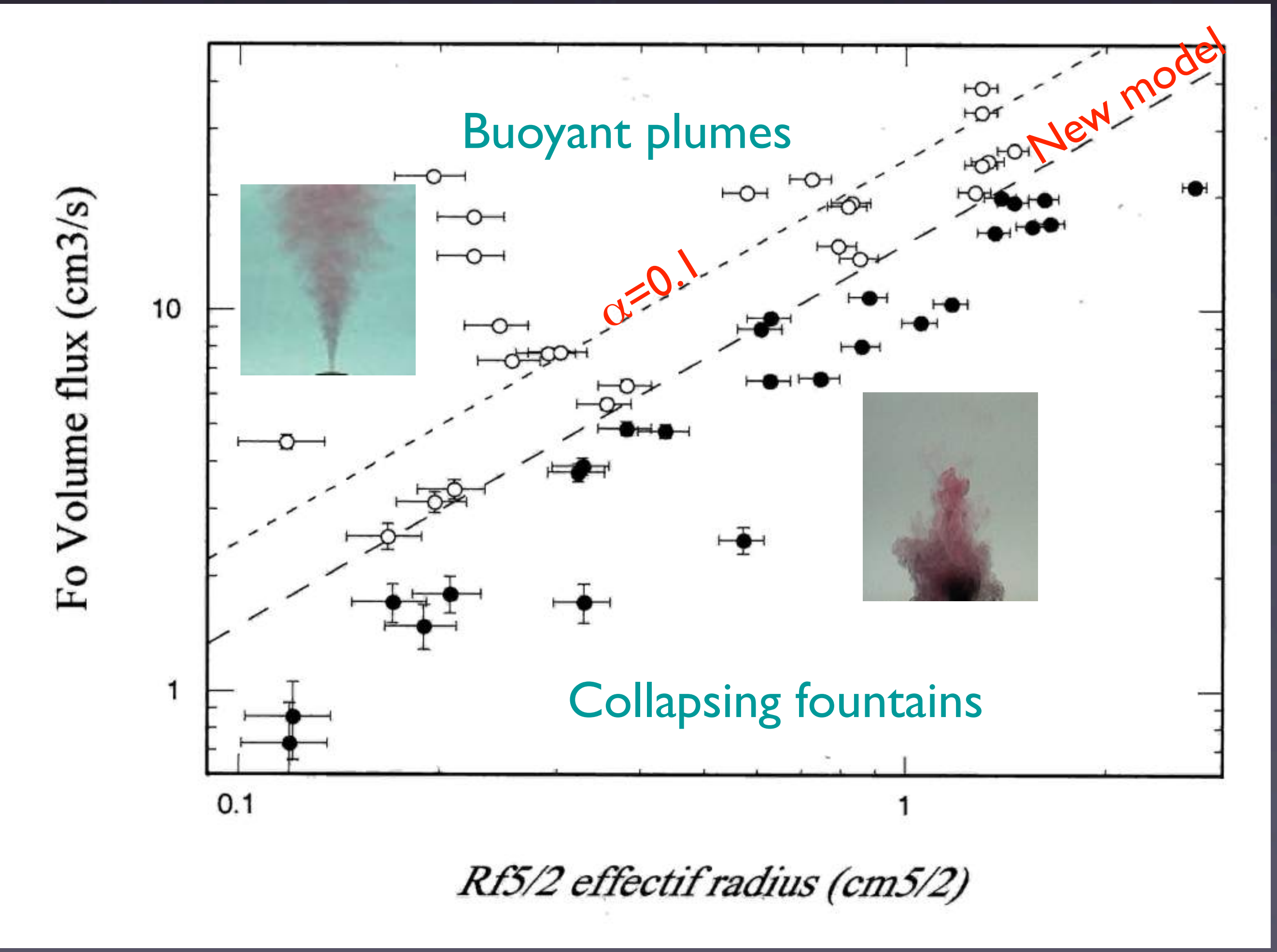

Comparison between new model predictions and field data

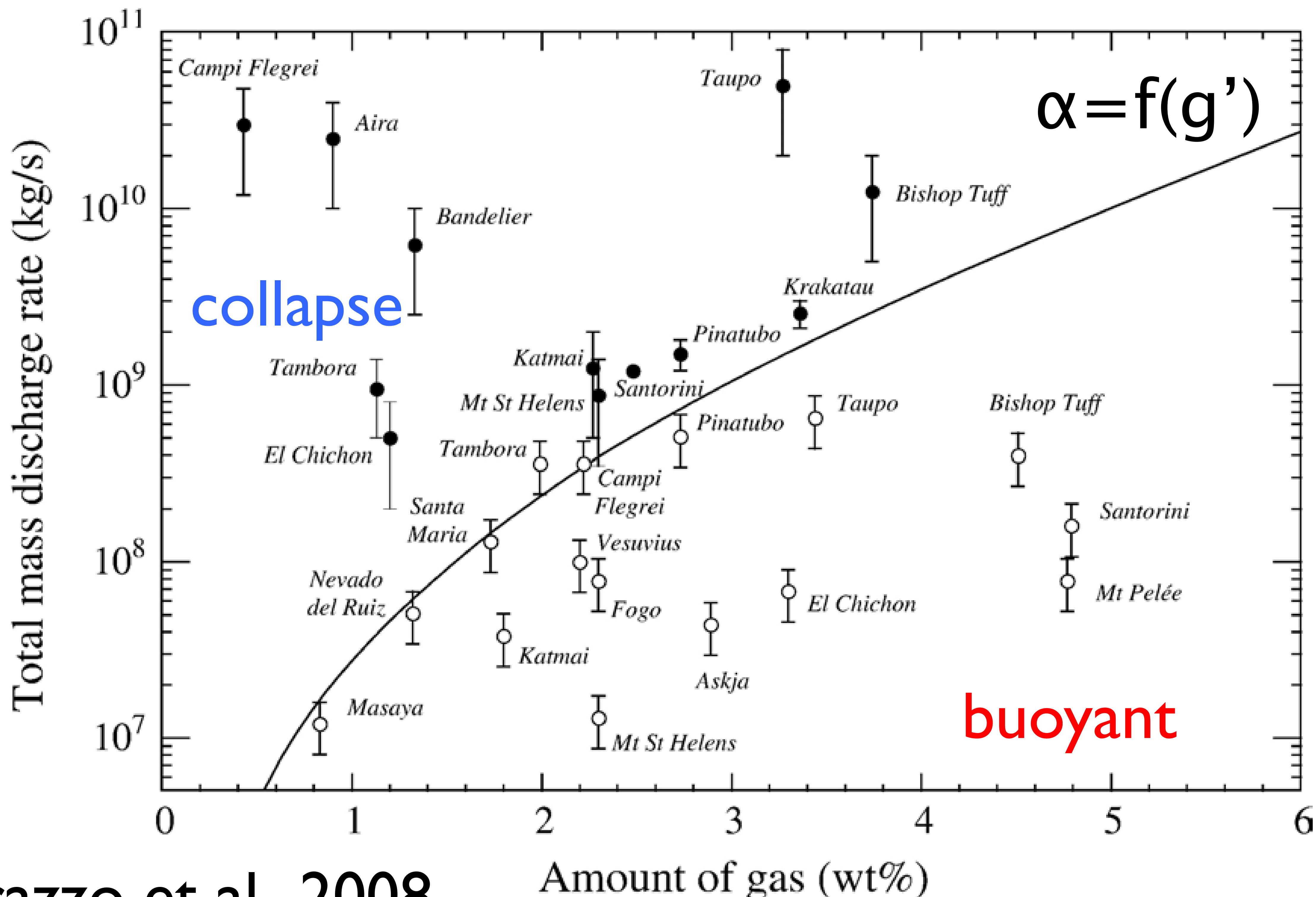

Carazzo et al., 2008

Modeling of volcanic plumes:

2/ maximum height of the volcanic column

3D numerical models

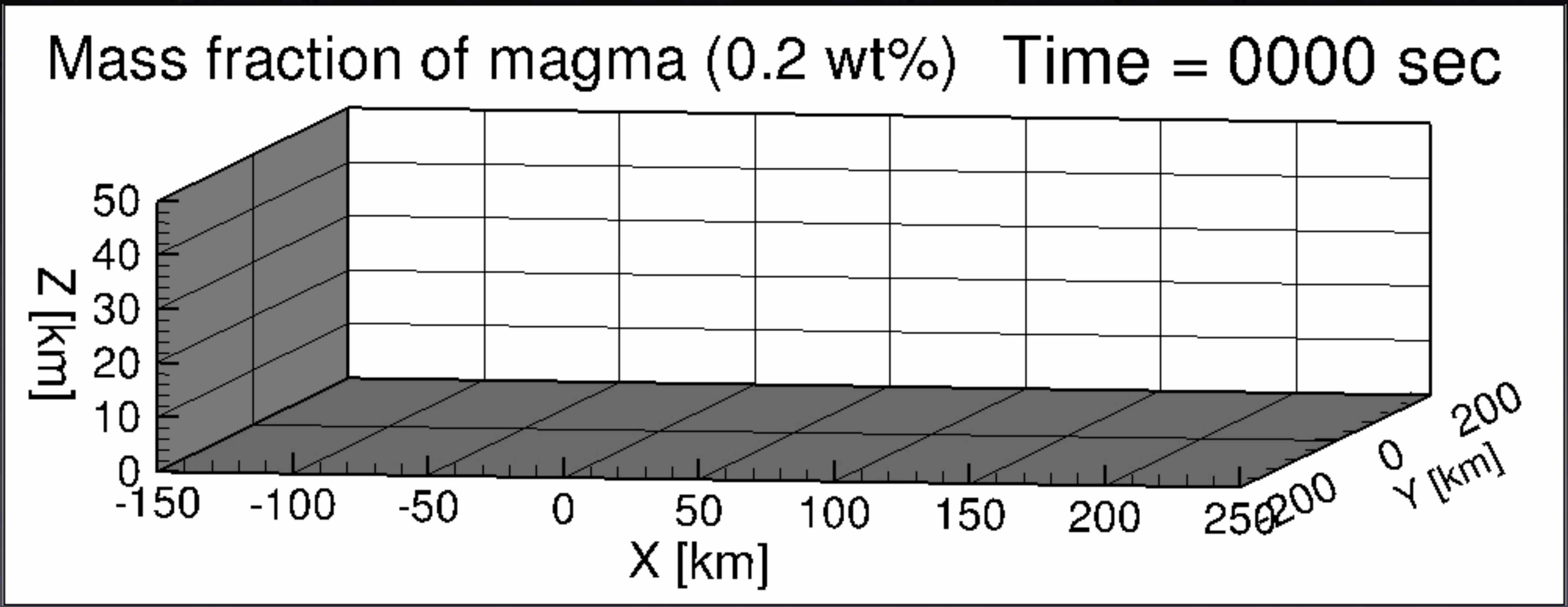

Suzuki, ERI Tokyo

Scaing analysis

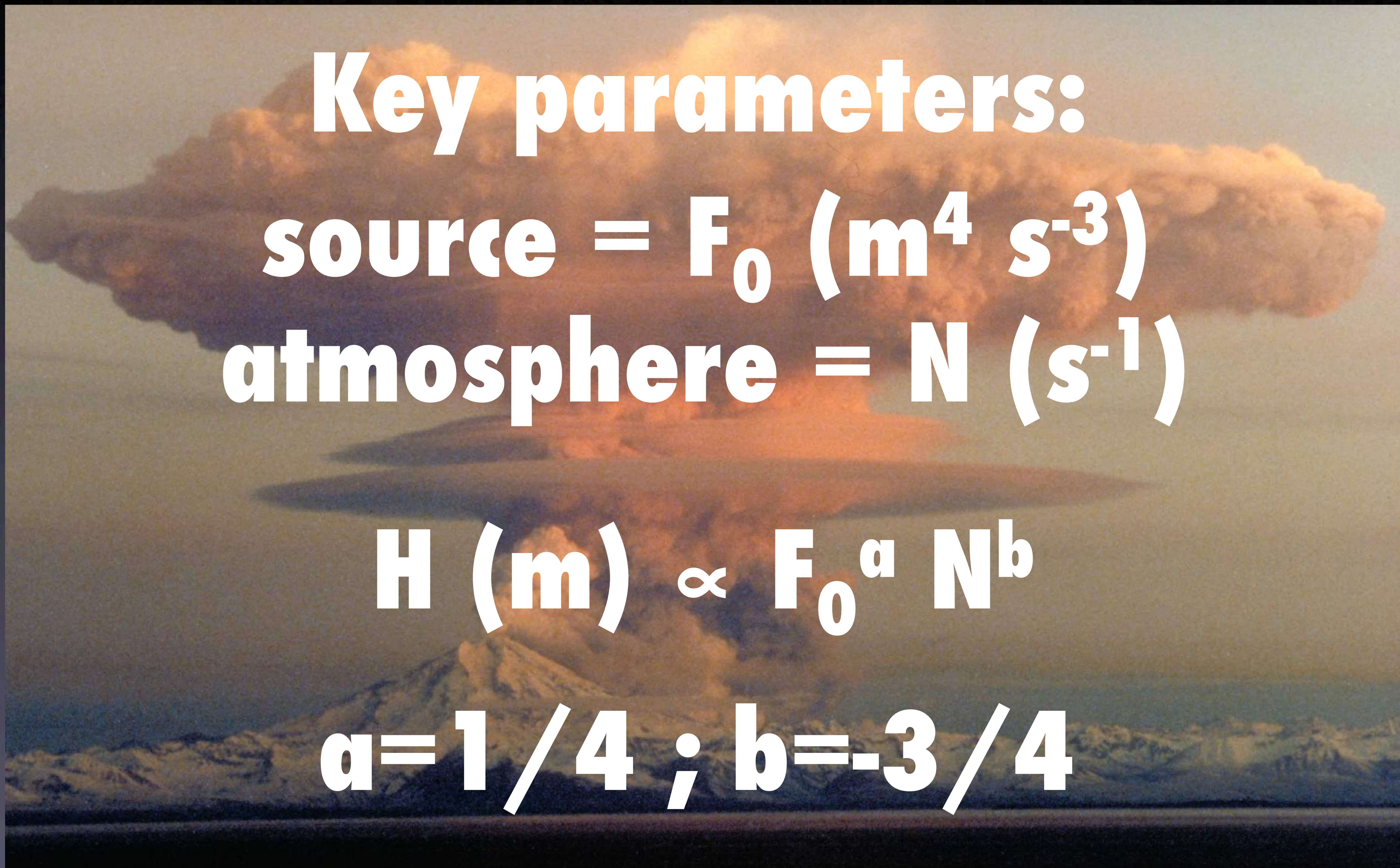

Test of scaling law

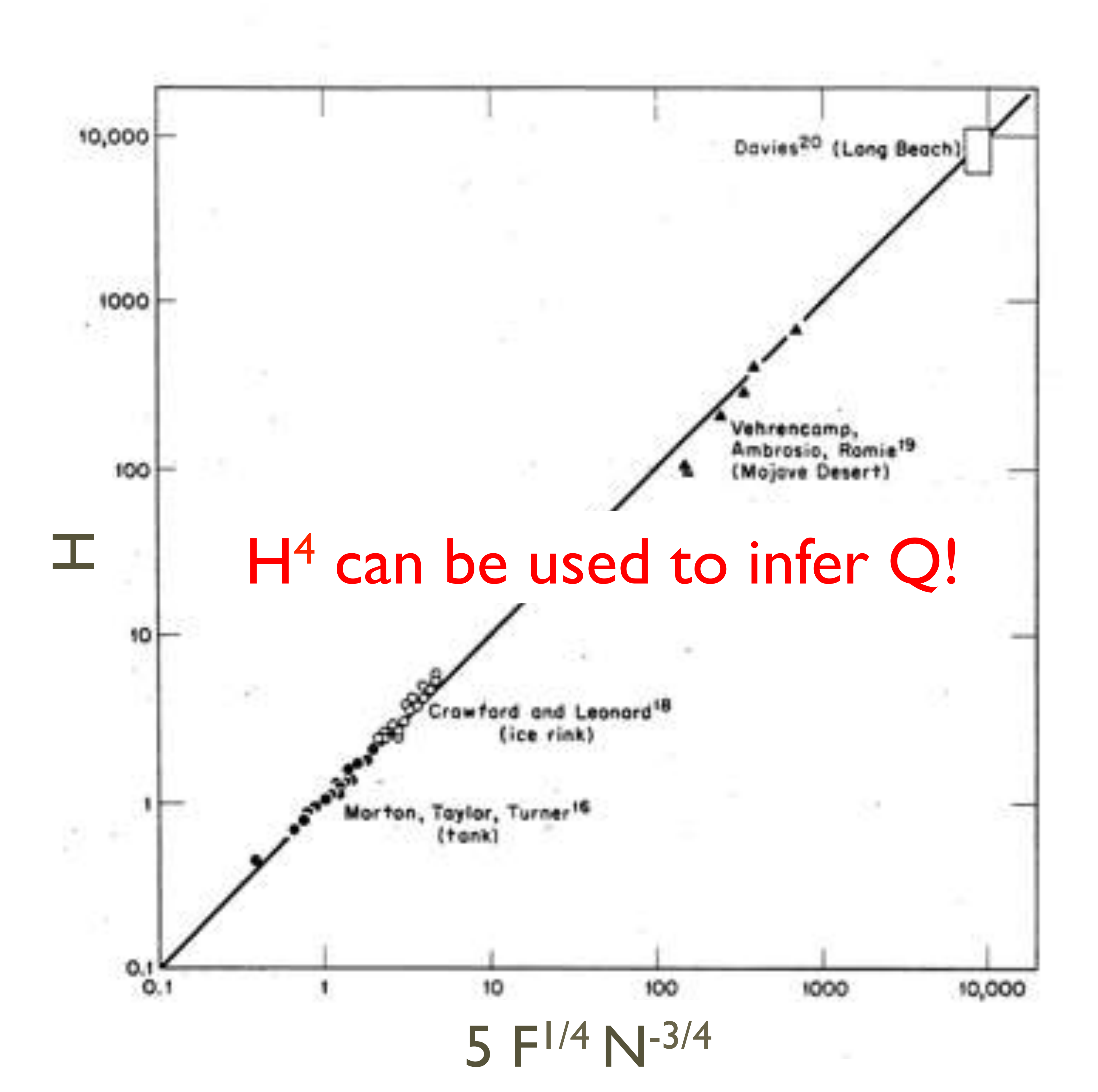

Briggs, 1969

Volcanic plume: effect of wind

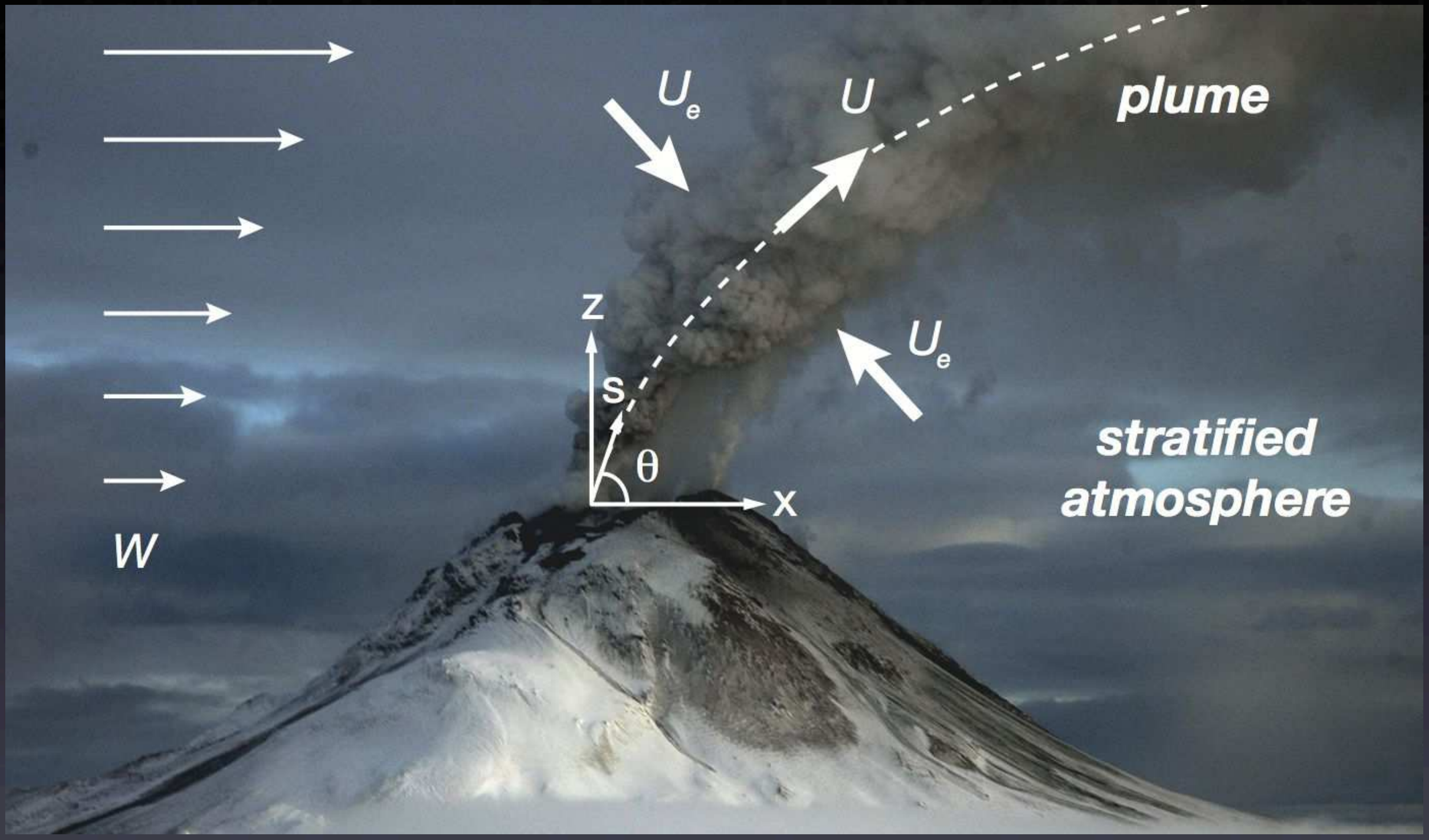

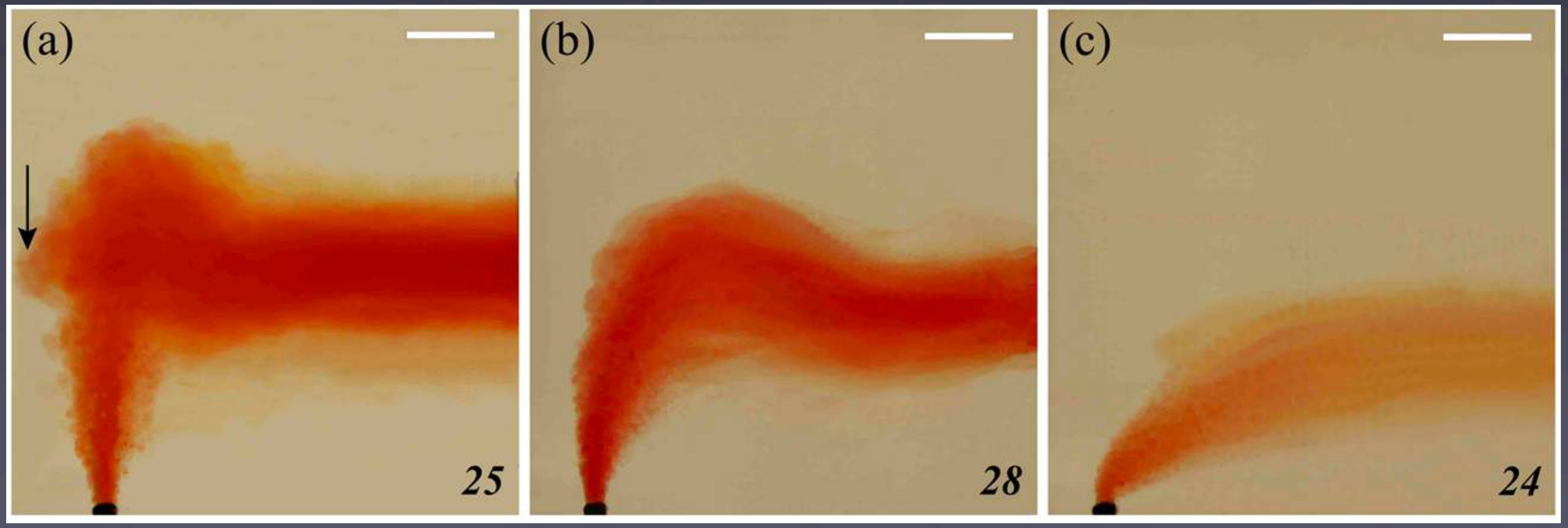

Carazzo et al., 2015

Volcanic plume: comparison model/data

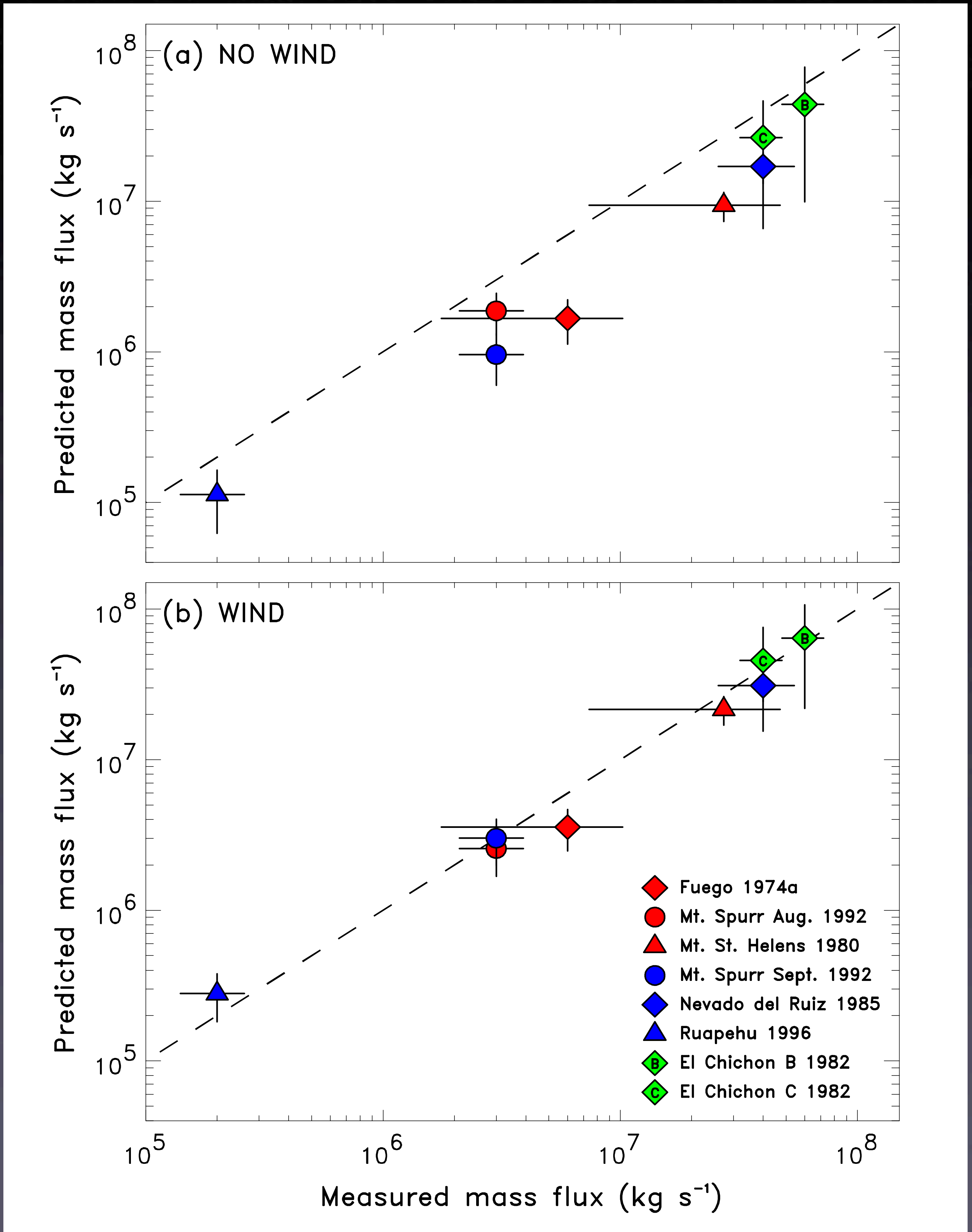

Girault et al., 2016